MONTHLY NOTICES

OF THE

ROYAL ASTRONOMICAL SOCIETY

Vol. 110 No. 6 1950

Published and Sold by the
ROYAL ASTRONOMICAL SOCIETY
BURLINGTON HOUSE
LONDON, W. 1

Price Nine Shillings

NOTICE TO AUTHORS

1. *Communications.*—Papers must be communicated to the Society by a Fellow. They should be accompanied by a summary at the *beginning* of the paper conveying briefly the content of the paper, and drawing attention to important new information and to the main conclusions. The summary should be intelligible in itself, without reference to the paper, to a reader with some knowledge of the subject; it should not normally exceed 200 words in length. **Authors are requested to submit MSS. in duplicate. These should be typed using double spacing and leaving a margin of not less than one inch on the left-hand side. Corrections to the MSS. should be made in the text and not in the margin.** Unless a paper reaches the Secretaries more than seven days before a Council meeting it will not normally be considered at that meeting. By Council decision, MSS. of accepted papers are retained by the Society for one year after publication; unless their return is then requested by the author, they are destroyed.

2. *Presentation.*—Authors are allowed considerable latitude, but they are requested to follow the general style and arrangement of *Monthly Notices*. References to literature should be given in the standard form, including a date, for printing either as footnotes or in a numbered list at the end of the paper. Each reference should give the **name and initials** of the author cited, irrespectively of the occurrence of the name in the text (some latitude being permissible, however, in the case of an author referring to his own work). The following examples indicate the style of reference appropriate for a paper and a book, respectively :—

A. Corlin, *Zeits. f. Astrophys.*, **15**, 239, 1938.
A. S. Eddington, *Internal Constitution of the Stars*, Cambridge, p. 182, Table 24, 1926.

3. *Notation.*—Authors should conform closely to the recommendations of Commission 3 of the International Astronomical Union (*Trans. I.A.U.*, Vol. VI, p. 345, 1938). Council has decided to adopt the I.A.U. 4-letter abbreviations for constellations where contraction is desirable (Vol. IV, p. 221, 1932).

4. *Diagrams.*—**These should be drawn about twice the size required in print and prepared for direct photographic reproduction except for the lettering, which should be inserted in pencil. Legends should be given in the manuscript indicating where in the text the figure should appear.** Blocks are retained by the Society for 10 years; unless the author requires them before the end of this period they are then destroyed.

5. *Tables.*—**These should be arranged so that they can be printed upright on the page.**

6. *Proofs.*—Costs of alterations exceeding 5 per cent of composition must be borne by the author. Fellows are warned that such costs have risen sharply in recent years, and it is in their own and the Society's interests to seek the maximum conciseness and simplification of symbols and equations consistent with clarity.

7. *Revised Manuscripts.*—When papers are submitted in revised form it is especially requested that they be accompanied by the original MS.

Reading of Papers at Meetings

8. When submitting papers authors are requested to indicate whether they will be willing and able to read the paper at the next or some subsequent meeting, and approximately how long they would like to be allotted for speaking.

9. Postcards giving the programme of each meeting are issued some days before the meeting concerned. Fellows wishing to receive such cards whether for Ordinary Meetings or for the Geophysical Discussions or both should notify the Assistant Secretary.

MONTHLY NOTICES

OF THE

ROYAL ASTRONOMICAL SOCIETY

Vol. 110 No. 6

MEETING OF 1950 NOVEMBER 10

Professor W. M. Smart, President, in the Chair

The election by the Council of the following Fellows was duly confirmed :—

James W. Dungey, 19 Warkworth Street, Cambridge (proposed by A. Beer);
Geoffrey Harold Ramsden, Fairleigh, Myddleton Villas, Ilkley, Yorkshire (proposed by F. J. M. Stratton); and
Nancy G. Roman, Yerkes Observatory, Williams Bay, Wisconsin, U.S.A. (proposed by S. Chandrasekhar).

The election by the Council of the following Junior Members was duly confirmed:—

Francis John Lowes, Department of Physics, University of Manchester (proposed by S. K. Runcorn);
Garry Ross Nankivell, 45 Gayhurst Road, Dallington, Christchurch, New Zealand (proposed by A. F. Jones); and
Vincent Cartledge Reddish, Penetang, Holcroft, Culcheth, Warrington, Lancashire (proposed by A. Hunter).

One hundred and three presents were announced as having been received since the last meeting, including:—

W. M. Smart, *Some Famous Stars* (presented by the author);
Survey of India, Technical Report, 1947. *Part III. Geodetic Work* (presented by the Survey of India); and
R. H. Phillimore, *Historical Records of the Survey of India.* Volume II, 1800–1815 (presented by the Survey of India).

SPECIAL GENERAL MEETING OF 1950 DECEMBER 8

Professor W. M. Smart, President, in the Chair

At a Special General Meeting of Fellows, held immediately preceding the Ordinary Meeting, amendments to the Bye-laws designed to remove from the Fellows the legal liability to pay their annual contributions, were proposed by

the Treasurer on behalf of the Council, and seconded by Dr A. Hunter. The amendments proposed by the Council were as follows :

(*a*) that Bye-law 24 be repealed;

(*b*) that Bye-laws 25 and 26 be renumbered 24 and 25 respectively;

(*c*) that a new Bye-law be enacted as follows :

> " 26. Every Fellow shall be considered as belonging to the Society until he has either signified in writing to the Society his desire to resign, or has ceased to be a Fellow under Bye-laws 21 or 25; when his name shall be erased from the List of Fellows.";

(*d*) that Form No. 2 in the Appendix, referred to in Bye-laws 19 and 20, be amended by the deletion of the words

> " after the payment of any annual contribution which may be due by me at that period, and ".

The Treasurer explained that these amendments were necessary to enable the Society to benefit in future by the recovery of income tax on annual contributions paid under seven-year covenants, and the motions were carried unanimously.

MEETING OF 1950 DECEMBER 8

Professor W. M. Smart, President, in the Chair

The election by the Council of the following Fellows was duly confirmed:—

Lawrence H. Aller, Associate Professor of Astrophysics, The Observatory, University of Michigan, Ann Arbor, U.S.A. (proposed by S. Chandrasekhar);

Roland Fabian Berrill, Upwood House, Caterham, Surrey (proposed by H. Bondi);

Edward George Bowen, Division of Radiophysics, C.S.I.R.O., Chippendale, New South Wales, Australia (proposed by R. v. d. R. Woolley);

Arthur Charles Clarke, B.Sc., 88 Nightingale Road, London, N.22 (proposed by M. W. Ovenden);

Frank Coop, F.R.Met.Soc., 638 Devonshire Road, Blackpool, Lancashire (proposed by H. A. Costigan);

Aidan Patrick FitzGerald, 17 Finaghy Park North, Belfast, Northern Ireland (proposed by E. M. Lindsay);

George Edwin Gray, 6 Winifred Road, Dagenham, Essex (proposed by F. M. Holborn);

D. ter Haar, D.Sc., The University, St. Andrews, Fife, Scotland (proposed by S. Chandrasekhar);

George William Hamstead, B.Sc., A.R.C.S., F.R.Met.Soc., 25 West End Lane, Bell's Hill, Barnet, Hertfordshire (proposed by R. W. B. Pearse);

Victor A. Hughes, M.Sc., Ridge End, Hook Hill Lane, Woking, Surrey (proposed by J. S. Hey);

Wasley Krogdahl, Dearborn Observatory, Evanston, Illinois, U.S.A. (proposed by S. Chandrasekhar);

Laurence Patrick Lee, Lands and Survey Department, Wellington, New Zealand (proposed by D. C. Berry);

Lilian Elenblad Lewis, 52 Campbell Street, East Kew, E.4, Victoria, Australia (proposed by J. F. Paterson);

Voislav V. Michkovitch, Director of the Institute for Theoretical and Applied Astronomy, Serbian Academy of Science, Belgrade, Yugoslavia (proposed by D. H. Sadler);

James Victor Morley, Old House Farm, Marton, Blackpool, Lancashire (proposed by W. M. F. Macfarlane);

Evelyn Musgrave, B.Sc., 30 Norman Avenue, Eccleshill, Bradford, Yorkshire (proposed by H. R. Didcock);

Kongot Nagappan Padmanabhan Nair, Doon School, Dehra Dun, United Provinces, India (proposed by L. M. Verghese);

William John Newall, 20 Ruth Street, Corinda, Brisbane, Australia (proposed by A. K. Chapman);

The Rt. Hon. Earl of Rosse, M.B.E., M.A., M.R.I.A., F.S.A.(Eire), Birr Castle, King's County, Eire (proposed by W. M. Smart);

George Frederick Suart, F.R.C.O., Naworth, Rossal School, Fleetwood, Lancashire (proposed by F. Holden);

Geofroy William Tory, B.A., Counsellor of Embassy, Commonwealth Relations Office, Downing Street, London, S.W.1 (proposed by W. M. Smart);

Jean Verhoogen, Ph.D., Associate Professor of Geology, University of California, Berkeley, California, U.S.A. (proposed by P. Byerly); and

James Tinley Wilson, A.B., Ph.D., Associate Professor of Geology, University of Michigan, Ann Arbor, Michigan, U.S.A. (proposed by P. Byerly).

The election by the Council of the following Junior Members was duly confirmed:—

Raymond Hide, 68 Victoria Park, Cambridge (proposed by S. K. Runcorn);
Harry Hughes, Caius College, Cambridge (proposed by S. K. Runcorn); and
Leon Mestel, Trinity College, Cambridge (proposed by F. Hoyle).

Eighty-five presents were announced as having been received since the last meeting.

Dr J. C. P. Miller and Mr K. C. Blackwell were appointed honorary auditors of the Treasurer's accounts for the year 1950.

A PRELIMINARY SURVEY OF THE RADIO STARS IN THE NORTHERN HEMISPHERE

M. Ryle, F. G. Smith and B. Elsmore

(Received 1950 August 25)

Summary

Observations with an interferometer of large resolving power have made it possible to locate 50 discrete sources of radio waves or " radio stars " in the Northern Hemisphere ; their positions and intensities (which cover a range of $7\frac{1}{2}$ in apparent magnitude) are given. The positions of the more intense radio stars can be determined with an accuracy of about 5 minutes of arc, but most of them can only be located to within 1°.

The angular distribution of the radio stars, unlike that of the general background radiation, shows no concentration in the galactic plane; this result suggests either that they are at distances small compared with the dimensions of the galaxy, or that they are situated outside the galaxy. Whilst there is evidence that a few of the weakest radio stars represent the total " background " radiation of some of the nearest extra-galactic nebulae, it is concluded that the majority of the radio stars must be situated within the galaxy. Estimates of the relative intensities of the radio stars and of the background radiation have suggested that they are distributed throughout the galaxy with an average population density comparable with that of visual stars.

Attempts to identify the radio stars with various types of visual body have been unsuccessful; it is therefore concluded that the radio star represents a hitherto unobserved type of stellar body, distributed widely throughout the galaxy, and one which is equally numerous in other spiral nebulae.

---

1. *Introduction.*—The existence of discrete sources of radio waves in the galaxy was first demonstrated by Hey, Parsons and Phillips (1946), and subsequently confirmed by the observations of Bolton and Stanley (1948) and Ryle and Smith (1948). In these experiments it was found that the angular diameters of the two most intense sources did not exceed 6 minutes of arc, whilst none of the sources appeared to coincide with a bright visual star.

More recent experiments at Cambridge have shown the absence of any measurable annual parallax; it was therefore concluded that the two most intense sources are situated at distances greater than $2 . 10^{16}$ cm. (Ryle, 1950). There is also some evidence (Ryle, 1949; Smith, 1950) that the sources are of stellar dimensions.

Observations of the discrete galactic sources have been maintained at Cambridge since 1948 May, using wave-lengths of 1·4, 3·7 and 6·7 m. The greater part of this programme has been concerned with a survey of the Northern Hemisphere on a wave-length of 3·7 m. In the present communication an account will be given of the results of this survey, including the positions and intensities of 50 sources which have been located.

The results have been analysed in an attempt to deduce the nature of the sources, and although it does not appear possible to relate them to any of the well-known types of stellar body, as observed at visual wave-lengths, there is good reason for believing that they are extremely common bodies distributed

throughout the galaxy. For this reason, and because of the greater convenience, the discrete sources of radio waves are here referred to as "radio stars", although there is, as yet, insufficient evidence to prove conclusively that they are of stellar dimensions.

Observations of the disturbing effects of irregularities in the terrestrial ionosphere (analogous to "bad seeing") were also made during this survey; the results obtained have already been described (Smith, 1950; Ryle and Hewish, 1950).

2. *The experimental methods.* (a) *The detection of the radio stars.*—The detection of discrete sources of radio waves presents considerable difficulty, partly because of the small radio-frequency power which is intercepted by the aerial system, but chiefly because of the problem of distinguishing between the radiation from an individual source, and the general background radiation from the galaxy. Even the largest "pencil-beam" radio telescopes which have been

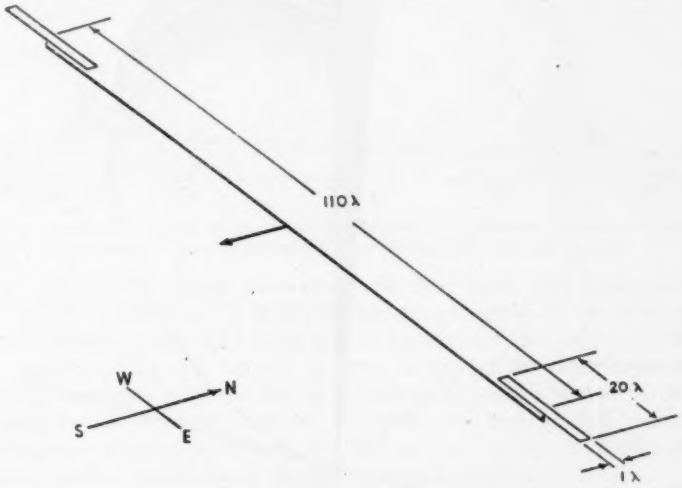

FIG. 1.—*Spaced-aerial interferometer used on a wave-length of 3·7 m.*

built have a resolving power which is very poor compared with a small visual telescope; it is therefore difficult to interpret the variations of received power as the system is directed to different parts of the sky, in terms of discrete sources, since similar variations are also produced by the angular structure of the general background radiation. This problem has been considered in some detail in a recent paper (Ryle, 1950) and it was there shown that the use of an interference system of considerable resolving power had great advantages over a conventional "pencil-beam" aerial system.

In the present series of observations an interferometer having an aperture of 110 λ has been used (see Fig. 1). The discrimination against the background radiation with this system corresponds to that of a conventional "pencil-beam" aerial having an aperture of about 1 km. The ability to separate two adjacent radio stars is, of course, a function of the solid angle over which the aerial system

is receptive, and is therefore related to the resolving power of the individual aerials of the interference system and not to their spacing.

As can be seen from Fig. 2, the reception pattern of each aerial is restricted to about $\pm 1\frac{1}{2}°$ in an East–West plane but covers about $\pm 45°$ in a North–South plane. The system is mounted horizontally at the latitude of Cambridge (52°) and the reception pattern therefore covers a narrow strip along the meridian, which extends from the pole to about declination $+10°$. The system is therefore analogous to a transit telescope, and each radio star may be observed when it

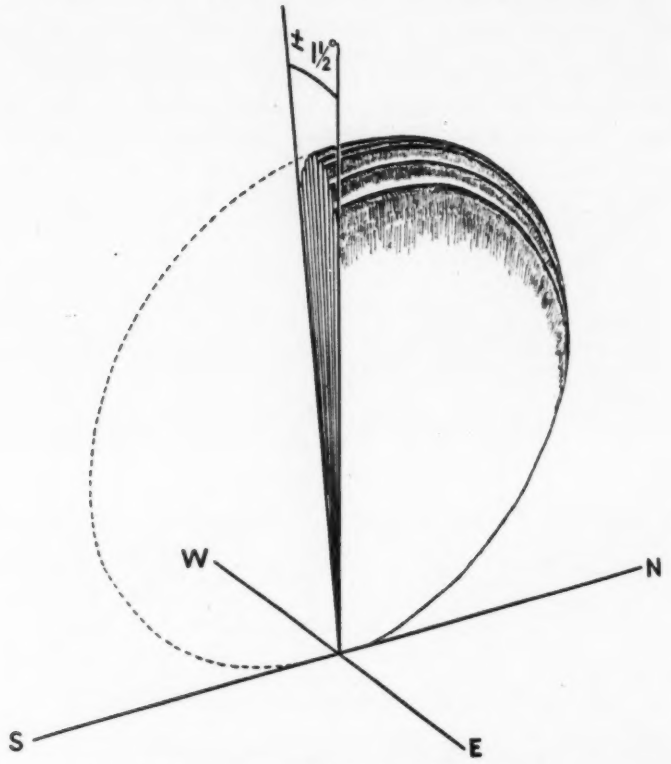

FIG. 2.—*Reception pattern of spaced-aerial interferometer.*

is within $\pm 1\frac{1}{2}°$ of the meridian. (This method of observation has considerable advantages over the "Lloyd's mirror" interferometer used by the Australian workers (Bolton and Stanley, 1948), since each radio star is observed when its zenith distance is a minimum. In the "Lloyd's mirror" method an interference pattern is produced by reflection at the surface of the sea, and observations are restricted to a few degrees above the horizon, where refraction in the troposphere and ionosphere may cause considerable errors.)

As the Earth rotates the interference pattern produced by the two aerials will be swept across the greater part of the Northern Hemisphere. The radiation due to the general background will produce a trace on the record which will

exhibit slow variations as the meridian strip includes more or less of the Milky Way; any discrete source of radiation, having an angular diameter small compared with the separation of the interference maxima (30 minutes of arc), will, on the other hand, produce a periodically varying trace whilst it is situated within $\pm 1\frac{1}{2}^\circ$ of the meridian. A typical record showing the transit of the two intense radio stars in the constellations of Cygnus and Cassiopeia and the slow variation of the background radiation is shown in Fig. 3.

Records of the type shown in Fig. 3 are satisfactory if the radio star to be observed produces a power in the aerial comparable with that produced by the background radiation. If, however, the background power is considerably greater, there is difficulty in measuring the small periodic variations produced on the record by the much smaller power from the radio star. It is clearly difficult to detect a radio star which produces a trace less than about $\frac{1}{50}$ of the full-scale deflection of the recorder, and it is therefore not possible with this system to observe radio stars which produce an aerial power much less than about $\frac{1}{50}$ of that due to the background radiation.

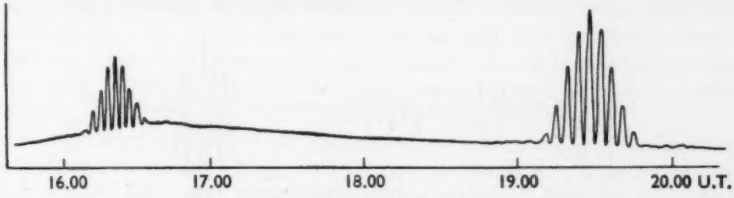

FIG. 3.—*Section of record obtained with spaced-aerial interferometer, showing the intense radio stars in the constellations of Cygnus* (16.20) *and Cassiopeia* (19.30).

In order to be able to make observations of weaker radio stars a new recording system has been developed, in which the power intercepted by the aerial system from an extended source, such as the general background, produces no deflection of the recorder. In this system the two aerials of the interferometer are connected alternately in phase and in anti-phase in such a way as to produce alternately two interference patterns, in which the maxima and minima are interchanged. This aerial system receives the same power from the general background in both positions of the phase-changing switch.

If, now, a radio star is situated near the meridian, it will produce a power in the aerial which depends on its position relative to the interference maxima and minima, and which will, in general, be different in the two switch positions. The output from the aerial will therefore contain a constant component due to the general background radiation and a component due to the radio star which varies periodically at the switching frequency (25 c./s.). The amplitude and phase of this component depend on the position of the radio star relative to the interference maxima and minima; as the Earth rotates the amplitude and phase of this component will change and by arranging that the deflection on the record is proportional to this periodic component it becomes possible to obtain a trace which shows the passage of the radio stars through the interference pattern. No deflection of the trace is produced in the absence of sources of small angular diameter, and a very much greater sensitivity may therefore be used; radio stars whose intensity is a very small fraction of that of the background radiation may then be observed.

A section of a typical record obtained with this system is shown in Fig. 4, in which the transit of a number of weaker sources can be seen. With this system it is found that the detection of very weak radio stars is limited not by the sensitivity of the recording apparatus, nor by the incidence of the background radiation, but by the confusion of the interference patterns produced by adjacent radio stars; under these conditions a further extension of the detection limit is only likely to be achieved by decreasing the solid angle of the envelope of the interference pattern, i.e. by increasing the resolving power of the individual aerials of the interferometer.

(b) *The determination of the position of a radio star.*—The use of an interference system of the type described, in addition to allowing better discrimination than a conventional "pencil-beam" radio telescope, has particular advantages when the positions of discrete sources are to be determined. By observing the precise time of the central maximum of the interference pattern on the record, it is possible to determine the time of transit and hence the Right Ascension of the source, with an accuracy which corresponds to the resolving power of a conventional "pencil-beam" system having an aperture of about 1 km.

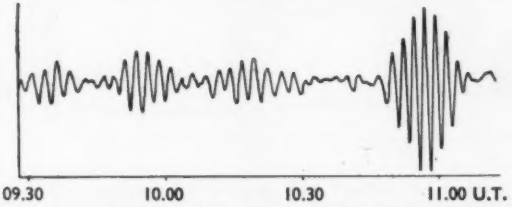

FIG. 4.—*Section of record obtained with "phase switching" system, showing a number of weak radio stars between R.A. 04.00 and 06.00. The recorder sensitivity is about 100 times greater than that of Fig. 3.*

The declination of a radio star may be obtained in the following way from another property of the spaced-aerial interferometer by observing the period of the interference pattern on the record. A radio star in the plane of the equator will give rise to a record whose periodicity (t_0) is given by the time taken for the Earth to rotate through the angle separating successive maxima of the interference pattern (for the present system $t_0 \simeq 2$ minutes). It can be shown that a radio star having a declination δ will produce a record whose periodicity is $t_0 \sec \delta$, so that a measurement of the periodicity enables $\sec\delta$ to be deduced. It is therefore possible to find both coordinates of the source from the same record.

A full account of the methods of determining the coordinates to take account of height and azimuth errors in the aerial alignment will be given elsewhere, together with calculations of the errors introduced by refraction in the terrestrial ionosphere.

The accuracy with which the coordinates of a radio star may be determined depends, of course, on the intensity of the source; for the two intense radio stars in the constellations of Cygnus and Cassiopeia, the time of transit may be determined from the record with an accuracy of 0·25 second, under conditions of "good seeing", but the Right Ascension cannot be determined with this accuracy owing to uncertainty in determining the electrical centres of the two aerial systems. An accuracy of about 5 seconds in time (corresponding to an angular accuracy of ½–1 minute of arc) is possible in Right Ascension, with an accuracy

of 5 minutes of arc in declination. For the weaker sources the accuracy is usually limited by difficulties arising from overlapping of the interference patterns of adjacent sources; in the limiting case of the weakest sources the trace on the record may be modified by the presence of nearby sources which are themselves too weak to be detected. Under such conditions the apparent position of a very weak source may be in error by an amount greater than that deduced from the accuracy with which the record may be read; the observed position may then approximate to the "centre of gravity" of two or more very close sources.

It is clear from the relation connecting the declination and the periodicity of the record that the accuracy with which the declination may be determined becomes poor for radio stars at low declinations, whilst for those near the pole the accuracy may be better than that of the Right Ascension.

3. *The results of observations of the Northern Hemisphere.*—Observations on a wave-length of 3·7 m. with the system described in the previous paragraph have enabled a preliminary catalogue of 50 radio stars in the Northern Hemisphere to be compiled. These sources are listed below, in Table I, with their positions. Since the determination of Right Ascension is usually more precise than that of declination, the sources have been numbered in each hour of Right Ascension, the last two figures representing the serial number of each radio star in order of its discovery. (In this initial list the radio stars have been arranged in order of intensity.)

The measured intensity of the radiation from each radio star is tabulated in column 4, and an apparent magnitude is given in column 5. Since the two most intense sources are about three magnitudes "brighter" than the "brightest" of the remaining sources (which are regularly distributed in apparent magnitude*) the zero of the magnitude scale has been arbitrarily chosen as corresponding to an intensity of 10^{-23} watts m.$^{-2}$ (c./s.)$^{-1}$. This flux is approximately that of the fourth most intense radio star (12·01) in the region surveyed.

The limits of accuracy of the positions of the radio stars which are quoted in the table include not only the probable error in reading the records and in determining the aerial alignment but an additional factor which depends on the confusing effect of neighbouring radio stars. As has already been explained in Section 2 (b) it is difficult to determine this factor for the radio stars of very small intensity, since the record may be modified by the presence of other sources which are themselves too weak to be detected. It is therefore possible that the positions of some of the very weak sources may be in error by an amount greater than that deduced; the observed position may then correspond to the "centre of gravity" of the main source and other weaker sources nearby.

Attempts have been made to measure the angular diameter of several of the more intense radio stars, but in no case has it been found to exceed the resolving power of the apparatus; the upper limit determined for the angular diameter of the two most intense sources (19·01 and 23·01) was about 3 minutes of arc.

4. *The distribution of the radio stars.*—Before attempting to make any deductions about the nature of the radio stars it is important to make some estimate of their distribution in space. Previous experiments made to measure the annual parallax of the two most intense radio stars have shown that they are situated at distances greater than $2 \cdot 10^{16}$ cm. (Ryle, 1950).

* The distribution of the radio stars in apparent magnitude has been discussed in an earlier paper (Ryle, 1950).

TABLE I

(Positions refer to Epoch 1950)

Number	R.A.			Declination			Intensity (watts m.$^{-2}$ (c./s.)$^{-1}$ $\times 10^{25}$)	Apparent Magnitude
	h	m	s	°	′	″		
00·01	00	42	± 6	38	±5		4	3·5
01·01	01	25	± 5	30	±3		8	2·8
01·02	01	09	± 3	43	15±1		4·5	3·3
02·01	02	16	± 3	44	15±2		6	3·0
02·02	02	25	± 3	35	30±2		5	3·2
02·03	02	45	± 3	45	15±0	45	4	3·5
03·01	03	50	±20	75	±1		14	2·1
03·02	03	12	± 3	43	45±0	30	9·5	2·5
03·03	03	58	± 1 3	41	±1	30	4·5	3·3
04·01	04	28	± 1	25	±2		33	1·2
04·02	04	56	± 2	33	±1	30	12·5	2·3
04·03	04	10	± 2	35	45±0	30	10·5	2·4
05·01*	05	31	37± 0 10	22	10±0	20	125	−0·2
05·02	05	02	± 3	37	±2		10	2·5
06·01	06	17	± 2	33	±2		8·5	2·7
06·02	06	57	± 3	47	30±1	30	3	3·8
07·01	07	19	± 3	51	51±1		4	3·5
07·02	07	35	± 4	42	±2	30	3	3·8
08·01	08	08	± 0 15	48	15±0	30	10	2·5
08·02	08	48	± 2	18	±5		7·5	2·8
08·03	08	22	± 3	36	±1	30	4	3·5
08·04	08	51	± 2	53	±1		2·5	3·9
09·01	09	16	± 4	47	±1		5	3·2
09·02	09	32	± 6	39	±2		3·5	3·6
09·03	09	57	± 2	56	30±1	30	3·3	3·8
10·01	10	00	30± 0 30	43	15±1		7·5	2·8
10·02	10	50	± 3	44	15±2		3·5	3·6
10·03	10	33	± 4	56	±1		3·3	3·8
11·01	11	03	± 3	39	45±1		6	3·0
11·02	11	48	± 4	64	±3		5	3·2
11·03	11	43	± 3	44	±2		3	3·8
12·01*	12	28	25± 1 10	12	±0	20	105	−0·1
13·01	13	26	± 4	48	±3		3·5	3·6
13·02	13	40	± 2 30	38	±1	30	3	3·8
14·01	14	01	± 2	51	±2		7·5	2·8
14·02	14	59	± 3	58	±1	30	4	3·5
15·01	15	00	± 2	70	±1		9	2·6
15·02	15	29	± 5	55	±1	30	4·5	3·3
15·03	15	01	± 2	36	±3		4	3·5
16·01	16	49	± 4	7	±9		30	1·3
16·02	16	01	± 4	66	30±1		7	2·9
16·03	16	24	± 1	38	±1	30	7	2·9
16·04	16	08	± 2	40	±4		3·5	3·6
17·01	17	03	± 6	63	30±1	30	5	3·2
18·01	18	40	±10	80	±1		9·5	2·5
18·02	18	00	± 0 30	47	30±0	30	8·5	2·7
18·03	18	27	± 3 30	47	45±1		7·5	2·8
19·01	19	57	46± 0 5	40	30±	7	1350	−2·9
19·02	19	01	± 4	57	30±1		3·8	3·5
23·01	23	21	12± 10	58	32±	4	2200	−3·4

* See opposite page.

Further information on the distances of the radio stars may be obtained in two different ways from an analysis of a number of them. The first of these analyses concerns the way in which the radio stars are distributed in galactic latitude; in the second, the distribution in intensity, or apparent magnitude, is investigated.

(a) *The distribution in galactic latitude.*—The earlier parallax observations had shown that the two most intense radio stars were situated outside the solar system. If radio stars are comparatively rare bodies situated within the galaxy, it would be expected that those already observed would be appreciably concentrated towards the galactic plane. If, on the other hand, radio stars are comparatively common objects, those which have so far been observed (the most intense) are likely to be situated at distances small compared with the dimensions of the galaxy, and an isotropic distribution would be expected. An isotropic distribution would also occur if the radio stars were situated outside the galaxy, since at a wave-length of 3·7 m. the obscuration even towards the galactic centre is likely to be negligible.

In carrying out the analysis of the experimental results, it is necessary to make allowances for the variation of the overall limit of detection in different regions of the sky. This variation is due to: (*a*) the variation of the receptivity of the aerial system in different directions along the meridian, and (*b*) the confusion in the neighbourhood of the most intense sources, caused by subsidiary maxima in the East–West reception pattern of the aerial system.

The second difficulty (*b*) was overcome by omitting from the analysis areas of the sky in the neighbourhood of the two intense radio stars. The difficulty which arose because the detection sensitivity varied with declination was overcome by restricting the analysis to the area between declinations $+32°$ and $+72°$ (over which the correction factor is small) and including only those sources whose corrected intensity exceeds a given figure. This figure was chosen so that any source producing this flux and situated anywhere within the chosen area would give a measurable trace on the record; the present survey includes all radio stars within the area "brighter" than magnitude 3·6.

An effectively uniform detection sensitivity having been obtained in this way, the average number of sources per unit solid angle was computed for each of a series of strips, 10° wide in galactic latitude, situated between latitudes $-30°$ and $+90°$. The result of this analysis is shown in Fig. 5. Although the number of sources which are available for this analysis is small, it is apparent that there is no marked concentration in the galactic plane, and that within the statistical fluctuations to be expected the distribution is isotropic.

---

* Since the axis of the interferometer does not lie precisely along a horizontal East–West line, the observation of the time of transit locates a source on a line which makes a small angle to an hour-circle. For sources of small declination, where the accuracy of the declination measurement is worse than that of the Right Ascension, it is therefore possible to specify the position of a source more precisely than is indicated in the table.

The Right Ascension of the source 05·01 may thus be represented:—

$$05^h\,31^m\,37^s \pm 6^s + 0{\cdot}4\Delta^s,$$

where the declination is $22°\ 10' + \Delta'$.

The Right Ascension of the source 12·01 may be represented:—

$$12^h\,28^m\,25^s \pm 7^s + 0{\cdot}3\Delta^s,$$

where the declination is $12°\ 55' + \Delta'$.

It may therefore be concluded either that radio stars are outside the galaxy or that they are comparatively common bodies situated within the galaxy; the distances of the sources which have so far been detected must in the latter case be small compared with the dimensions of the galaxy. The possibility that the sources are outside the galaxy will be discussed in greater detail in Section 5. Additional evidence that radio stars are comparatively common bodies situated within the galaxy is provided by an analysis of their intensities in relation to the general background radiation of the galaxy, and this evidence will now be examined.

(b) *Radio stars in relation to the general background radiation.*—Early theories put forward to account for the observation of radio waves from the galaxy assumed emission from the interstellar gas (e. g. Henyey and Keenan, 1940). The subsequent observation of discrete sources of small angular diameter not only demonstrated the existence of another mechanism for the emission of intense radio waves but also suggested that this mechanism might in fact be responsible for the general background radiation; the existence of a large number of discrete sources distributed throughout the galaxy might produce an apparently diffuse background radiation when observed with aerial systems of comparatively small resolving power. The two alternative theories have been discussed in some detail in two recent survey papers (Unsöld, 1949; Ryle, 1950).

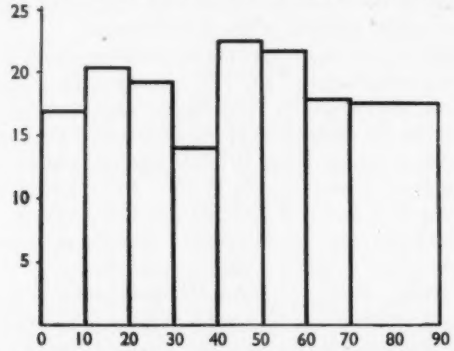

FIG. 5.—*Density of radio stars "brighter" than magnitude 3·6 plotted as a function of galactic latitude. (For latitudes 0° to 30° the average of the northern and southern strips is plotted.)*

Ordinates: Number of radio stars per steradian.
Abscissae: Galactic latitude in degrees.

Whilst the early theories of emission from the interstellar gas might have provided a satisfactory explanation for the observations of galactic radiation on wave-lengths of less than about 3 m., very great difficulties were raised by later observations on longer wave-lengths. Thus observations on 10 m. indicated a well-defined concentration near the galactic plane, and showed that even at this wave-length the galaxy must be "optically thin". The intensity of radio waves emitted by the interstellar gas would therefore be appreciably less than that emitted by a black-body radiator at the temperature of the gas. Furthermore the intensity emitted at any shorter wave-length would be a still smaller fraction of that from a black body, owing to the decrease in the "optical depth" of the interstellar gas with wave-length. Calculations based on the observed intensity

at a wave-length of 10 m. and on the observation that even at this wave-length the galaxy is "optically thin" showed that the observed intensity of the background radiation *at any wave-length* could only be accounted for by assuming a temperature of the interstellar gas of at least 10^5 deg. K. At the same time it is difficult to account theoretically for the maintenance of an interstellar temperature much greater than 10^3 deg. K., except in the neighbourhood of early-type stars (Woolley, 1947).

It must therefore be concluded that unless a considerably greater temperature is permissible for the interstellar matter, it is impossible to account for more than about 1 per cent of the observed background radiation at any wave-length, by theories based on the emission from the interstellar gas.

It is therefore important to examine, in greater detail, the possibility that the background radiation is the integrated radiation from a large number of radio stars distributed throughout the galaxy; it is suggestive that the ratio of the intensities of the most intense radio stars to that of the background radiation is of the same order of magnitude as the ratio of the visual intensities of the brightest stars to that of the total integrated starlight.

In order to investigate this possibility further an analysis has been made of the relative intensities of the 25 most intense radio stars, in relation to the integrated radiation from the Northern Hemisphere (Ryle, 1950). The results of this analysis have indicated that all the existing measurements of galactic radiation could be accounted for if there were a large number of radio stars distributed throughout the galaxy, and having an average population density of the same order of magnitude as that of the visual stars.

5. *The nature of the radio stars.*—The analysis of the previous section has suggested two possibilities which must now be examined. They are :

(*a*) The radio stars are situated outside the galaxy, and the general background radiation is due to the interstellar gas; in this case it is necessary to account for the maintenance of a very much greater temperature of the interstellar gas than is predicted by present theoretical work.

(*b*) The radio stars are situated within our galaxy with a population density which is comparable with that of visible stars.

The two alternatives will now be examined in greater detail.

(a) *Sources outside the galaxy.*—The observation of the general background radiation from the galaxy suggests that similar radiation is likely to be emitted by other spiral nebulae; this conclusion is independent of the mechanism responsible for the background radiation. Although there is some evidence (Ryle, 1949; Smith, 1950) that the intense discrete sources are of stellar dimensions, the only direct measurements of angular diameter have indicated a figure less than a few minutes of arc. It is therefore possible that certain extra-galactic nebulae might be of sufficiently small angular diameter, and of sufficient intensity to account for the present observations of "discrete" sources.

The background radiation from directions near the galactic centre produces a flux (at a wave-length of 3·7 m.) of about 10^{-20} watts m.$^{-2}$ (c./s.)$^{-1}$ (steradian)$^{-1}$. If account is taken of the angular variation of intensity as observed from the solar system, it can be shown that it is possible to deduce an effective diameter of the galaxy for radio emission. If now it is assumed that the Andromeda nebula is similar to our galaxy, the emission at a wave-length of 3·7 m. should produce a flux at the Earth of about 10^{-24} watts m.$^{-2}$ (c./s.)$^{-1}$; the effective angular diameter

of the source would be 20–30 minutes of arc. This intensity is greater than the detection limit of the present apparatus, and it might therefore be expected that on any theories of galactic radiation "discrete" sources of small angular diameter should be detected in the positions of the nearest extra-galactic nebulae.

An analysis has therefore been made in Section 6 (a) to relate the positions of the radio stars with those of the major extra-galactic nebulae. It has been found that of the five largest nebulae, two coincide with the positions of weak radio stars, while two more are sufficiently near other radio stars to suggest a relationship. Furthermore it has been found that the observed intensities of these sources are in good agreement with the values expected on the assumption that the "background radiation" emitted by other spiral nebulae is comparable with that from our own galaxy. It is therefore likely that whatever mechanism is responsible for the emission of radio waves from our own galaxy is also operative in other galaxies.

It is now important to examine the possibility that all the radio stars might be accounted for by the emission from extra-galactic nebulae. It must first be noted that the intensities of the four sources whose positions are near those of the major extra-galactic nebulae are relatively very small. (For instance, the detection of the source which coincides with the Andromeda nebula is made extremely difficult by the proximity of the intense source in Cassiopeia (23·01) which produces a flux approximately 750 times as great.)

It is therefore necessary to decide whether certain extra-galactic nebulae, which produce a very small visual emission, could produce an intensity of radio waves at the Earth some 750 times that produced by the Andromeda nebula. Although local dust obscuration might be responsible for the absence of any intense visual emission, it seems most improbable that such a condition could apply to all the major radio stars, particularly since many of them are situated in regions where the general obscuration is small. At the same time the emission of radio waves of this intensity by an extra-galactic nebula appears to present very great theoretical difficulties; the observations carried out on the two most intense radio stars have indicated that their intensities, at a wave-length of 3·7 m., are of the order of $2 \cdot 10^{-22}$ watts m.$^{-2}$ (c./s.)$^{-1}$, whilst their angular diameters are less than 3 minutes of arc. If the radiation were due to the emission from the interstellar gas of the nebula it would be necessary to postulate an average temperature of at least 10^8 deg. K.; the maintenance of this temperature appears to present insuperable difficulties, even without the cooling mechanism described by Menzel and Aller (1941).

It would therefore only be possible to account for the majority of the radio stars in terms of the emission from sources outside the galaxy, on the assumption of some new type of body which produces little visible radiation but very intense radio waves. The mechanisms required for such a body seem to present far greater difficulties than those involved in assuming a special body situated at a relatively much smaller distance, within our own galaxy. As has already been shown, the presence of such bodies within our galaxy would not only provide a simpler explanation for the radio stars but would at the same time account for the general background radiation from the galaxy. The presence of similar bodies in the other major extra-galactic nebulae would in the same way account for their observed radio emission.

(b) *Sources within the galaxy.*—The second possibility, that the sources are inside our galaxy, will now be examined.

Several different theories have been proposed concerning the nature of the radio stars. Ryle (1949) suggested that they were a new type of stellar body in which the radio emission was very much greater than that of the Sun, whilst the visual emission was small. This condition could arise if the envelope of a star were maintained at a very great temperature, and he suggested that certain stars, whose surface temperature was small but which had a large magnetic field and rotational velocity, could account for the observed intensity of radio emission.

Bolton, Stanley and Slee (1949), on the other hand, have noted that one of the radio stars is near the position of the Crab nebula, which is thought to be the shell of a past supernova, while two others are near unresolved nebulae. Unsöld (1949) has suggested that the basic mechanism may be analogous to that of the emission from sunspots, and suggests a possible relation to late-type stars.

Now that a considerably greater number of radio stars have been located, it is possible to make a more detailed analysis of these and other possibilities, and the new experimental evidence will now be examined from this point of view.

6. *Identification of the radio stars with visual bodies.*—In the following sections attempts will be made to relate the radio stars to various types of visual body; this will be done by comparing the positions of the radio stars with those of the outstanding examples of each type of visual body.

In carrying out an analysis of this type, it is important to remember that the accuracy with which the positions of most of the radio stars may be found is poor; it is therefore likely that the positions of visual bodies will occasionally fall within the limits of the position of a radio star even if there is no genuine relationship. It is therefore important to calculate the probability of random coincidences in each analysis, in order to determine whether any observed correlation can be regarded as significant.

The survey has been restricted to the region between declinations $+12°$ and $+82°$, an area which covers a solid angle of 4·9 steradians. The total solid angle occupied by the limits of accuracy of all the radio stars which have so far been observed in this area is 0·05 steradians; there is therefore a probability of 1 in 100 that a randomly chosen position will coincide with one of the radio stars. If a total of n visual bodies is examined in any particular analysis, it is therefore likely that about $n/100$ coincidences will be observed even if there is no relation between the visual bodies and the radio stars. In each analysis the number of observed coincidences must therefore be related to the figure for random coincidences in order to determine whether there is a genuine relationship.

(i) *Extra-galactic nebulae.*—The positions of 309 extra-galactic nebulae within the selected area were compared with those of the radio stars, and nine coincidences were found. This number does not greatly exceed the expected figure for random coincidences, but when the analysis was restricted to the five major extra-galactic nebulae a more significant result was obtained; two of the radio sources were found to coincide, while two others each have one coordinate in good agreement, with an error in the other coordinate which is only slightly greater than the error deduced from the record. All four sources are of extremely small radio intensity and, as has already been shown, it is difficult to make accurate allowance for the presence of other undetectable sources when deducing the errors of observation of weak sources. The result of this analysis is therefore regarded as very suggestive.

The five major extra-galactic nebulae in the selected area are listed in Table II, together with the radio sources which appear to be associated with them.

Further confirmation of this association has been provided by an estimate of the expected intensities from the above nebulae. On the assumption that their characteristics are identical with those of our own galaxy, it is possible to estimate the intensity which each would produce at the Earth from the visual observations of their angular diameters. In order to determine the intensity which would be recorded by the present apparatus, it is also necessary to take account of the fact that such a source can no longer be regarded as small compared with the angular separation of the maxima of the interference pattern. The expected intensities, derived in this way, are found to be of the same order of magnitude as those observed experimentally. (A direct measurement of the angular diameters of these particular radio sources would, of course, provide powerful independent evidence for their association with extra-galactic nebulae; unfortunately it has not yet been possible to make measurements of angular diameter on sources as weak as these four.)

TABLE II

Nebula	Position		Radio Source	Position		Magnitude
	h m	° ′		h m	° °	
M31 (Andromeda)	00 40	41 0	00·01	00 42±6	38±5	3·5
M33	01 31	30 24	01·01	01 25±5	30±3	2·8
M101	14 01	54 36	14·01	14 01±2	51±2	2·8
M81	09 52	69 19	None observed			
M51	13 28	47 28	13·01	13 26±4	48±3	3·6

There is no significant statistical evidence relating more distant nebulae with other radio stars and indeed it has already been shown that there are strong theoretical reasons for supposing that all the radio stars so far observed, except those listed in Table II, are situated within the galaxy.

(ii) The remaining analysis has therefore been based on the assumption that the majority of radio stars are situated within the galaxy. Although there is some evidence (Ryle, 1949; Smith, 1950) that the sources are of stellar dimensions, the analysis has not been restricted to correlations with different types of star but has been extended to include various galactic nebulae and diffuse bodies.

(a) *Identification with stars.*—The positions of the radio stars were first compared with those of visual stars brighter than magnitude 4·0 and lying within the selected area (Schlesinger, 1930). It was found that not one of the 146 visual stars included in this category fell within the limits of accuracy of the position of a radio star. The visual stars examined included the brightest examples of most of the main spectral types (9 O-type, 45 B, 20 A, 19 F, 39 G, 8 K and 6 M).

Attempts to identify individual radio stars with unusual but fainter visual stars were equally unsuccessful; the areas enclosed by the limits of error of the two most intense radio stars (23·01 and 19·01) contain no visual star brighter than 11th magnitude. The positions of other radio stars are not known with comparable accuracy, but it was found that the probability of finding a visual star of given magnitude within the area of a radio source was not significantly different from that of finding one in an equal area chosen at random in a neighbouring region of the sky.

Since the present observations suggest that the radio stars may be relatively abundant, it is likely that those which have been observed at the present time

are situated near to the solar system. If the radio sources are stars in which the ratio of radio emission to visual emission is very much greater than that of the Sun (due, perhaps, to the maintenance of a large temperature in the envelope with a comparatively small photospheric temperature), it is possible that the most intense radio stars might be identified with some of the nearest visual stars, without regard to their apparent visual magnitude. An analysis was therefore made of the positions of the radio stars and those of the 90 nearest stars falling within the selected area (Kuiper, 1942). One of these stars (Wolf 424a) falls within the limits of error of the position of a radio star, but the relation is not significant.

A similar analysis was also made for stars having a large proper motion (Luyten and Ebbighausen, 1936, and elsewhere). It was found that there was no correlation down to 10th magnitude for stars having $\mu > 0''{\cdot}1$ per annum. For the two most intense radio sources, stars having $\mu > 0''{\cdot}05$ per annum were examined, and no correlation was found down to 14th magnitude.

(b) *Novae and supernovae.*—The positions of 21 novae in the selected area were examined (Norton's star atlas); no correlation with radio stars was found.

The proximity of the radio source in Taurus (05·01) to the Crab nebula, which is thought to be the shell of the supernova of 1054, has been noted by Bolton, Stanley and Slee (1949). Although the analysis of Section 4 has already shown that an origin in such a rare body as a supernova is unlikely, the positions of the two other outstanding supernovae in the selected area (areas 1572 and 1604) were also examined; no radio star was found near either position. It therefore seems unlikely that radio stars are related to novae or supernovae.

(c) *Galactic nebulae and clusters.*—The positions of 38 planetary nebulae and 29 diffuse nebulosities in the selected area (*Publications of the Lick Observatory* (1918), Vol. 13) were compared with those of the radio stars, but in neither case were any coincidences found. Thirty-one star clusters were also examined, and again no correlation was found.

7. *Conclusions.*—An interferometer of large resolving power has been used to find the positions of 50 radio stars (covering a range of 7·3 magnitudes) in the Northern Hemisphere. The positions of the weaker radio stars cannot be determined with very great precision, but the two most intense ones can be located with an accuracy of about 3 minutes of arc.

The observation of a considerable number of these bodies has made it possible to carry out various analytical investigations in an attempt to deduce their nature; these investigations were not possible with the small number of sources which were known previously.

It has been found that the radio stars, unlike the general background radiation, show no detectable concentration in the galactic plane. It is therefore concluded either that they are situated at distances small compared with the dimensions of the galaxy, or that they are outside the galaxy.

On the supposition that other spiral nebulae produce a total "background" radiation comparable with that of our own galaxy, it was possible that the radio stars might represent nothing more than the background radiation of extra-galactic nebulae, since all except the nearest are of sufficiently small angular diameter to be unresolved by the present apparatus. An analysis has shown that several of the weakest radio sources coincide with the positions of major

extra-galactic nebulae, and that their intensities are in good agreement with those predicted on the hypothesis mentioned above. It may therefore be concluded that whatever mechanism is responsible for the background radiation in our own galaxy, also occurs in other spiral nebulae.

It does not, however, seem possible to suppose that the majority of the observed radio stars are outside our galaxy, both because of the theoretical difficulties encountered in attempting to explain the very great intensities of the more intense radio stars and because of the absence of correlation with other extra-galactic nebulae.

It is therefore concluded that most of the radio stars are situated within the galaxy.

It has already been shown (Ryle, 1950) that the presence of a large number of such bodies distributed throughout our own galaxy would not only provide a satisfactory explanation for the remainder of the observations of radio stars but would at the same time account for the general background radiation from the galaxy; the poor resolving power of the present apparatus would only make it possible to resolve those sources which were nearest, and which would therefore be distributed isotropically, whereas the distribution of the unresolved background radiation would, as is found experimentally, conform closely to the shape of the galaxy. The great difficulties involved in accounting for more than about 1 per cent of the background radiation on theories based on the emission from the interstellar gas are in themselves a powerful argument in favour of the existence of numerous isolated radio sources distributed throughout the galaxy.

In order to obtain further evidence concerning the nature of the radio stars, attempts have been made to identify them with various types of stellar body. No correlation was found with either the brightest or the nearest visual stars or with novae.

Although there is some evidence that the sources are of stellar dimensions, attempts were also made to identify them with various types of diffuse body within the galaxy, and with planetary nebulae and star clusters, but no significant correlation was found with any such type of body.

In the absence of further evidence it is therefore concluded that the radio stars represent a hitherto unobserved type of stellar body, in which a very intense radio emission is associated with a very small visual intensity. One possible mechanism for the emission from such a body has been suggested in a previous communication (Ryle, 1949).

We are indebted to Mr D. E. Blackwell and Mr M. W. Ovenden of the Solar Physics Observatory for their assistance in providing us with various astronomical data used in the analyses.

Figs. 1, 2 and 3 appeared in a recent paper published in "Reports of Progress in Physics" and we are grateful to the Council of the Physical Society for permission to use them here.

This work was carried out as part of a programme of radio research at the Cavendish Laboratory, supported by a grant from the Department of Scientific and Industrial Research.

Cavendish Laboratory,
Cambridge:
1950 *August* 11.

References

Bolton, J. G. and Stanley, G. J., 1948, *Nature*, **161**, 312.
Bolton, J. G., Stanley, G. J. and Slee, O. B., 1949, *Nature*, **164**, 101.
Henyey, L. G. and Keenan, P. C., 1940, *Ap. J.*, **91**, 625.
Hey, J. S., Parsons, S. J. and Phillips, J. W., 1946, *Nature*, **158**, 234.
Kuiper, G. P., 1942, *Ap. J.*, **95**, 201.
Luyten, W. J. and Ebbighausen, E. G., 1936, *Astr. J.*, **45**, 188.
Menzel, D. H. and Aller, L. H., 1941, *Ap. J.*, **94**, 30.
Ryle, M., 1949, *Proc. Phys. Soc.*, A, **62**, 491.
Ryle, M., 1950, *Rep. Prog. Phys.*, **13**, 184.
Ryle, M. and Hewish A., 1950, *M.N.*, **110**, 381.
Ryle, M. and Smith, F. G., 1948, *Nature*, **162**, 462.
Schlesinger, F., 1930, *Catalogue of Bright Stars*, Yale University Observatory.
Smith, F. G., 1950, *Nature*, **165**, 422.
Unsöld, A., 1949, *Zeit. f. Astrophys.*, **26**, 176.
Woolley, R. v. d. R., 1947, *M.N.*, **107**, 308.

SOME SOUTHERN STARS INVOLVED IN NEBULOSITY

A. D. Thackeray

(Received 1950 September 11)

Summary

An outer shell of nebulosity surrounding Eta Carinae is described. AG Carinae, HD 138403 and Co.D $-46°$ 11816 are found to be surrounded by nebulous disks or shells with [*O* III] weak or absent. These three stars all have Harvard classification of P Cygni type and resemble planetaries of low excitation. The spectrum of HD 138403 has some affinity to that of the nebulosity round T Tauri. Diffuse nebulosities near HD 92207 and CPD $-59°$ 2661 in the neighbourhood of Eta Carinae are also described. A complex field of bright and dark nebulosity at $11^h\ 36^m\ -63°07'$ indicates close interaction between stars and nebulosity. The small dark areas are highly irregular in outline and also appear to lie close to stars.

This paper describes observations with the Radcliffe reflector of a number of cases of stars involved in nebulosity. Some, of regular form, might be classed as planetaries, but they appear to be of unusually low excitation, while others are irregular and suggest the interaction of stars with nebulosity through which they happen to be passing. None of them, apart from Eta Carinae, seem to have been reported before.

Eta Carinae.—The very complex gaseous halo surrounding this star has been described by Gaviola (**1**) and by the writer (**2**) in a preliminary note on the basis of early observations with the Radcliffe reflector. In his latest paper Gaviola has given an excellent description of the complex inner structures of the halo. The more detailed photographs obtained with the Radcliffe reflector since 1948 July confirm this structure, and in this paper it is only proposed to consider the outer structure where the Cordoba photographs differ in some respects. In particular, Gaviola apparently doubts the existence of an outer elliptical shell (see his Fig. 3(*a*)* from an Ilford Ortho Process plate). The apparent discrepancy can, in the writer's opinion, be entirely attributed to the use of an emulsion insensitive to the red region, in particular to *Hα*. The accompanying plate shows three photographs of Eta Carinae as follows:

Plate	Date	Emulsion	Filter	Exp. time	Region
12 (*a*)	1949 June 23	Ilf. Astra 8	W 25	30 m.	*Hα*
12 (*b*)	1950 June 18	Kod. 103 aE	W 12	3	*Hα*
12 (*c*)	1950 May 6	Kod. 103 J	W 59	15	N1, N2

The lighter of the two red pictures, 12(*a*), shows the two brightest portions of the elliptical shell (formations which Gaviola denotes by *k* and *l*) clearly joined by a fainter portion of the same shell in PA 200°–220°. Moreover, unlike Gaviola's isophotes (his Fig. 5), both formations *k* and *l* are separated from the inner structure by minima of intensity. The formation *m* (PA 25°) shows an

* Note that Gaviola's reproductions are reversed left and right compared with those in this paper; the latter are all shown with north at top and preceding to *right*, as seen in the southern sky.

extension widening towards the star which is probably to be identified with Gaviola's (Fig. 2*a*) "radial cylindrical column"; however, the accompanying Plate 12 (*a*) shows that in red light at least it is also separated from the inner structure by a minimum of intensity.

Plate 12 (*b*), another red picture of much greater density, shows the outer shell blacked out into an oval mass with major axis approximately in PA 125°–305°, and numerous condensations lying still further out. That these condensations are *Hα* emission patches rather than stars is rendered certain, partly on account of their diffuseness, but also on comparison with Plate 12 (*c*), a green photograph isolating N1, N2 in which the condensations fail entirely to appear despite the stellar images being generally much denser. Twenty such patches have been measured for position at distances ranging from 7″ to 23″ of arc from the central star. Gaviola has found evidence that the structure at distances up to 7″ of arc is expanding at a rate which suggests that it is associated with the brightening of Eta Carinae in 1843. If the condensations appearing at much greater distances in Plate 12 (*b*) are associated with the same outburst, then they must be expanding at much greater velocities; they will therefore eventually provide a more sensitive criterion for measurement of the expansion. On the other hand, five of the most distant condensations (including three very bright ones) lie close to a star in approximate position $d = 20''$, PA 118°, relative to Eta, and it seems probable that some of these condensations are connected with the fainter star rather than with Eta itself.

Plate 12 (*c*) is more or less comparable with Gaviola's Fig. 3(*a*) in showing the halo around Eta roughly circularly symmetrical, in strong contrast to the elongated red shell of Plate 12 (*b*). It is not clear to what extent this symmetry should be attributed to diffusion from the bright stellar image, but it may be regarded as established that outside of a circle 10″ of arc radius from Eta—about the limit of Gaviola's isophotes—the green radiation of the star's nebulosity is very weak and merges with the general nebulosity of NGC 3372.

The example of the Crab nebula shows that in addition to *Hα* the [*N* II] pair 6548, 6584 may make a significant contribution to the red halo of Eta Carinae. This region of the spectrum cannot easily be reached with the Newtonian spectrograph and attempts to settle the question have not met with success owing to insensitivity of the available film. However, Spencer Jones (**3**) recorded only *Hα* without any [*N* II].

AG Carinae ($10^h\ 54^m.2$ −60° 11′; 1950).—This star * appeared near the edge of a survey plate of the region of NGC 3372. The existence of a nebulous shell surrounding the star was immediately confirmed on plates centred on the star (1950 April 16). The shell appears as an elliptical ring, 39 × 30″ in outer diameter, with major axis in PA about 150°; see Plate 12 (*d*). The ring is about 5″ of arc wide. From PA 30 to 75° a fairly straight nebulous mass, about 20″ long, appears tangential to the ring in PA 80°. Within the main ring on the preceding side of the central star there are two other straightish streaks about 9″ from the star. The ring, which is not uniform in intensity, gives the impression of a helix viewed almost along the axis. However, the true form may be an irregularly illuminated spheroidal disk, for faint nebulosity can be seen between the ring and the star; in particular, two faint curved wisps extend from the ring to the star joining the latter in approximate PA 90 and 120°. The nebulosity can

* Classified as P Cygni type by Miss A. J. Cannon, *H.A.*, **76**, No. 3, 1916, Table III.

be seen visually with the 74-inch reflector, despite the brightness of the central star, and appears decidedly red. However, blue photographs also show it well.

A 30-minute exposure with the Newtonian spectrograph, isolating the southern portion of the ring, shows $H\beta$ and $H\gamma$ faintly on a still fainter continuous spectrum, possibly due to overlapping light from the star. No N1, N2, 3727 or other emission lines were detected. The star and envelope are reminiscent of BD $+30^\circ 3639$ (Campbell's hydrogen envelope star); but regarded as a planetary nebula the system is remarkable for the brightness and variability of the central star (6·5–8·0), which must account partly for the failure of previous visual or photographic observations to exhibit the surrounding ring.

Although it is quite possible that the presence of the nebulous ring might affect magnitude estimates on dense images of small-scale photographs even if the photographs were made on blue-sensitive plates, it does not seem likely that the observed variations in brightness can be ascribed to this cause. Independent evidence from Harvard (**4**) and Johannesburg (**5**) plates agree that the object was unusually bright in 1911. It is more likely that the amplitude of variations is to be ascribed to variations of the central star than of the surrounding shell. Observations of the relative brightness of shell and star during and after a bright maximum would be especially interesting.

AG Carinae appears to be a remarkable object in combining the properties of a low-excitation planetary nebula and a P Cygni type star with slow irregular variations in light. In this respect it holds an interesting place in Beals' (**6**) scheme linking Wolf-Rayet stars with novae, P Cygni and α Cygni stars.

It should be remembered however that Miss Cannon's classification of the spectrum as of P Cygni type was based on the strength of the hydrogen emission and absence of N1, N2. Nowadays the P Cygni characteristic connotes rather an emission line with sharp violet absorption suggestive of ejection of matter on a gentle scale compared with the usual nova. Whether the emission spectrum of AG Carinae has this characteristic cannot unfortunately be determined with equipment at present available at the Radcliffe Observatory.

HD 138403 ($15^h\,32^m{\cdot}3\;-71^\circ\,45'$; 1950. $9^m{\cdot}7$ Pec).—This star was examined on account of its inclusion, with AG Carinae, in *H.A.*, **76**, No. 3, 1916, Table III, Miss A. J. Cannon's list of P Cygni objects. Visual examination on 1950 April 28 showed the star to be surrounded by a circular disk, about 5″ of arc in diameter, of distinctly reddish hue, thus resembling Campbell's hydrogen envelope star. Red exposures of 30 and 10 seconds on Kodak O–E plates through Wratten 25 filter showed disks which had measured diameters of 6″·3 and 4″·9 respectively. Heavier exposures showed no faint extensions. A spectrum obtained on 1950 May 29 showed the hydrogen lines bright and strong from $H\beta$ to $H3835$ (and possibly two other Balmer lines) superposed on a strong continuous spectrum. The [*O* III] pair 5007, 4959 does not appear, but [*O* II] 3727 is strong—intermediate in intensity between $H\gamma$ and $H\delta$—despite absorption in the glass prisms. The only other emission lines detected are the [*S* II] pair 4068, 4076, perhaps stronger than $H3835$.

The spectrum bears some resemblance to the nebulosity surrounding T Tauri in which Herbig (**7**) has found [*O* II] and [*S* II] but not [*O* III]. T Tauri is classed as dG5; in the case of HD 138403 it is not possible to say from the available spectra whether the star is of such late type, but the nebulosity must be

Scale 1″·5 = 1 mm. N. prec. = top right.

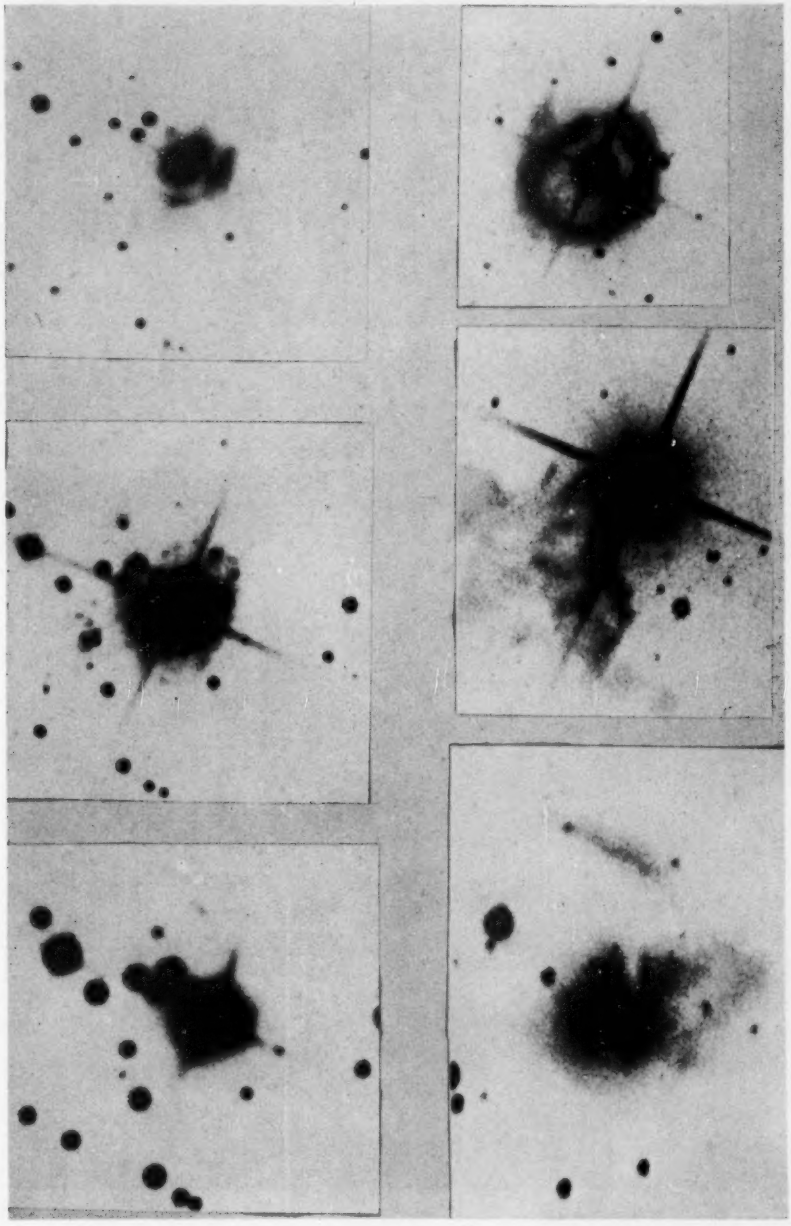

(*a*), (*b*) η Carinae, Hα
(*c*) η Carinae, N_1, N_2
(*d*) AG Carinae, Hα
(*e*) HD. 92207, Hα
(*f*) CPD —59° 2661, Hα

A. D. Thackeray, Some Southern Stars involved in Nebulosity.

Nebulosity near HD. 92207.
Scale 7′·5 = 1 mm.
(N. at top. Prec. to right).

A. D. Thackeray, Some Southern Stars involved in Nebulosity.

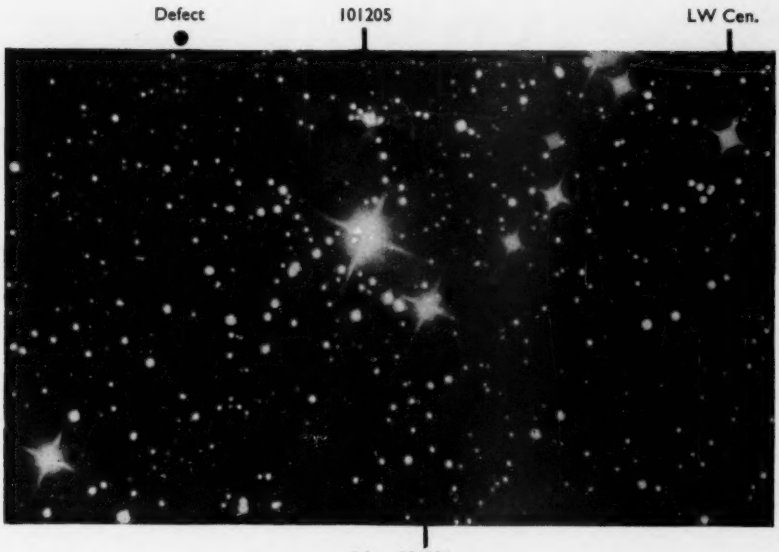

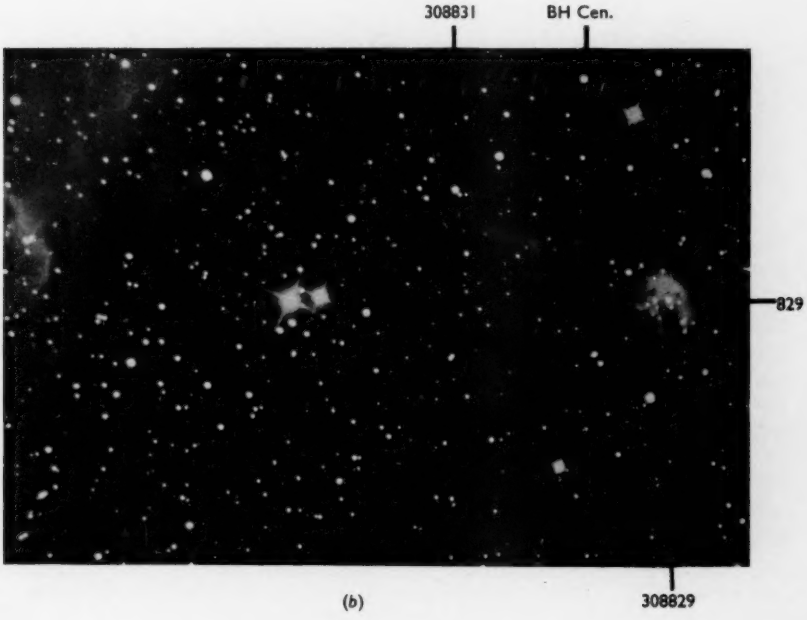

Nebulosity at $11^h\ 36^m$, $-63°\ 7'$
Scale: 5′·8 = 1 mm.

A. D. Thackeray, Some Southern Stars involved in Nebulosity.

regarded as of low excitation in view of the apparently complete absence of the nebulium pair.

Co.D −46° 11816 ($17^h\ 42^m{\cdot}0$ −46° 04′; 1950. 10^m).—This star was also examined on account of its inclusion in *H.A.*, **76,** No. 3, Table III. On 1950 May 15 visual examination showed it to be at the centre of a nebulous envelope without however the red hue of HD 138403. Photographs show a disk brightening towards the edge to form an almost circular ring about 9″·6 in outer diameter and 1″·7 thick at the edge. The ring is not quite uniformly intense all round. The field of this star and of HD 138403 (from red plates) is shown in Fig. 1.

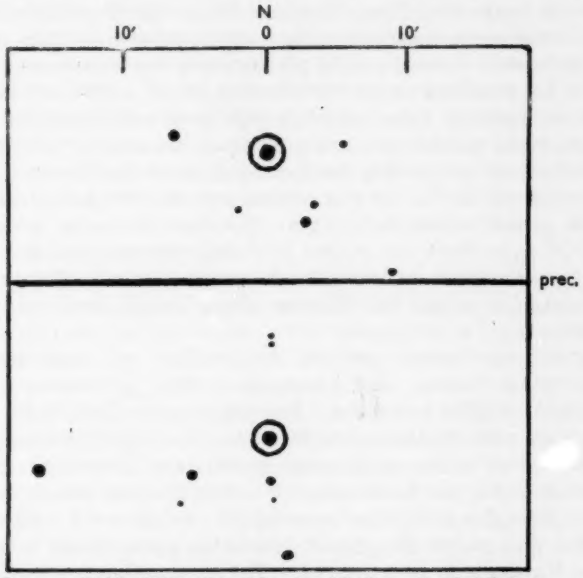

FIG. 1.—*Fields of HD* 138403 (*above*) *and Co.D* −46° 11816 (*below*).

The spectrum resembles that of a planetary nebula except that the hydrogen lines are strong relative to the [*O* III] pair 5007, 4959. The relative intensity $H\beta$: N1 : N2 is estimated from a Newtonian spectrogram to be 10:8:3. [*O* II] 3727 appears as strong as $H\beta$ despite glass absorption.* A very faint emission feature appears at 4363 which is probably to be attributed to [*O* III]. No lines of *He* have been detected but the film contains defects which hamper certain identification of faint features. The continuous spectrum of the star is strong with no detectable absorption lines; its strength relative to the nebulosity probably accounts for the failure to detect N1, N2 hitherto.

The object should be regarded as a planetary nebula, to be added to the list of those with diameters greater than 8″ of arc (**8**). But it is probably of lower excitation than any in Wyse's list on account of the nebulium lines being weaker than $H\beta$.

* Miss A. J. Cannon (*H.C.*, No. 224, 1911) later found [*O* II] 3727 without N1, N2 and Miss D. Hoffleit (*H.B.*, No. 892, 1933) therefore suggested that the star might be surrounded by a nebula.

Other Stars in H.A., **76,** *No.* 3, 1916, *Table III.*—CPD $-59°$ 2855 (GG Carinae).—This star is in the same field as AG Carinae. Visual examination and direct photographs showed no signs of surrounding nebulosity. The star has been classed as an eclipsing binary (9·47–9·95) with a period of 62 days. Its spectrum (Be) would be well worth observing through eclipses.

Co.D $-30°$ 15469.—No nebulosity found.

P Cygni and BD $+11°$ 3673.—As a formality, these two well-known northern objects were examined visually in conditions of poor seeing but no nebulosity was found.

The remaining four stars in *H.A.*, **76,** No. 3, Table III, including S Doradus, belong to the Large Magellanic Cloud and fall outside the scope of this paper.

Stars involved in nebulosity within diffuse nebulae.—While the foregoing objects show some resemblance to planetaries of low excitation, the remaining objects to be described under this heading are of a different nature. They comprise examples of stars intimately associated with external nebulosity, the association arising possibly as a result of chance encounter. We can be confident that the nebulosity surrounding Eta Carinae originated in the star itself and there is no direct proof, as Gaviola has pointed out, that the star is actually located within the general nebula NGC 3372. But there are many examples of stars within NGC 3372 where the evident interaction between star and nebulosity is such as to place them certainly at the same distance. Two are shown in Plate 12 (*e*), (*f*), while AG Carinae (Plate 12 (*d*)) lies only just outside NGC 3372.

HD 92207.—($10^h 35^m.5$ $-58°$ 28′; 1950).—This 5th mag. star (A2p) lies about 80′ Np Eta Carinae. Bok's isophotes of NGC 3372 show it to be involved in an "island" of faint nebulosity. Red photographs (Kodak 103 aE + Wratten 25 filter) taken with the Radcliffe reflector reveal a magnificent semi-circular arc with emission rim ending to the south at HD 92207 (Plate 13). Details of the nebulosity near the star itself, where it is brightest, are shown in Plate 12 (*e*). Exposures through a green filter isolating N1, N2 show the emission rim to be less marked than on the $H\alpha$ plates*, but in the portion close to HD 92207 the ratio N1 : $H\alpha$ seems to be enhanced. The observations are consistent with a higher degree of ionization close to the star than along the emission rim. HD 92207 is clearly a supergiant, since a note in the HD Catalogue points out the resemblance of the spectrum to that of α Cygni. It is worthy of note that the 8th mag. star 7′ north of 92207 which is not far from the centre of the semi-circular emission rim is classified by Harvard as type B (HD 92206).

CPD $-59°$ 2661.—($10^h 43^m.9$ $-59°$ 41′; 1950).—This 10th mag. star is well within NGC 3372 but the nebulosity shows a very marked brightening in its immediate neighbourhood, to an extent which probably must affect estimates of magnitude on small-scale photographs. (See Plate 12 (*f*): this photograph was centred on another part of the nebula and the images consequently show coma.) The two most remarkable features are the dark lane pointing north from the preceding side of the star, and the detached bar of nebulosity lying due north of the star.

A spectrum of the star and nebulosity (not trailed) shows a narrow strong continuous spectrum with absorption near $H\epsilon$ as the only recognizable

* In confirmation of the effect found spectrophotometrically in the emission rims of M16, etc., *M.N.*, **110,** 343, 1950.

discontinuity. *Hβ* and possibly N1 are visible as faint emission crossing the spectrum. The star is not classified in the Henry Draper Extension.

HD 101191, *HDE* 308829, 308831.—($11^h\ 36^m{\cdot}6 - 63°\ 07'$; 1950).—This field (see Chart 148, Henry Draper Extension, *H.A.*, **112**) was investigated on account of faint nebulosity being visible on the Franklin-Adams Charts. *Hα* photographs exhibit most interesting complex patterns of bright and dark nebulosity. Near the right-hand edge of Plate 3 (*b*) appears the star HDE 308829 surrounded by bright curved wisps, with a straight dark lane on the southern side. Within this dark lane is a very narrow bright streak pointing directly at the star. The curved wisps diffuse out towards the east and north, and join again around the star HDE 308831. In the area between these two stars there is a rich mass of faint wisps curving out from a central starless area. The impression gained from a careful examination of the photographs is that of interstellar nebulosity being distorted into a streamlined pattern and attracted by passing stars. Near the upper left edge of Plate 14 (*b*) is another faint star (not classified in HDE) with two curved arcs of nebulosity meeting the star at opposite points.

The HDE classifications of the two stars 308829, 308831 are B8, B9 respectively. A 25-minute Newtonian spectrogram of HDE 308829 with the Radcliffe reflector fails to add anything to this classification and to record any sign of the surrounding nebulosity.

Plate 14 (*a*) centred on the bright star HD 101205 (B2), only 7'·5 N.W. of Plate 14 (*b*), shows some highly irregular dark nebulae sharply silhouetted against the general background of nebulosity. The irregularity of their outlines does not permit classification as "globules" in the sense used by Bok and Reilly (**9**). The largest, 1'·4 N.W. of 101205, also shows some signs of bright nebulosity crossing the dark area. This important fact renders it likely that the dark nebulae are partly enmeshed within the bright nebulosity rather than that they happen to be projected against it and to lie much nearer to the Earth. 1'·4 S.W. of 101205 is the 8th mag. star HD 101191 (B2) with some six small dark nebulae on the west side; most of them exhibit an elongated shape pointing roughly towards 101205. Of the many dark patches visible on Plate 14 (*a*), only one is a plate defect and this is indicated on the upper left edge; all the others have been confirmed on duplicate plates.

Of special interest in connection with this field is the fact that it contains two eclipsing variables of *β* Lyrae type. LW Centauri, period 1·0025 days, is in the right-hand top corner of Plate 14 (*a*); BH Centauri, period 0·7915 days, is near the top right-hand corner of Plate 14 (*b*).

Conclusion.—The objects described in this paper form a very small sample of a heterogeneous group. Beals' scheme links together a number of objects in which matter is being ejected from a central star. There is no clear indication that objects such as those illustrated in Plates 13 and 14 (*b*) can be incorporated in such a scheme, and it would be premature to attempt a general synthesis. The results are collected together in this paper merely as descriptions of new instances of stars surrounded by nebulosity without enquiry into the question of how the association came about. It is hoped that further observations of the numerous examples of such associations to be found in the Magellanic Clouds may throw fresh light on the problem. However, in dealing with the Magellanic Clouds there will be a stronger tendency to favour intrinsically bright objects than in observing galactic objects.

I am indebted to Dr R. H. Stoy and to Dr D. S. Evans for reading the manuscript and for offering some helpful comments.

Note added in proof.—Spectra of AG Carinae taken with the Radcliffe Cassegrain spectrograph are now available (1951 April). They show that the hydrogen emission is indeed accompanied by violet absorption as in the typical P Cygni spectrum, and on one plate at least the same phenomenon is apparent with some lines due to *He* I. The spectrum appears to be variable.

Radcliffe Observatory,
Pretoria :
1950 *August* 20.

References

(1) E. Gaviola, *Revista Astronomica*, **18,** 252, 1946; *Nature*, **158,** 403, 1946; *Ap. J.*, **111,** 408, 1950.
(2) A. D. Thackeray, *The Observatory*, **69,** 31, 1949. (The writer regrets that he overlooked the publications of Gaviola in 1946 listed above.)
(3) H. Spencer Jones, *M.N.*, **91,** 794, 1931.
(4) N. K. Greenstein, *Harvard Bulletin*, No. 908, 1938, where the irregular variations during many years are plotted.
(5) R. Innes, *Union Obs. Circ.*, **1,** 203, 1915.
(6) C. S. Beals, "Novae and White Dwarfs", *Colloque International d'Astrophysique*, Paris, **1,** 109, 1939.
(7) G. H. Herbig, *Ap. J.*, **111,** 11, 1950.
(8) D. S. Evans and A. D. Thackeray, *M.N.*, **110,** 429, 1950.
(9) A. J. Bok and E. F. Reilly, *Ap. J.*, **105,** 255, 1947.

MAGNITUDES OF BRIGHT STARS IN THE E REGIONS OBSERVED BY THE FABRY METHOD

A. W. J. Cousins

(Communicated by H.M. Astronomer)

(Received 1950 November 9)

Summary

This paper describes the Fabry photometer attached to the Cape Astrographic Telescope and its use to determine photographic, photovisual and " blue " magnitudes of the brighter stars in the Harvard E Regions. 258 Pg, 209 Pv and 66 blue magnitudes have been determined with a standard error that does not normally exceed $\pm 0^m.007$. The scale was fixed by means of rotating sectors. Most of the stars are brighter than 8·3 Pg or 7·5 Pv. The systematic errors affecting the method are carefully discussed and their effect found to be less than 0·01 mag. The accidental errors are analysed and the standard error of a single observation is found to be $\pm 0^m.01$, excluding the effect of the sky. This is closely approached on the best nights.

The Fabry magnitudes have been compared with one another (Pg and blue) and with magnitudes obtained with the Cape Photometric Cameras. The Fabry colours have been compared with colours measured photoelectrically. The colour corrections are linear. The standard deviations are $\pm 0^m.013$, $\pm 0^m.025$ and $\pm 0^m.033$ for the magnitudes and $\pm 0^m.028$ for the colours. The corresponding external errors are $\pm 0^m.009$, $\pm 0^m.017$, $\pm 0^m.024$ and $\pm 0^m.024$. It is concluded that standard magnitudes should be determined with a precision of at least $\pm 0^m.02$ but that there is not much to be gained by pressing the accuracy beyond $\pm 0^m.01$. A final section discusses the relative merits of the photoelectric and Fabry methods.

Introduction.—The potentialities of the Fabry method for stellar photometry had already been demonstrated* when it was decided to adopt the method at the Cape Observatory, where the method has been made more effective by the introduction of rotating sectors. These serve as neutral filters to reduce the light of the stars by accurately known amounts and so limit the range in photographic density without any change in exposure time. The magnitude scale is no longer primarily dependent on the plate calibration curve, but on the constants of the rotating sectors.

The use of rotating sectors in photographic photometry has been questioned because of the well-known reciprocity failure of photographic emulsions, but experience has shown that rotating sectors give reliable results provided the speed of rotation is sufficiently high.

The Fabry method has several advantages over in-focus methods of stellar photometry. The images are large and uniform and their structure is virtually unaffected by seeing conditions, by small guiding errors or by the colours of the stars. The plates can be calibrated with a sensitometer, and if the light from the brighter stars is reduced by means of rotating sectors, the density of the

* H. Grouiller, *Annales d'Astrophysique*, **2**, 418, 1939. E. G. Williams and H. Knox-Shaw, *M.N.*, **102**, 226, 1942. R. O. Redman, *M.N.*, **105**, 212, 1945. A. W. J. Cousins, *M.N.*, **103**, 154, 1943.

photographic images can be kept within a limited range on the steep part of the calibration curve.

The Fabry method is very suitable for setting up a magnitude scale because the latter is fixed by the constants of the rotating sectors and the sensitometer, both of which are dependent on geometrical measurements alone. The images vary so little in structure and density that there should be no risk of a change of colour equation with magnitude. Moreover, as the stars are observed individually, there are no complications due to distance corrections.

This paper gives an account of the observations that have been made with a Fabry photometer attached to the 13-inch Astrographic Refractor to determine the magnitudes of the brighter stars in the Harvard Standard (E) Regions at $-45°$ declination. Three programmes provide photographic, photovisual and "blue" magnitudes. These latter are on the colour system of the Cape Bright Star * Programme which was started in 1945 and aims at providing accurate photographic magnitudes for all stars south of the Equator whose H.R. magnitudes are brighter than 5·0.

The photographic programme was commenced in 1947 to provide magnitudes for a sufficient number of stars to define the scale above the eighth magnitude and to include all stars brighter than 7·0 in an area 6° by 6° centred on each E region. Stars above $6^{m}\cdot8$ are too bright to be measured satisfactorily on the short-exposure plates taken with the photometric cameras as a separate part of the Cape E-region programme, but are needed to provide a link with the Bright Star observations.

The photovisual programme was started a few months later. It includes most of the stars in the photographic programme whose photovisual magnitudes are brighter than 7·6 and a few additional late-type stars too faint to be included in the photographic list. These magnitudes serve to fix the scale above magnitude 7·5. In conjunction with the photographic magnitudes, they provide the colour indices needed to convert one system of magnitudes to another.

The third programme is designed to provide standard stars for the Bright Star Programme. The original plan had been to observe these stars in series at equal altitudes, both east and west of the meridian, and build up a homogeneous system of magnitudes by means of stars common to several plates. This method did not prove satisfactory in practice because there is nearly always a progressive change in the atmospheric transparency during the night and frequently a difference from one azimuth to another. An obvious solution was to use standard stars located at intervals of R.A. round the sky, and the brighter stars in the E regions were chosen for the purpose because they would also provide a link with the fainter stars. As the Bright Stars are being observed with a blue filter these magnitudes differ from ordinary photographic magnitudes and colour corrections are needed to convert the one system to the other. The brightest stars in the E regions have been re-observed with the blue filter and a few selected from these serve as standards for the Bright Star Programme.

The Fabry method is now being used in conjunction with the Victoria Telescope to observe fainter stars. The practical limits with one-minute exposures are about 10·8 Pg and 9·3 Pv. Observations are being made to obtain magnitudes for stars whose parallax has been measured at the Cape, and to check the magnitude scales in the E regions to the limits given above.

* Capital letters are used hereafter to differentiate between stars observed in this particular programme and bright stars in general.

Equipment and observing procedure.—The Fabry unit is constructed to take the place of a standard plate holder on the Astrographic Refractor and can be removed or replaced at will without interfering with the adjustments. The unit carries the Fabry lens, a simple plano-convex lens of about 8 mm. focus, adjusted to give a sharp image of the objective on the plate. Immediately in front of the lens is a diaphragm located in the focal plane of the telescope objective.

The small plate holder used with the unit is provided with cross motions. This permits a maximum of 216 images arranged in 9 rows of 24 in an area 20 mm. by 23 mm. In practice it is found preferable to leave a space between every pair of images, thus reducing the maximum number by one-third. Fig. 1, which is approximately to scale, shows the arrangement of the images on a photographic plate.

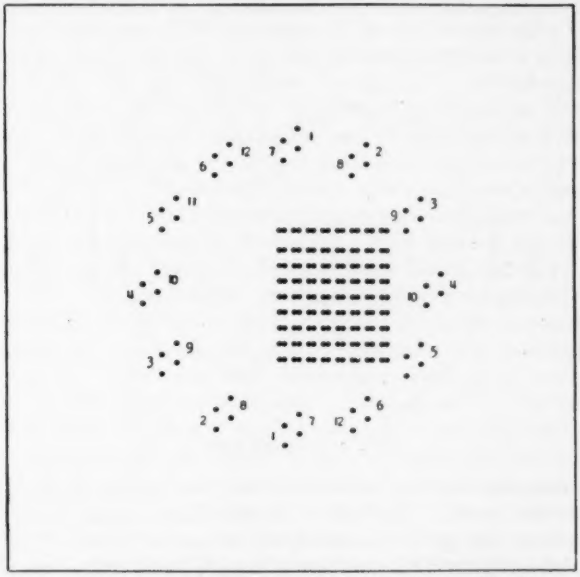

FIG. 1.—*Arrangement of images on* $3\frac{1}{4} \times 3\frac{1}{4}$ *inch photographic plate.*

A stepped rotating sector (see Fig. 2) driven by a small electric motor is mounted inside the telescope tube. It can be moved in and out to the desired position without disturbing the Fabry unit, and takes only a few seconds to change from one step to another. In earlier work a series of interchangeable sectors had been used and an appreciable time was spent in changing these between exposures. The stepped sector is designed with half-magnitude steps from 0 to 2·5. When very bright stars are observed, the original sectors with constants of 3, $3\frac{1}{2}$, 4 and 5 magnitudes still have to be used. The actual values of the constants have been computed from measurements made with a Hilger measuring machine. The 4 and 5 magnitude sectors have only one opening, but the others interrupt the light twice every revolution. The speed of the motor normally exceeds 3000 r.p.m.

Each plate was calibrated in a sensitometer, two exposures of one-minute duration being given before and two after the star observations.

In each region two (or sometimes three) stars, usually of spectral type F, were chosen as local standards and used as comparison stars. If these stars are designated A and B and the remainder a, b, c, d, e, etc., then the observing sequence would be: A a b B c d A e, etc.; every two observations of other stars being preceded and followed by an observation of one of the standards. This serves as a check on any drift in the zero point due to variations in the atmospheric transparency or unevenness of the plate. It was often necessary to use different standards for the stars of the different programmes.

Except for some of the fainter stars in the photovisual programme, each star was given two exposures of one-minute duration. This appears to be the most economical number of images per star with this equipment. From 15 to 20 stars, including the standards, could be observed per hour. Observations were restricted to one region at a time, but several regions were often observed on the same night.

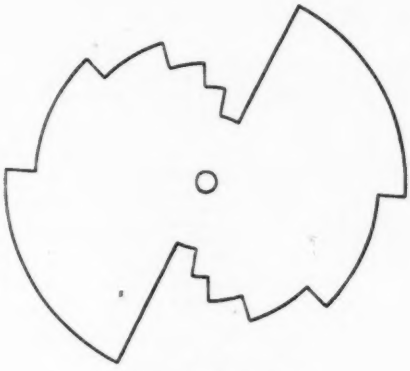

FIG. 2.—*Stepped sector.*

Routine observations were limited to the time during which a region was within 35° of the zenith. The risk of trouble from clouds, smoke, local haze and the loom from city lights increases rapidly at lower altitudes. The differential extinction between individual stars was in consequence always small and rarely exceeded $0^m{\cdot}02$. The telescope was, however, fitted with a clinometer graduated to give the relative air-mass (sec z) directly and the reading was recorded for each star at the time of observation.

All plates were developed in M.Q. developer (ID—2 formula) without rocking or agitation of any kind. The Eberhard effect is easily seen, but there is little unevenness over the plate.

Sky light.—The diaphragm in front of the Fabry lens admits light from the sky as well as from the star being observed and from any other stars that happen to be sufficiently close. When companions were seen and could not be avoided by setting out of centre, the fact was recorded. Such stars are not suitable for standards, as the measured magnitude will depend on the photometric procedure. The effect of the sky light can and should be allowed for.

Since 1947 June routine observations of the brightness of the sky have been included in the photographic and photovisual programmes. This is not necessary for the Bright-Star observations as the effect is negligible. In order to

obtain images of suitable density with an exposure of one minute, and so avoid complications due to different exposure times, a lens working near $f/1$ is required. For some months a common aspherical "bulls-eye" lens was used, but this was later replaced by a microscope condenser mounted so that it could be quickly interchanged with the regular Fabry lens. The effective relative speeds of the sky lens and the regular Fabry lens, with their respective diaphragms, were determined empirically with the help of rotating sectors and the inverse-square-law apparatus previously used for sector tests.*

Tests show that, for moderately small zenith distances, the brightness of the sky increases approximately as $\sec z$. It is therefore possible to reduce the results to the zenith. The mean photographic brightness was $12^m{\cdot}0$ per square minute of arc compared with a star reduced to the zenith. Values above $12^m{\cdot}2$ were rare; below $11^m{\cdot}8$ they were usually associated with a hazy sky. Observations made at the same time, but of different areas of the sky, usually agree within a few hundredths of a magnitude, indicating that the sampling error is small. Only in the case of the Milky Way region E7 (centre: $\lambda = 312°, \beta = -7°$) were the measures systematically brighter by about $0^m{\cdot}1$. The Moon increases the brightness 45° away by about 1 magnitude at First Quarter and 3 magnitudes at Full Moon.

The photovisual brightness of the night sky is both brighter and more variable than the photographic. Values brighter than $11^m{\cdot}4$ and fainter than $11^m{\cdot}8$ per square minute of arc are not uncommon, but exceptional nights can usually be recognized from the appearance of the sky. The western sky is noticeably brighter than the eastern, due to the lights of Cape Town, and this is confirmed by the measures. No observations were made in bright moonlight, but photoelectric measures show that the colour index of the sky is then negative.

Measurement and reduction.—All plates were measured with the modified Schilt photometer. Two analysing diaphragms were used, with projected diameters of 0·24 and 0·32 mm. respectively. (The diameter of the Fabry images was about 0·8 mm.) With the smaller diaphragm the star and calibration images were trailed, but with the larger one they were measured centrally. There is no apparent difference in the accuracy and the latter method is quicker. Before taking a reading the plate was trailed about 1 mm. away from the images and the lamp rheostat adjusted to give a galvanometer deflection of 100·0 for the plate background. The reading of the galvanometer scale then gave the percentage transmission of the images directly. A plate with 200 images can be measured in three-quarters of an hour.

A calibration curve was plotted for each plate and used to convert the readings from the star images into magnitudes. These magnitudes were then corrected for the effect of the sector (if one had been used), the differential extinction to the zenith and the light of the night sky.

The extinction correction was computed from the formula: $-m = -p(\sec z - 1)$. The values assumed for p were 0·50 for the photographic and 0·25 for the photovisual observations. These values are only approximate and there are considerable variations from night to night. Should the actual value differ from the assumed one there will be an apparent change in the mean zero point of the region as the altitude changes. This cannot, in general, be distinguished from a progressive change in the atmospheric transparency, and no attempt was made to separate the two effects. The differential extinction between the stars in a region was

* A. W. J. Cousins and R. H. Stoy, *M.N.*, **106**, 287, 1946.

always small and the error introduced by using the assumed coefficients can rarely have exceeded 0·01 magnitude.

The magnitudes were then reduced to a provisional system by means of the standard stars. There was nearly always a drift of the apparent zero point during the period of observation, due to variations in the transparency of the atmosphere and possibly also to photographic effects.

At a later stage, when a number of plates had been reduced for a given region and provisional magnitudes had been obtained for most of the stars, it was possible to re-examine the drift of zero point and determine the weight to be assigned to the observations. Unit weight was given when the average difference between the observations and the provisional mean magnitudes of the stars was $0^m{\cdot}01$. When several regions occur on a plate each was considered on its own merits.

It was considered desirable that a star should be observed on at least three different nights and have a minimum weight of 3. When the individual observations of a star were not in good agreement, additional observations were made, but only obviously discordant results were rejected. The final magnitudes are the weighted means of all the usable observations, with small adjustments to the zero point of each region to conform as closely as possible with the zero point determined by Stoy from plates taken with the photometric cameras.

Several attempts were made to determine the relative zero points by means of the Fabry method, either by direct comparisons between the E regions or by comparisons with σ Octantis. These showed a considerable amount of observing would be necessary to obtain definitive results. It should be noted that a single comparison in one direction without a return to the first region is of little value because of changes in the extinction; and that each comparison involves a reversal of the telescope to the other side of the pier. The weakness of the polar comparison lies in the low altitude of the pole (34°) at the Cape. The zero points are now being checked as part of the Bright Star Programme, both by direct inter-comparisons between the standard stars and by means of stars compared independently with two E regions. Preliminary results suggest that some small changes may be necessary. Colours, now being measured photoelectrically, will assist in checking the photovisual zero points. The use of the "S" magnitudes derived by Stoy for zero point determinations is justified by the fact that the initial purpose of the present series was to fix the scale for these magnitudes, but it is possible that errors of the order $0^m{\cdot}02$ may have been introduced, due to scale and zero point errors since Stoy's zero points were determined at about $9^m{\cdot}0$.

The photographic programme.—Unbacked Ilford Zenith plates without a colour filter were used for the photographic programme. A star of magnitude 7·7 gave an image of photographic density 0·3 with an exposure of one minute. The earlier observations were made with a diaphragm 2 mm. in diameter in front of the Fabry lens, but this was later replaced by one of half that aperture to reduce stray light from the sky background. It is possible that a still smaller one could be used, but this would have no practical advantage (except in bright moonlight) to compensate for the extra care needed in setting and guiding and the risk of trouble due to the chromatic aberration of the objective. With the present diaphragm bad definition has practically no effect on the observations, provided it is not accompanied by variations in transparency, but with a further reduction in aperture the photometer would not possess this immunity. On a dark night

stars observed through the 1 mm. diaphragm need only small corrections, not exceeding $0^m.03$, for sky light. Only some of the brighter stars were observed in moonlight, the corrections then being of the same order.

The plates were calibrated in a tube sensitometer for which the adopted constants, computed from the measured diameters of the apertures and the sequence of the tubes (see Fig. 1), are as follows:—

m	No.	m	No.	m.	No.
0·00	5	0·97	6	1·96	7
0·27	8	1·34	9	2·26	1
0·51	11	1·52	12	2·50	10
0·71	2	1·71	3	2·66	4

The plate was moved 3 mm. between the first and second exposures and reversed for the third and fourth. This produced twelve compact groups of four spots arranged in a circle 5 cm. in diameter. A group containing two images from tube n also contained two from tube $n+6$ and vice versa. This reduces the errors due to unevenness of the plate. The lamp is fitted with a blue filter similar to that used for the Bright Star Programme.

Twenty-five plates of uniformly good quality would have been sufficient to complete this programme. The actual number taken was 87. Of the 3900 observations, 1100 received full weight. The average weight was 0·47.

The photovisual observations.—The Ilford H.P.3 plates used for the photovisual observations were taken from three batches, but the selective colour sensitivities were not noticeably different. The first batch was backed, the others not. The last batch was appreciably faster than the others and the reciprocity failure less.

A colour filter was fitted about an inch in front of the Fabry lens. For about a year a Zeiss Ikon II filter was used. This was then replaced by an Omag 301. Approximate transmission factors for these filters were measured with a monochromator and 1P21 photomultiplier tube. The change of filter produced a change in the colour system that can be expressed in the form

$$(\text{Zeiss Pv.} - \text{Omag Pv.}) = 0{\cdot}07(\text{Pg.} - \text{Omag Pv.}).$$

The second colour system is very near that obtained by Redman with an Ilford Delta filter and aluminized mirror.

The 2 mm. diaphragm was used for all the observations in the best compromise focus of the 13-inch objective (which is photographically corrected). This is about 8 mm. beyond the usual focus. A 1 mm. diaphragm would not pass all the light to which the plate and filter combination is sensitive. This meant that sky corrections as large as $0^m.10$ were occasionally needed for the fainter stars with a poor sky. A few observations of the brighter stars were made with the Moon present.

The plates were calibrated with the slit sensitometer used for photovisual observations in Durban*, with an Ilford Gamma filter over the light source. The apparatus was adapted for use with plates and provided with a mask having two rows of twelve holes spaced at 2·5 mm. centres ($0^m.25$ intervals). The spots are of similar size to the star images. The plate was rotated 90° between exposures, producing eight rows of spots arranged in pairs and bordering

* A. W. J. Cousins, *M.N.*, **103**, 154, 1943.

a hollow square. The adjacent rows of a pair are graded in opposite directions to compensate for unevenness of the plate. Normally only four rows of spots (two pairs) were measured. The star images, arranged as on a photographic plate, lie within the square.

The H.P.3 plate and filter combination is more than a magnitude slower han a Zenith plate, a photographic density of 0·3 resulting from a $6^{m}\cdot2$ star with the early plates and Zeiss filter and a $6^{m}\cdot7$ star with the recent plates and Omag filter. In order to reach a $7^{m}\cdot5$ star it was necessary to give two-minute exposures. The same standard stars were used for these but with a sector $0^{m}\cdot5$ greater. A two-minute exposure was sufficient for the sky with the new plates (and filter) but four minutes were necessary with the earlier ones.

3260 observations were made to complete this programme and 950 received full weight. The average weight was 0·51—slightly higher than for the photographic programme. This is at least partly due to the better observing conditions in 1949. 67 plates were used.

The Bright Star standards.—Ilford Special Rapid plates and a blue filter are being used for the Bright Star Programme. The first observations were made on backed plates, but practically all those used for observing the standard stars were unbacked. In other respects the equipment and observing technique were the same as those used for the photographic programme. No sky corrections were required. 580 observations were made of the Bright Star standards, apart from their routine use in the Bright Star Programme. The average weight was 0·7.

Systematic accuracy.—A magnitude system is normally defined by stating the scale, colour equation and zero point relative to some standard system. The scale should be a normal Pogson scale, but the colour system and therefore the adopted zero point will depend on the method and conditions of observation. The system should be homogeneous throughout and there should be no variation in colour equation with magnitude. The relation to another system can be found only by direct comparison between the magnitudes of individual stars.

The scales of the present magnitude systems depend primarily on the rotating sectors and to a lesser extent on the sensitometer calibrations. In both cases the constants are computed from geometrical measurements and it is believed that they are accurate to within one per cent.

The constants of the rotating sectors have also been measured photoelectrically, using a 1P21 photo-multiplier tube with the inverse-square-law apparatus previously used to make similar measures photographically.* The lamp was used (*a*) bare, as for the photographic tests, (*b*) with a coarse ground-glass window and (*c*) with a flashed opal window. The last gives the most accurate results with the greatest loss of light. Small empirical corrections (averaging $0^{m}\cdot01$ and $0^{m}\cdot003$ per magnitude for (*a*) and (*b*) respectively) were applied when the first two arrangements were used. The response of the cell-galvanometer combination is sensibly linear. The measured values are given in Table I. The agreement between these and the values computed from the geometrical measurements is satisfactory.

Tests made with Ilford Zenith, H.P.3 and Special Rapid plates have shown that when these plates are used with rotating sectors the photographic effect of the rapidly flickering light is essentially the same as that produced by a steady

* A. W. J. Cousins and R. H. Stoy, *M.N.*, **106**, 287, 1946.

light of the same average intensity. These tests can be considered conclusive within $0^m.01$ or $0^m.02$ over a range of three or four magnitudes.

The two sensitometers have been compared with one another, using similar blue filters. No difference in scale could be detected. The Fabry images and the sensitometer spots are of nearly the same size, so no errors are expected from this cause. When the measures of the spots are compared with the calibration curve the residuals are little if any larger than would be expected from a knowledge of the errors and give no reason to suspect the accuracy of the individual constants.

TABLE I

Measurements of Sector Constants

Stepped Sector

Step	Magnitude Reduction: Geometrical Measures	Photoelectric Measures	Adopted Value
1	0·497	0·498	0·50
2	0·993	0·991	0·99
3	1·489	1·486	1·49
4	1·986	1·979	1·98
5	2·483	2·480	2·48

Original Sectors

Nominal Magnitude	Geometrical Measures	Photoelectric Measures	Adopted Value
1·0	1·002	0·998	1·00
1·5	1·502	1·502	1·50
2·0	1·999	1·997	2·00
2·5	2·500	2·495	2·50
3·0	2·989	2·983	2·99
3·5	3·435	3·432	3·43
4·0	4·009	4·008	4·01
5·0	4·852:	4·846:	4·85

Occasionally a star was observed with two different sectors in succession, permitting a comparison between the sectors and sensitometer. The following results were obtained with the tube sensitometer and Zenith plates :—

Sectors used	$0^m.5$–$0^m.0$	$1^m.0$–$0^m.5$	All others
No. of comparisons	22	42	38
Average difference	$-0^m.001$	$+0^m.005$	$+0^m.003$
Standard error	$\pm 0^m.006$	$\pm 0^m.004$	$\pm 0^m.004$

The mean of 76 similar comparisons using H.P.3 plates and the slit sensitometer is $+0^m.011 \pm 0^m.002$ for a half-magnitude difference. This difference, though small, may be real and possibly due to a change in plate characteristic with wave-length. A change from the Ilford Gamma to the blue filter produced an apparent change of scale of 6 per cent with these plates. On the other hand the Zenith plates showed no difference in the calibration curve when the blue filter was omitted. If the calibration of the photovisual plates is in error by 2 per cent this may have affected individual magnitudes by $0^m.01$ but should not have introduced any scale error, since the scale is mainly dependent on the rotating

sectors. An error of $+0^{m}\cdot01$ is possible at and below $7^{m}\cdot0$ due to the effect of selection. It is intended to re-observe these stars with the 18-inch visual component of the Victoria Telescope.

No direct evidence of the homogeneity of the present magnitude systems is available. Comparisons with other systems are given in a later section. A comparison between the results from a number of individual photographic plates and the mean magnitudes shows that there is little change in colour equation from night to night and that differences greater than 1 per cent are rare. Changes in the atmosphere might account for these.

Errors of observation.—The accidental errors of observation are due partly to the method and partly to the sky. They vary from night to night and even from region to region on the same plate. The best observations have a standard error of $\pm0^{m}\cdot01$.

The average standard error attributed to the sky for all the observations under discussion is $\pm0^{m}\cdot013$. On the best nights (of which there are about two per month, on the average, at the Cape) the sky error is less than $\pm0^{m}\cdot010$. The average value obviously depends on the observer's choice of nights. There is inevitably a compromise between the ideal of working only on the best nights and the desire to complete a programme in a reasonable time.

The errors due to the method are predominantly due to the photographic plate, its measurement and reduction. They vary according to the density of the images and somewhat from plate to plate but an estimate of their size under actual conditions can be made from the measures themselves. The errors have been analysed under a number of different heads:—

(*a*) The measuring errors.
(*b*) The intrinsic errors.
(*c*) Calibration curve errors.
(*d*) Timing errors.

The results are given in Table II.

TABLE II

Accidental Standard Errors of Method

Ilford Plates used	Zenith	H.P.3	Special Rapid
	m	m	m
Measuring error	±0·006	±0·005	±0·004
Error due to background setting	0·006	(0·003)	0·002
Intrinsic error	0·009	0·012	0·006
Error of calibration	0·005	0·007	0·005
Error of timing exposure	0·004	0·004	0·004
Combined error for pair of images	0·011	0·012	0·008

(*a*) *The measuring errors.*—Two errors arise in measuring a plate: an error made in adjusting the reading for the plate background and an error in measuring the density of each image. These are due partly to errors in setting and reading the Schilt photometer and partly to sampling effects. It is generally accepted that the exposed portion of a plate should be measured relative to the unexposed background in preference to making absolute measurements of the transmission of the image. This procedure obviates the necessity for a separate check on the constancy of the light source, but it introduces an error due to random variations in the plate background. It would appear that either procedure could have been used with the present plates with little or no change in the accuracy.

The measuring and background errors can be obtained by re-measuring plates. Normally one background reading serves for the two adjacent images of each star. The measured percentage difference between the two nearly equal images of a pair is independent of errors in the background setting (to a first order of accuracy) while the actual (or average) percentages are not. If D_{a1} and D_{b1}, D_{a2} and D_{b2} are two sets of measures of images a and b, and ϵ_m and ϵ_b are standard errors of measurement and background setting respectively, then

$$\overline{[(D_{a1}-D_{b1})-(D_{a2}-D_{b2})]^2}=4\epsilon_m^2$$

and

$$\overline{[(D_{a1}+D_{b1})-(D_{a2}+D_{b2})]^2}=4\epsilon_m^2+8\epsilon_b^2,$$

where ϵ_m and ϵ_b are in units of 1 per cent deflection but can be converted into magnitude differences by means of the calibration curves.

The measuring errors, ϵ_m (in magnitudes) for the three brands of plates used are $\pm 0^m{\cdot}006$ (Zenith), $\pm 0^m{\cdot}005$ (H.P.3) and $\pm 0^m{\cdot}004$ (Special Rapid). The corresponding values of the background errors, ϵ_b, for Zenith and Special Rapid plates are $\pm 0^m{\cdot}006$ and $\pm 0^m{\cdot}002$. Two independent attempts to obtain ϵ_b for H.P.3 plates by this method of differences led to values sensibly zero.

An alternative method of estimating ϵ_b is to measure the background variations. Typical plates were measured at intervals of about 2 mm., using the larger diaphragm in the photometer. The average difference between successive readings (in units of 1 per cent deflection) is a measure of the background variation and the effect of these variations on the measures of an image can be computed with the aid of the plate calibration curves. Standard errors, computed for images of 50 per cent transmission, are as follows:—

Ilford Plate	Zenith	H.P.3	Special Rapid
Plate stationary	$\pm 0^m{\cdot}008$	$\pm 0^m{\cdot}007$	$\pm 0^m{\cdot}003$
Plate trailed	$0^m{\cdot}005$	$0^m{\cdot}003$	$0^m{\cdot}003$

(*b*) *The intrinsic errors.*—By intrinsic error is meant the departure from equality of equally exposed images. It is purely a photographic effect and depends on the density and separation of the images and the area integrated by the photometer. When expressed as a percentage of full-scale deflection it is smallest for very dense images, but owing to the slope of the characteristic curve the minimum expressed in magnitudes occurs in the neighbourhood of 30 per cent transmission. When the images are widely separated the errors are larger than when they are close. Unevenness of the sensitivity or development of the plate gives rise to "local errors"* even when the plates are fresh.

An estimate of the intrinsic error can be obtained from the sensitometer spots since the relative intensities of the twelve spots are fixed by the constants of the sensitometer and only the zero point varies from exposure to exposure. The values given in Table II are based on images between 25 per cent and 75 per cent transmission and about 3 mm. apart when measured with the larger diaphragm in the photometer. The value of the measuring error previously determined was assumed in each case. No background error is involved, as the same setting is used for both the images. The local error may amount to $0^m{\cdot}01$ over a distance of 5 cm. on a Zenith plate.

(*c*) *Calibration curve errors.*—Errors arise from the plotting and reading of the calibration curves. These curves are based on the measures of images that

* G. de Vaucouleurs, *Publ. Obs. Houga*, No. 10, 1944.

are subject to appreciable local errors, only partly removed in the mean. The average error of a normal point based on the measures of four spots is $0^{m}\cdot01$. Special care was taken to draw the curves as smoothly as possible, giving due weight to all the points. The errors given, which include that of reading the graph, are based on the differences between the calibration curves of plates developed together but measured and plotted independently.

(*d*) *Timing error*.—The timing error quoted, which is equivalent to an average error of 0·25 sec. per minute, is added for completeness but contributes little to the errors of observation.

It is clear that a plate can only attain unit weight (s.e. $\pm0^{m}\cdot015$) if the errors from other sources are small, and there are apparently few nights when the sky above the Cape Observatory is good enough for this. Slow and gradual changes in the transparency are not objectionable as they can be allowed for by a change in zero point, but rapid changes are generally irregular.

The finer grain and clearer background of the Special Rapid plate give it a distinct advantage over the faster plates, as shown by the larger proportion gaining unit weight (42 per cent compared with 28 per cent for Zenith and 29 per cent for H.P.3).

Results.—The detailed results are not given here. They will be published at a later date together with the magnitudes of fainter stars, but may be obtained in mimeographed form on application to the Cape Observatory. Some small adjustments in zero point from region to region may still be necessary.

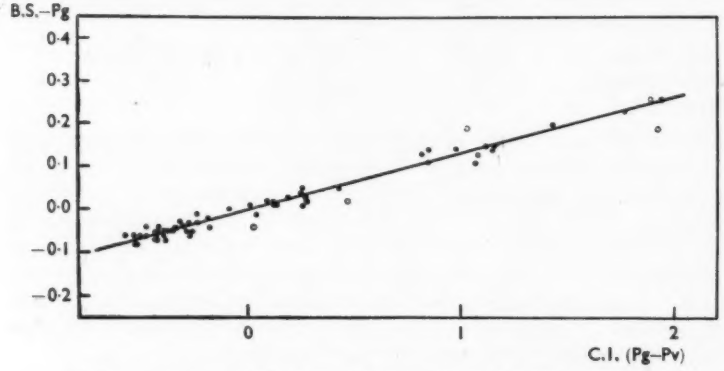

FIG. 3.—*Colour relation between photographic and bright-star magnitudes*

The average weight per star, excluding the local standards, is 5 for both the photographic and photovisual series, corresponding to a standard error of $\pm0^{m}\cdot006$. The error deduced from the internal consistency of the observations of each star exceeds $\pm0^{m}\cdot007$ in 13 cases, but only 6 of these (4 Pg and 2 Pv exceed $\pm0^{m}\cdot008$. These latter stars, and four others for which the observations indicated an internal standard error for unit weight of $\pm0^{m}\cdot020$ or greater, include two of spectral type Mb that are probably slightly variable, 5 with Pg magnitudes fainter than 7·9, and one that was difficult because of a nearby companion. Faint stars are liable to larger accidental errors because the images are weaker than the optimum, but the possibility of slight variability cannot be

overlooked. There is no obvious explanation for the remaining two stars (of spectral types A0 and F2), for which the discordance is noted in one colour only.

Table III gives a comparison between the magnitudes of Bright Stars obtained with the blue filter and equivalent magnitudes derived from the photographic and photovisual series by means of a colour coefficient.

The first column (Table III) gives the number in the *Cape Zone Catalogue* for 1900; the second the spectral type from the *Henry Draper Catalogue* and the third the revised type (when available) from the *Publications of Lick Observatory*, Vol. XVIII. The fourth, sixth and eighth columns contain the colour index (=Pg–Pv), and the photographic and Bright Star magnitudes as observed by the Fabry method. The ninth column gives the differences in the sense B.S.–Pg. These differences are plotted against C.I. in Fig. 3. They can be well represented by the straight line:—

$$B.S.-Pg = 0.132\ C.I.$$

The seventh column in the table, Pg′, gives the magnitude obtained by adding the colour correction computed with this formula to the observed photographic magnitudes in the preceding column. The tenth column gives the residuals B.S.–Pg′.

TABLE III

C.Z.C.	Spectral Type H.D.	Lick	C.I. Fabry	C.I. Pe	Magnitudes Pg	Pg′	B.S.	B.S.–Pg	B.S.–Pg′ m.×100	C.F.–C.Pe m.×100
500	K0	G4	+0·85	+0·65	4·11	4·22	4·22	+0·11	0	+3
510	A3	...	−0·09		5·21	5·20	5·21	0·00	+1	
577	G0	G0	+0·43	+0·37	5·38	5·44	5·43	+0·05	−1	−2
652	K0	G8	+1·07		6·39	6·53	6·50	+0·11	−3	
680	K5	M1	+1·77		4·99	5·22	5·22	+0·23	0	
703	K0	G4	+0·98	+0·76	4·84	4·97	4·98	+0·14	+1	+1
707	A0	...	−0·19		6·07	6·04	6·05	−0·02	+1	
2092	F0	...	+0·13	+0·15	5·10	5·12	5·11	+0·01	−1	−2
2120	K0	K1	+1·15	+0·88	4·89	5·04	5·03	+0·14	−1	+2
2147	F5	...	+0·09	+0·12	4·40	4·41	4·42	+0·02	+1	−2
2168	K0	K2	+1·12	+0·85	6·33	6·48	6·48	+0·15	0	+3
3572	B9	...	−0·35	−0·25	5·51	5·46	5·47	−0·04	+1	+4
3736	B5	...	−0·48		6·49	6·43	6·43	−0·06	0	
3742	B8	...	−0·42	−0·27	2·87	2·81	2·83	−0·04	+2	−1
3770	K0	G7	+0·82	+0·66	5·67	5·78	5·80	+0·13	+2	−2
3806	B8	...	−0·44		6·31	6·25	6·24	−0·07	−1	
3933	F2	F4s	+0·26	+0·28	5·43	5·47	5·45	+0·02	−2	−2
3978	B9	...	−0·40		6·16	6·11	6·10	−0·06	−1	
4077	A0	...	−0·28	−0·15	6·03	5·99	6·00	−0·03	+1	−3
7024	K5	cK4	+1·94	+1·31	3·90	4·16	4·16	+0·26	0*	
7091	B5	B3	+0·03	+0·01	5·01	5·01	4·97	−0·04	−4*	
7103	B3	(B3s)	−0·53	−0·38	5·35	5·28	5·27	−0·08	−1	+3
7119	B8	(B8nn)	−0·39	−0·30	5·25	5·20	5·18	−0·07	−2	+6
7132	B9	...	−0·31	−0·20	5·69	5·65	5·65	−0·04	0	+1
7142	B5	...	−0·43	−0·28	5·51	5·45	5·46	−0·05	+1	0

TABLE III (*contd.*)

C.Z.C.	Spectral Type H.D.	Lick	C.I. Fabry	Pe	Magnitudes Pg	Pg′	B.S.	B.S.−Pg	B.S.−Pg′ m.×100	C.F.−C.Pe m.×100
7145	B3	(B5n)	−0·43	−0·32	4·89	4·83	4·83	−0·06	0	+5
7171	A0	...	−0·36	−0·22	5·98	5·93	5·93	−0·05	0	−1
7327	B5	...	−0·48	−0·25	5·89	5·83	5·85	−0·04	+2	−9
7333	B9	...	−0·40	−0·24	5·90	5·85	5·85	−0·05	0	−3
9812	B8	...	−0·43	−0·28	4·95	4·89	4·90	−0·05	+1	0
9884	K0	K4	+1·43	+1·10	5·72	5·91	5·92	+0·20	+1	0
10051	F0	F5	+0·26	+0·23	5·41	5·44	5·42	+0·01	−2	0
10111	A0	...	−0·26	−0·16	5·17	5·14	5·12	−0·05	−2	+1
10121	A2	...	+0·04	+0·06	5·85	5·86	5·84	−0·01	−2	+1
12297	B3	B3	−0·51	−0·32	4·16	4·09	4·10	−0·06	+1	−3
12300	F8	F1	+0·27	+0·22	4·62	4·66	4·65	+0·03	−1	+2
12309	A3	...	+0·12	+0·15	5·98	6·00	6·00	+0·02	0	−3
12353	B9	...	−0·36	−0·23	5·24	5·19	5·19	−0·05	0	0
12445	B3p A2p	B3ne	−0·52	−0·34	1·94	1·87	1·86	−0·08	−1	−1
12549	B2	B2s	−0·53	−0·35	1·89	1·82	1·82	−0·07	0	−1
12618	A0	...	−0·18	−0·10	5·66	5·64	5·62	−0·04	−2	0
12713	B5	B6	−0·43	−0·33	4·00	3·94	3·93	−0·07	−1	+6
12780	B9	(B9)	−0·32	−0·20	5·42	5·38	5·39	−0·03	+1	0
12813	B2p	B3n	−0·58	−0·35	2·23	2·15	2·17	−0·06	+2	−6
12828	B3	B2s	−0·54	−0·36	2·71	2·64	2·65	−0·06	+1	−1
12915	B5	B5n	−0·43	−0·31	3·57	3·51	3·50	−0·07	−1	+4
15844	G5	G2	+0·85	−0·70	5·85	5·96	5·99	+0·14	+3	−4
15868	F2	A7n	+0·25	+0·23	3·61	3·64	3·65	+0·04	+1	−1
15997	B9	...	−0·29	−0·18	5·58	5·54	5·53	−0·05	−1	0
16087	B3p	B3nne	−0·38	−0·26	4·92	4·87	4·87	−0·05	0	+2
16121	B8	...	−0·34	−0·21	4·89	4·85	4·85	−0·04	0	−1
16195	B9	(B9)	−0·31	−0·20	5·07	5·03	5·03	−0·04	0	+1
16407	A0	...	−0·27	−0·17	4·42	4·38	4·36	−0·06	−2	+1
16458	F0	cF1	+0·26	+0·22	2·16	2·19	2·21	+0·05	+2	+1
16476	B9	...	−0·31	−0·20	5·89	5·85	5·85	−0·04	0	+1
16540	A0	...	−0·24	−0·13	5·64	5·61	5·61	−0·03	0	−2
18469	K0	...	+1·16	+0·88	5·14	5·29	5·29	+0·15	0	+3
18533	A5	...	+0·13	+0·13	5·93	5·95	5·94	+0·01	−1	+1
18762	A0	...	−0·24	−0·11	5·40	5·37	5·39	−0·01	+2	−4
18771	A3	...	+0·01	+0·05	5·68	5·68	5·69	+0·01	+1	−1
19883	F0	...	+0·19	+0·21	5·83	5·86	5·86	+0·03	0	−4
19939	G5	G2	+1·03	+0·81	4·91	5·05	5·10	+0·19	+5*	
19946	Mb	M4	+1·92		5·80	6·05	5·99	+0·19	−6*	
20067	G0	...	+0·47	+0·40	6·43	6·49	6·45	+0·02	−4*	
20068	Mb	M6	+1·89		3·73	3·98	3·99	+0·26	+1*	
20077	K0	G5	+1·08	+0·79	5·82	5·96	5·95	+0·13	−1	+7

* These stars appear to be slightly variable on the evidence of the Bright Star Programme. The observed range is $0^m{\cdot}10$ for C.Z.C. 19946 and 20067; somewhat more for C.Z.C. 20068 and less for the other stars. The variation of C.Z.C. 20068 was noted in the photographic observations, but none of the other stars attracted attention in either the photovisual or the photographic series.

The average value of the residuals, omitting those stars marked with an asterisk, which appear to be variable is $0^m.010$, corresponding to a standard deviation of $\pm 0^m.013$. The average standard error of the individual magnitudes is $\pm 0^m.006$, and the internal error of the differences $\pm 0^m.008$, leaving a standard error of $\pm 0^m.009$ unaccounted for.

Uncertainties in the adopted colour indices and colour coefficient do not introduce appreciable errors, but detailed features of the spectra may produce some departures from a strictly linear relationship. There is not, however, any appreciable general correlation between the sign or magnitude of the residuals and the spectral types of the stars.

When the differences are grouped according to magnitude, only the brightest stars show a systematic difference as large as $0^m.010$, viz.:

Magnitude Group	<3·0	3·0–4·0	4·0–5·0	5·0–5·5	5·5–6·0	>6·0
Mean difference (B.S.–Pg′)	+0·010	0·000	−0·001	−0·006	+0·002	−0·003
No. of stars	6	3	13	14	17	7

Since individual magnitudes are largely dependent on particular sectors and different sectors were used for the two series, the smallness of the differences is evidence of the general consistency of the adopted sector constants and the resulting magnitude scales.

Of the six stars that appear to be variable, only one, C.Z.C. 20068 (β Gruis) had been suspected in the course of the photographic or photovisual observations.

Discussion of results.—The fainter stars observed in the photographic and photovisual series can be compared with the brighter stars measured on the Cape photometric camera plates. The SPg, SPv and Fabry magnitudes are mutually dependent with regard to scale and zero point, so the comparison can give little information about systematic errors in the Fabry magnitudes, but the comparison is interesting because the magnitudes were determined by radically different methods.

Dr Stoy has made a comparison between the Fabry results and the magnitudes obtained from the Cape series* of plates. The latter are the observed magnitudes with a distance correction applied. The colour relations between the series can be expressed:—

$$\text{Fabry Pg–Cape Pg} = -0{\cdot}03 + 0{\cdot}07 \text{ C.I.}$$
$$\text{Fabry Pv–Cape Pv} = +0{\cdot}04 + 0{\cdot}07 \text{ C.I.}$$

The magnitudes were adjusted to remove zero point differences. No scale correction was applied to either series, since a comparison, region by region, failed to show any significant differences in this respect.

After applying the above corrections the average differences are $0^m.020$ (161 stars) for thePg and $0^m.026$ (125 stars) for the Pv magnitudes. The internal average deviations of the photometric camera magnitudes (over the same range) are $0^m.014$ and $0^m.017$ for Pg and Pv respectively. Assuming that the corresponding value for the Fabry magnitudes (both series) is $0^m.005$, the average differences should be $0^m.015$ and $0^m.018$, leaving $0^m.013$ (s.e. $\pm 0^m.017$) for Pg and $0^m.019$ (s.e. $\pm 0^m.024$) for the Pv not accounted for.

Most of the stars in Table III are included in the photoelectric colour programme at the Cape Observatory and preliminary results have been supplied

* Two later series taken in Pretoria with longer exposures are less suitable because there are fewer stars in common.

by Mr Menzies for 57 of these stars with four or more observations. Differences in zero point have been removed, region by region, and the results are given in column five. The relation between the photoelectric and Fabry colour indices is approximately linear and can be expressed:

$$\text{C.I. (Fabry)} = 1{\cdot}35 \times \text{C.I. (Photoelectric)}.$$

The residuals, after reducing the photoelectric colours to the Fabry system, are given in the last column of the table. The average (omitting stars suspected of variability) is $0^{m}{\cdot}022$, equivalent to a standard error of $\pm 0^{m}{\cdot}028$. The average internal standard errors of the photoelectric and Fabry colour indices, reduced to the Fabry system, are $\pm 0^{m}{\cdot}011$ and $\pm 0^{m}{\cdot}009$, respectively, leaving $\pm 0^{m}{\cdot}024$ to be accounted for.

The photoelectric colours used for this discussion are only preliminary and may not be strictly homogeneous. A critical analysis will be made when the photoelectric programme has been completed and it is possible that slightly smaller external errors will result.

These comparisons show that the unexplained differences, after applying linear colour corrections, are not large. It is possible that these arise from undetected systematic errors. On the other hand, colour corrections are not strictly linear even with black-body radiation, and larger variations may be expected with actual stars.

To be generally useful a magnitude or colour index should be convertible to some standard system, and the accuracy with which this can be done decides the accuracy it is worth while aiming at in a programme of general photometry. The indication from the above comparisons is that an error of one- or two-hundredths of a magnitude would remain after allowing for internal errors. It is clearly worth while determining the magnitudes of standard stars with an accuracy of $\pm 0^{m}{\cdot}02$, but probably not worth while to press the standard error below $\pm 0^{m}{\cdot}01$.

Conclusion.—During the period that the Fabry method has been in use at the Cape Observatory photoelectric photometry has greatly increased in popularity. It is no longer a difficult technique with limited applications and there are those who believe that it has rendered photographic methods obsolete where high precision is desired.

This point of view is perhaps too sweeping. There is probably little difference, either in accuracy or in time spent on observation and reduction, between the photoelectric and Fabry methods when used for fundamental magnitude work on the brighter stars. Either method should give the accuracy desired with three observations made under favourable atmospheric conditions, though more are desirable to reduce the risk of undetected variability.

While the sky imposes an ultimate limit to the accuracy, the rate of observation is usually limited by the speed of the recording device and the amount the observer has to do. A reduction in the number or duration of the exposures adopted for the Fabry programmes would have little effect on the observing rate. The time taken to set the telescope and sector would not be affected and the observer might find that he had not sufficient time to record an observation and select another star while shorter exposures were in progress. On the other hand, the method becomes less efficient for faint stars because of the increase in the exposure time needed to obtain images of suitable density. While

other methods of photometry also become less efficient for faint stars, their practical limit for a given size of telescope is usually somewhat fainter. The Fabry method is further handicapped by its unsuitability for use with a reflector (except in Herschelian form).

The Fabry method can be used with the same plates and colour filters that are used for other photometric programmes. While this is no guarantee that the colour systems will be identical, they are likely to be sufficiently close to present no difficulties in converting one to the other. This is apparently not always true when " photographic " magnitudes are determined photoelectrically.

When an observatory already possesses a Schilt or similar photometer capital cost is strongly in favour of the Fabry method, especially when it is desired to equip more than one telescope. In the case of a twin telescope it is possible to observe photographic and photovisual magnitudes simultaneously with little reduction in the rate of observation.

A few observations are lost due to mistakes on the part of the observer, wrong adjustments or faulty processing of the plates, but the largest cause for rejection is poor observing conditions. Naturally, when good nights are few, there is a tendency to use some doubtful nights, with the result that a fair number of observations have to be rejected or given reduced weights after measuring the plates. This is possibly the most serious objection to the Fabry method. An observer using a photoelectric photometer can usually see when conditions are too bad.

It is a pleasure to express my thanks to Dr Jackson and Dr Stoy for much encouragement and helpful criticism during the progress of the work. My thanks are also due to Dr Stoy and Mr H. C. Davies for assistance in taking the plates and to Professor Redman and others who read this paper in draft form and have given me the benefit of their criticism.

Royal Observatory,
Cape of Good Hope :
1950 *October* 31.

THE IMPORTANCE OF ROTATION IN STELLAR EVOLUTION

P. A. Sweet

(Communicated by the Director of the University Observatory, Glasgow)

(Received 1950 October 13)*

Summary

Eddington's assessment (1) of the rate of circulation in meridian planes in the Sun, produced by its rotation, is reviewed, using a first-order perturbation theory. The resulting velocity is found to be of the order of 10^{-10} cm./sec., as compared with Eddington's figure of 2×10^{-4} cm./sec., a reduction of importance when considering the amount of mixing of material in the Sun during its lifetime.

The theory is applied to stars in general, and the equatorial rotation velocity necessary to provide a significant rate of stirring in a star is found in terms of its magnitude and effective temperature. These rotation rates are found to lie within the range actually observed for early-type stars, but are in excess of those for the later types.

In view of the widely held opinion that giants are stars with non-uniform composition, the distribution of rotation rates among the stars thus assumes an added interest. The rotation rate can similarly govern the possibility of local exhaustion of hydrogen in the core, with its consequent effects on evolution.

---

1. *Introduction.*—Circulation currents in the radiative envelopes of stars may have a considerable effect on their structure and evolution. In the absence of mixing currents the composition of the radiative envelope, apart from the possible accretion of interstellar material, must remain almost constant during the life of a star, while the molecular weight in the convective core increases slowly as the hydrogen there is transformed into helium. According to the theory of stellar structure the resultant discontinuity of molecular weight at the core surface would cause the star to expand. Although it is doubtful whether in light stars this increase in radius would be sufficient to produce giants, in the heavy stars where the polytropic index in the core is nearer its maximum value 3 it is possible that the effect might be sufficient to account for giants. The effect could not occur in well-stirred stars. Further, the work of Schönberg and Chandrasekhar (**2**), and its subsequent development by M. Hall Harrison (**3**), on the effects of a local exhaustion of hydrogen in the core, show that the evolution of a star in which there were no general mixing would differ significantly from a star in which stirring allowed hydrogen from all parts of the star to be consumed. Finally, the work of Hoyle and Lyttleton (**4**) and Hen and Schwarzschild (**5**) on the possible production of giant stars through accretion of interstellar material producing a non-uniformity in molecular weight in the outer part of the radiative envelope, shows that a star which has consumed hydrogen from its radiative envelope is more likely to become a giant than a star whose hydrogen content in the radiative envelope has not been affected. On this accretion theory, therefore, a well-stirred star stands more chance of becoming a giant than an unstirred one.

* Received in original form 1950 August 28

In order to allow non-uniform composition to develop, the meridian-plane circulation velocity must not exceed a value of the order of magnitude of the radius of the star divided by the time-scale of its evolution. In the Sun, for example, taking a radius of 7×10^{10} cm., together with a time of 3×10^{9} years, this maximum velocity is seen to be of the order of 7×10^{-7} cm./sec. Thus Eddington's figure of 2×10^{-4} cm./sec. would preclude an appreciable difference in the compositions of the core and radiative envelope, while the figure of 3×10^{-10} cm./sec. derived in the present paper involves a negligible mixing rate.

A survey of the problem included in Wasiutynski's work (**6**) on stellar hydrodynamics shows that in the past great difficulty has been experienced in attempting to assess the rate of circulation produced by rotation. The main difficulty has been that, with an arbitrary distribution of angular velocity, the boundary conditions adopted for the flow cannot be satisfied simultaneously at the surface of the star and on the surface of the convective core. In consequence much of the work in this field has been restricted to general theorems, emphasis being laid mostly on the relationship between the circulation velocity, the thermal equilibrium and the variation of angular velocity throughout the star. Schwarzschild, for example, has shown (**7**) that thermal equilibrium could be maintained without meridian-plane circulation if the star possessed a certain special distribution of angular velocity. However, even if a star could develop such a differential angular velocity, it is difficult to see how it could maintain it against viscosity drag, and more especially, magnetic forces, without meridian-plane circulation, since the other forces are all directed in meridian planes. It will be seen later that the boundary conditions adopted were unnecessarily severe.

The first quantitative investigation of the effect of rotation was made by Eddington (**1**) in 1929. A few years previously, in 1924, H. von Zeipel had shown, in a famous theorem (**8**), that the radiative transfer of energy in a star is upset slightly by rotation and that thermal equilibrium would only be possible, in a rigid star, if the rate of generation of energy obeyed a special law. This law is clearly not satisfied in any real star; the first effect of radiative transfer alone attempting to maintain thermal equilibrium is therefore to produce a slight rise in temperature over some parts of any given equipotential surface and a slight fall over other parts. The resulting variation in pressure over the surface must set up convection currents in meridian planes. The circulation settles down to a steady state sufficient to maintain thermal equilibrium. An exception to this would be in a region where the molecular weight was already strongly non-uniform. In such a case circulation would only proceed for a short time, until the distortion of the surfaces of constant molecular weight prevented further motion. This effect is referred to in more detail later.

It was by equating the rate of transport of energy out of any region, by the circulation, to the amount by which radiative transfer alone fails to get rid of it, that Eddington derived an approximate value for the radial component of the circulation velocity, viz.:

$$v_r = q\bar{\epsilon}_1 / \{1/\gamma - 1/4(\gamma - 1)\} g, \qquad (1.1)$$

where $\bar{\epsilon}_1$ is the mean rate of generation of energy per gram of material interior to the point in question, g is the local acceleration of gravity, γ is the ratio of the specific heats of the gas and q is a dimensionless factor depending on the distortion

of the equipotential surfaces by the rotation. In Eddington's treatment of the problem the factor q can only be obtained by assessment, and for some reason Eddington took a value which is far too high. This resulted in an estimate of 2×10^{-4} cm./sec. for the radial velocity. In a more accurate treatment the velocity distribution correct to the first order in the ratio of the centrifugal acceleration to acceleration of gravity can be found, using a first-order perturbation theory. The calculations made are used to form a relationship between the maximum equatorial rotation velocity which would allow a star to develop a non-uniform composition, and its position in the H–R diagram. The results show that the magnitude of that rotation which has a critical effect on the structure of a star is within the range actually observed.

2. *A generalized first-order perturbation theory.*—The first step is to derive an expression for the distortion of the equipotential surfaces due to the rotation. The following procedure is an extension of a method given by Chandrasekhar (**9**). The equations of hydrostatic equilibrium, neglecting viscosity and the inertia of the circulation itself, and assuming conditions to be symmetrical about an axis through the centre of the star *, are

$$\left.\begin{aligned} \partial P'/\partial r &= \rho' \partial \phi'/\partial r + \rho' f_r, \\ \partial P'/\partial \theta &= \rho' \partial \phi'/\partial \theta + r\rho' f_\theta, \end{aligned}\right\} \tag{2.1}$$

where $\rho' f_r$, $\rho' f_\theta$ are the components of the disturbing force (e.g. the centrifugal force of rotation or magnetic forces), ϕ' is the gravitational potential of the star itself, P', ρ' are the hydrostatic pressure and density of the material, and (r, θ) are the distance from the centre and the angular distance from the axis of symmetry. Dashes are used to denote values in the perturbed star.

On eliminating P' from equations (2.1) we have

$$\frac{\partial \rho'}{\partial \theta} = -\frac{\chi}{g}\frac{d\rho}{dr} + \frac{1}{g}\left\{\rho \frac{\partial f_r}{\partial \theta} - \frac{\partial}{\partial r}(r\rho f_\theta)\right\} \tag{2.2}$$

correct to the first order, where g is the local acceleration of gravity and $\chi = \partial \phi'/\partial \theta$. Poisson's equation,

$$\nabla^2 \phi' = -4\pi G \rho', \tag{2.3}$$

can be used to substitute for $\partial \rho'/\partial \theta$ in (2.2), giving

$$\begin{aligned} \frac{1}{r^2}\frac{\partial}{\partial r}\left(r^2 \frac{\partial \chi}{\partial r}\right) + \frac{1}{r^2}\frac{\partial}{\partial \theta}\left(\frac{1}{\sin\theta}\frac{\partial}{\partial \theta}\{\chi \sin\theta\}\right) \\ = +\frac{4\pi G}{g}\frac{d\rho}{dr}\chi + \frac{4\pi G}{g}\left[\frac{\partial}{\partial r}(r\rho f_\theta) - \rho \frac{\partial f_r}{\partial \theta}\right]. \end{aligned} \tag{2.4}$$

The form of the left-hand side of (2.4) suggests expanding χ in a series of associated Legendre polynomials $P_n^1(\cos\theta)$. If we therefore expand f_r and f_θ in the forms

$$f_r = \sum_{s=0}^{\infty} a_s(r) P_s, \quad f_\theta = \sum_{s=1}^{\infty} b_s(r) P_s^1 \dagger, \tag{2.5}$$

---

* It is the neglect of the inertia of the circulation which enables the assumption of axial symmetry to be made, for the remaining perturbing effect, that of rotation, for example, is axially symmetrical. In an exhaustive treatment it would have to be shown that no permanent asymmetrical state, with consequently large circulation currents, is possible. Such states would probably produce non-axially symmetrical effects at the surface of the star. No such effects are observed on the solar surface, however.

† f_θ can always be expanded in this form, since it must vanish at $\theta = 0, \pi$ in order to avoid a singularity on the axis of symmetry.

while noting that $\partial P_n/\partial\theta = -P_n^1$, the general solution of (2.4) can be written

$$\chi = \sum_{s=1}^{\infty} c_s(r) P_s^1, \tag{2.6}$$

where

$$\frac{1}{r^2}\frac{d}{dr}\left(r^2\frac{dc_s}{dr}\right) - \left[\frac{s(s+1)}{r^2} + \frac{4\pi G}{g}\frac{d\rho}{dr}\right]c_s = \frac{4\pi G}{g}\left[\frac{d}{dr}(r\rho b_s) + \rho a_s\right]. \tag{2.7}$$

The boundary conditions for the cs are obtained as follows. We have $\chi \to 0$ as $r \to \infty$, hence

$$c_s \to 0 \text{ as } r \to \infty, \quad s \geqslant 1. \tag{2.8}$$

The inner boundary conditions may be obtained in terms of the temperature variation over the core surface. This variation of course depends on conditions within the core which are not dealt with in detail in this paper. If it is known that the turbulence in the core does not affect the equations of hydrostatic equilibrium appreciably, then the solutions of (2.7) can be extended right to the centre of the star. The boundary conditions in this case are

$$c_s = 0 \text{ at } r = 0, \quad s \geqslant 1. \tag{2.9}$$

The functions $\partial\rho'/\partial\theta$ and $\partial T'/\partial\theta$ can then be determined; the next step is to find the velocity components v_r and v_θ of the meridian-plane circulation in terms of these. The actual circulation is governed by the equation of thermal equilibrium. This can be written in the entropy form

$$\rho' \boldsymbol{v} \,.\, \text{grad}\, S'/\mu' = (\rho'\epsilon' - \text{div}\, \boldsymbol{H})/T', \tag{2.10}$$

where $S' = \dfrac{\mathfrak{R}}{\gamma' - 1}\log\left(\dfrac{P'}{\rho^{\gamma'}}\right)$, the entropy per g. mol. of the gas,

$\mathfrak{R}$ = gas constant,

γ' = ratio of specific heats of the gas,

μ' = molecular weight of the gas,

$\boldsymbol{H}$ = flux of radiation, and

ϵ' = rate of production of nuclear energy per gram.

In this equation the radiation pressure has been neglected. The equation can be written correct to the first order as

$$\rho\frac{Tv_r}{\mu}\frac{dS}{dr} = \rho'\epsilon' - \text{div}\, \boldsymbol{H} \tag{2.11}$$

since the left-hand side is already a first-order quantity. We can write, correct to the first order,

$$\frac{\partial}{\partial\theta}(\rho'\epsilon') = \rho\epsilon\left[\frac{\partial}{\partial T}(\log\rho\epsilon)\frac{\partial T'}{\partial\theta} + \frac{\partial}{\partial\rho}(\log\rho\epsilon)\frac{\partial\rho'}{\partial\theta}\right], \tag{2.12}$$

all quantities on the right-hand side being known. Further

$$\frac{\partial}{\partial\theta}(\text{div}\, \boldsymbol{H}) = \frac{1}{r^2}\frac{\partial}{\partial r}\left(r^2\frac{\partial H_r}{\partial\theta}\right) + \frac{1}{r}\frac{\partial}{\partial\theta}\left\{\frac{1}{\sin\theta}\frac{\partial}{\partial\theta}(H_\theta \sin\theta)\right\}, \tag{2.13}$$

in which, using the equation of radiative transfer, we have

$$\left.\begin{aligned} \frac{\partial H_r}{\partial \theta} &= -\tfrac{4}{3}ac\left[\frac{\partial}{\partial\theta}\left(\frac{T'^3}{k'\rho'}\right)\frac{\partial T'}{\partial r} + \frac{T'^3}{k'\rho'}\frac{\partial}{\partial r}\left(\frac{\partial T'}{\partial\theta}\right)\right], \\ H_\theta &= -\tfrac{4}{3}ac\frac{T'^3}{k'\rho'}\cdot\frac{1}{r}\frac{\partial T'}{\partial\theta}, \end{aligned}\right\} \tag{2.14}$$

k' being the opacity. (2.13) can therefore be written, correct to the first order, in the form

$$\frac{\partial}{\partial\theta}(\operatorname{div}\boldsymbol{H}) = \frac{1}{r^2}\frac{\partial}{\partial r}\left[r^2H\left\{\frac{\partial}{\partial T}\left(\log\frac{T^3}{k\rho}\right)\frac{\partial T'}{\partial\theta} + \frac{\partial}{\partial\rho}\left(\log\frac{T^3}{k\rho}\right)\frac{\partial\rho'}{\partial\theta} + \frac{1}{dT/dr}\frac{\partial}{\partial r}\left(\frac{\partial T'}{\partial\theta}\right)\right\}\right] + \frac{H}{r^2dT/dr}\frac{\partial}{\partial\theta}\left[\frac{1}{\sin\theta}\frac{\partial}{\partial\theta}\left(\frac{\partial T'}{\partial\theta}\sin\theta\right)\right], \tag{2.15}$$

all quantities on the right-hand side again being known. By differentiating (2.11) with respect to θ we can now write

$$\partial v_r/\partial\theta = Q(r,\theta),$$

where Q is a known function. Hence

$$v_r = \int_0^\theta Q\,d\theta + Q_1(r),$$

where $Q_1(r)$ is a function which can be determined immediately from the condition that the total rate of outflow of material over any sphere must vanish. We thus have finally

$$v_r = \int_0^\theta Q\,d\theta - \tfrac{1}{2}\int_0^\pi \sin\theta_1\int_0^{\theta_1} Q(r,\theta)d\theta\,d\theta_1. \tag{2.16}$$

The lines of flow can be found by introducing a stream function C given by

$$v_r = \frac{1}{\rho r^2\sin\theta}\frac{\partial C}{\partial\theta}.$$

C can then be expressed as

$$C = \rho r^2\int_0^\theta v_r\sin\theta\,d\theta, \tag{2.17}$$

while

$$v_\theta = -\frac{1}{\rho r\sin\theta}\frac{\partial C}{\partial r}. \tag{2.18}$$

The method just given will be used in the next section to determine the meridian-plane circulation velocity in uniformly rotating stars. This provides the simplest example of its use, although the effect of a simple non-uniform distribution of angular velocity is not essentially more difficult to handle, and does not introduce any intrinsically new factor.

3. *Calculation for uniformly rotating stars.*—The discussion will be restricted to the point-convective model with uniform molecular weight, neglecting radiation pressure and the guillotine factor in the opacity law. The Cowling model (**10**) will be used; in this case the density ρ and the temperature T are expressed in units of their central values ρ_c and T_c, while z is the radial coordinate r in Emden units given by

$$z = r\{8\pi\mu G\rho_c/5\mathfrak{R}T_c\}^{1/2}.$$

If the mass interior to any point, as expressed in units of $4\pi\rho_c\{5\mathfrak{R}T_c/8\pi\mu G\rho_c\}^{3/2}$, is denoted by m, the equation of hydrostatic equilibrium and the mass equation for the unperturbed model are given by

$$\left.\begin{aligned} dT/dz &= -5m/2(n+1)z^2, \\ dm/dz &= \rho z^2, \end{aligned}\right\} \tag{3.1}$$

where n is the effective polytropic index $d\log\rho/d\log T$. These equations will be used at several stages to simplify various expressions.

The disturbing functions f_r and f_θ are given by

$$\left.\begin{aligned} f_r &= r\Omega^2\sin^2\theta, \\ f_\theta &= r\Omega^2\sin\theta\cos\theta, \end{aligned}\right\} \tag{3.2}$$

where Ω is the angular velocity of the star. Following the method of the previous section we then find

$$\chi = r^2\Omega^2(h-1)\sin\theta\cos\theta, \tag{3.3}$$

where h is given by

$$\frac{d^2h}{dz^2} + \frac{6}{z}\frac{dh}{dz} + \frac{5n\rho}{2(n+1)T}h = 0. \tag{3.4}$$

The boundary conditions for h are

$$\left.\begin{aligned} &h \text{ finite at } z=0, \\ &h\to 1 \text{ as } z\to\infty. \end{aligned}\right\} \tag{3.5}$$

In the core of the Sun the convective equilibrium has no effect on the hydrostatic equations, significant in this problem. The velocity u of the currents is of order 2×10^3 cm./sec. according to Cowling's work (**10**). The Reynolds stresses $\frac{1}{2}\rho u^2$ are therefore of order 10^8 dynes/cm.^{2}. The gas pressure in the core is of order 10^{17} dynes/cm.^{2} and the effect of rotation, which can alter this value at any point by a factor of order 10^{-5}, reduces this to a pressure change of order 10^{12} dynes/cm.^{2}. The Reynolds stresses are therefore negligible.

The equation of thermal equilibrium (2.11) reduces to

$$\rho_c g\rho\frac{n-\frac{3}{2}}{n+1}v_r = -\operatorname{div}\boldsymbol{H}, \tag{3.6}$$

from which, following the method laid down in Section 2, we have finally

$$v_r = (1-\tfrac{3}{2}\sin^2\theta)p(z)LM^{-3}R^5(\Omega/\Omega_\odot)^2 \text{ cm./sec.} \tag{3.7}$$

In this expression M, L and R are the mass, luminosity and radius of the star in solar units, and $\Omega_\odot$ is the Sun's angular velocity, taken as $2{\cdot}85\times10^{-6}$ radians/sec., while

$$p(z) = \frac{1{\cdot}7\times10^{-12}z^5(n+1)}{m^3(n-\frac{3}{2})}\left[h\left(3-\frac{\rho z^3}{m}\right)+z\frac{dh}{dz}\right]. \tag{3.8}$$

The values of v_r calculated from this expression are given for the Sun in Table I, using the Cowling model, and the resulting circulation system is illustrated in Fig. 1.

TABLE I

Circulation velocity along rotation axis of Sun (units of 10^{-10} cm./sec.)

z	1·2	2·0	2·8	3·6	4·4	5·2	6·0	7·0
$[v_r]_{\theta=0}$	17·9	0·72	1·11	2·59	6·33	14·6	30·5	67·3

At the surface of the core the divisor $n-\frac{3}{2}$ in the expression for v_r vanishes. The resulting singularity, however, is only a formal one, since the formula is only valid when v_r is small compared with the rotation velocity. The layer in which $n-\frac{3}{2}$ is small enough to involve values of v_r of the order of magnitude of the rotation velocity is of course extremely thin, and is certainly thinner than the transition layer between the core and the radiative envelope. It will be noticed also that v_r does not vanish at the surface of the star. It has often been assumed in the past that v_r must vanish at the surface, in which case no steady state could exist in a star constrained to rotate uniformly. However, the actual physical requirement at the surface is that the radial flow of material should vanish. The required boundary condition is therefore simply that v_r is finite, and this is satisfied in this case.

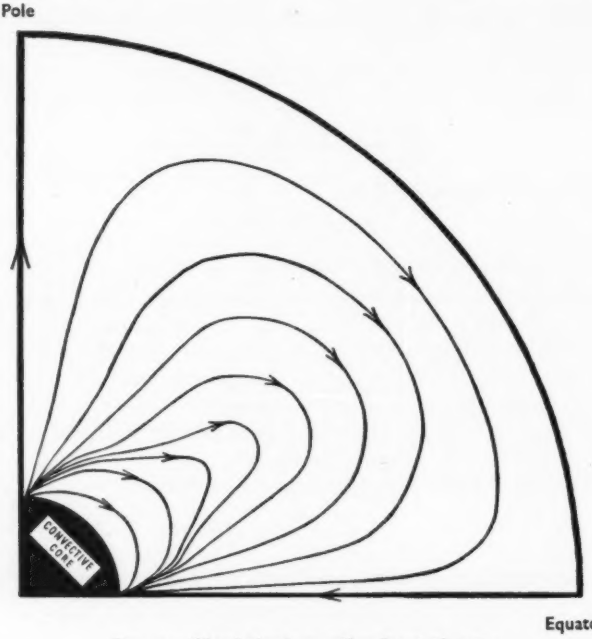

FIG. 1.—*Circulation in a uniformly rotating star*

The total time taken for material to travel from the core of the Sun to the surface along the axis of rotation is given by

$$t_\odot = \int_{r_{\text{core}}}^{R} \frac{dr}{[v_r]_{\theta=0}} \sim 8 \times 10^{12} \text{ years.}$$

4. *The maximum rotation velocity allowing non-uniform molecular weight.*—The results obtained in the previous section for the Sun can be extended to give an approximate time for circulation for stars in general by adopting the Cowling model for these also. The approximation will therefore be good for light stars, but will fall off in accuracy with increasing stellar mass, as electron scattering becomes important. Equation (3.7) shows that

$$v_r \propto L M^{-3} R^5 \Omega^2,$$

hence for stars in general the time taken for material to travel from the core to the surface along the axis of rotation is given by

$$t = L^{-1}M^3R^{-4}(\Omega/\Omega_\odot)^{-2}t_\odot \sim 8 \times 10^{12} L^{-1}M^3R^{-4}(\Omega/\Omega_\odot)^{-2} \text{ years.} \quad (4.1)$$

In discussing this expression it will be more convenient to use the equatorial rotation velocity v_0 in place of the angular velocity Ω. On taking the solar equatorial rotation velocity to be 2 km./sec. we have

$$v_0 = 2R(\Omega/\Omega_\odot) \text{ km./sec.};$$

the time t can then be written

$$t \sim 3{\cdot}2 \times 10^{13} L^{-1}M^3R^{-2}/v_0^2 \text{ years.} \quad (4.2)$$

The maximum rotation velocity which would allow the star to develop a non-uniform molecular weight is therefore given roughly by

$$v_{\max}\sqrt{10^{-9}t_1} \sim 180 L^{-1/2}M^{3/2}R^{-1} \text{ km./sec.}, \quad (4.3)$$

where t_1 years is the time which the star would normally take to develop the non-uniformity. The factor 10^9 has been introduced as a suitable time scale for t_1. By expressing R in terms of L and of T_e the effective temperature, we have

$$v_{\max}\sqrt{10^{-9}t_1} \sim 180 L^{-1}M^{3/2}(T_e/T_{e\odot})^2 \text{ km./sec.}, \quad (4.4)$$

where $T_{e\odot}$ is the Sun's effective temperature. This expression contains M, but since the range of mass is much less than the range of luminosity among stars, and since moreover there exists a rough mass-luminosity relationship, we can express M in terms of L from this relationship without undue loss of accuracy. The empirical mass-luminosity relation adopted for the purpose is given in Table II; here m denotes absolute bolometric magnitude, with $m_\odot = +4^{\mathrm{m}}{\cdot}62$.

TABLE II

Mean mass-luminosity relation adopted

m	-6	-4	-2	0	$+2$	$+4$	$+5$	$+8$
$\log_{10}M$	$+1{\cdot}35$	$+1{\cdot}08$	$+0{\cdot}80$	$+0{\cdot}53$	$+0{\cdot}28$	$+0{\cdot}06$	$-0{\cdot}17$	$-0{\cdot}42$

The results are given in graphical form in Fig. 2; here T_e has been reduced to spectral type, using the mean temperature scale for main sequence stars given by Kuiper (**11**). Stars brighter than 0^{m} begin to depart from the model used as the effect of electron scattering increases. The $v_{\max}\sqrt{10^{-9}t_1}$ curves may therefore lose accuracy above the zero magnitude line.

It must also be noted that if the star is expanding, the equation of thermal equilibrium in the form (2.10) does not hold. The effect of an expansion can be allowed for, however, by introducing an energy sink term on the right-hand side, equal to the rate at which the gravitational energy of the material at the point in question is increasing. This, like the normal energy production term and the div $\boldsymbol{H}$ term, will be spherically symmetrical to the zero order, and of the same order of magnitude as H/r. It would therefore have no essentially new effect on the circulation.

In interpreting the results embodied in Fig. 2, consider for example stars of types around A0. Such stars would take times of order 10^9 years to change

composition appreciably, due to consumption of hydrogen, this figure decreasing with increasing luminosity from star to star. On taking $t_1 = 10^9$ years, therefore, Fig. 2 shows that an Ao-type star with rotation velocity greater than 50 km./sec. would normally maintain uniform composition. Such a star could not therefore develop an isothermal core in the early part of its life, as in Chandrasekhar's work (**2**). Neither could it become a giant as the result of a discontinuity of molecular weight at the core surface, even if that were otherwise possible. On the other hand, certain theories of structure in connection with accretion of interstellar material put forward by Hoyle and Lyttleton (**4**) and by Hen and Schwarzschild (**5**) show that it might temporarily become a giant even if its rotation velocity exceeded this limit. This could take place if the non-uniformity in the outer part of the radiative envelope, due to the addition of a layer of interstellar material on the surface, were built up more rapidly than the internal circulation currents could smooth it out. Once such a non-uniformity were established it would take a far larger rotation rate than normal to smooth it out again, since the forces tending to restore a distorted surface of constant molecular weight in a region of non-uniformity are comparable with the gravitational forces themselves.

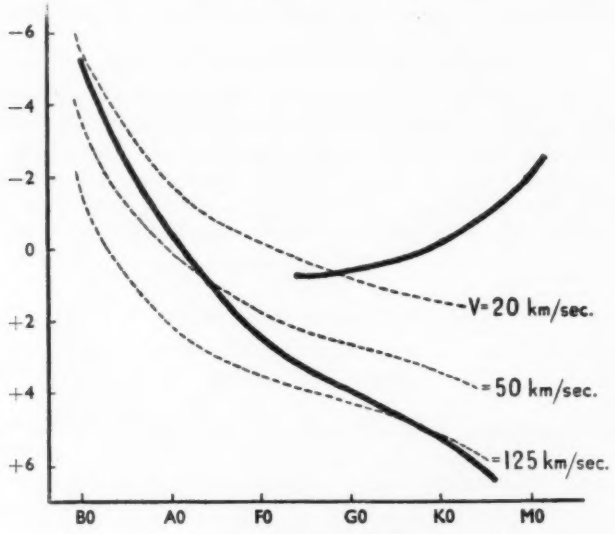

FIG. 2.—*H–R diagram*

$V_{max} = V\sqrt{10^9/t_1}$.

Turning now to the actual observed rotation velocities, using Struve's 1945 survey (**12**), it is interesting to note that A- and B-type stars (which would be massive enough to form giants) do in fact rotate with velocities in the neighbourhood of 50 km./sec.

5. *The effects of magnetic fields and viscosity.*—The most important effect is that the angular velocity is constrained, by magnetic fields, to be constant along the lines of force, according to the Ferraro–Alfvén law of isorotation (**13**). In thus preventing any special distribution of angular velocity from being set up

by the meridian-plane circulation a magnetic field would play an important part in stabilizing the circulation against breaking up into cellules. A magnetic field also exerts a force in meridian planes and can contribute, along with the centrifugal force of rotation, to the net rate of circulation. The mechanical force exerted by a field of H gauss produced by electric currents in a region of dimensions of order l cm. is of order $H^2/4\pi l$ dynes/cm.^{3}. In the inner part of the radiative envelope of the Sun, for example, if H is taken as 10^4 gauss and $l \sim 10^{10}$ cm. this force would be of order 10^{-3} dynes/cm.^{3}. This is negligible compared with the centrifugal force which is of order 1 dyne/cm.^{3} in this region. The action of the field in impeding the circulation is also negligible. The author has shown (**14**) that the action of a magnetic field on material moving in it is like that of a semi-permeable membrane. A force $\sigma H^2 v$ dynes/cm.^{3} is exerted by the field opposing the motion of material moving across the lines of force, where σ e.m.u. is the conductivity of the material and v cm./sec. is the relative velocity of the material perpendicular to the lines of force. Taking $\sigma \sim 10^{-4}$ e.m.u. together with $v \sim 10^{-10}$ cm./sec. and $H \sim 10^4$ gauss, this force is of order 10^{-6} dynes/cm.^{3}; this again is negligible as compared with the centrifugal force. The relative effect of the magnetic field may increase in the outer regions where the density is less, but Table I shows that the time of circulation is determined principally by conditions in the inner part of the radiative envelope where v is least. These rough considerations show that magnetic effects are not likely to contribute directly to the general mixing throughout the star, except possibly in individual giant stars in the unlikely event of their having low angular velocity accompanied by a strong magnetic field.

With circulation velocities as small as involved in the theory, viscosity plays a negligible part in the equations of motion in meridian planes. The only appreciable influence which viscosity effects could have is through the viscous production of heat affecting the thermal equilibrium. Here again the normal viscosity effect is negligible, although turbulent viscosity in non-uniformly rotating stars might give rise to an appreciable source of heat. The usual conditions for turbulent flow in a fluid cannot however apply in a radiative envelope owing to the high degree of thermal stability there. It is therefore doubtful whether differential rotation could produce turbulence.

6. *Conclusions.*—(i) Meridian-plane circulation currents in stars are much slower than has been supposed hitherto.

(ii) In fast-rotating stars, except possibly where no magnetic field is present, the meridian-plane circulation in radiative envelopes stirs material from the convective core throughout the whole star.

(iii) The resulting homogenizing effect on the chemical composition would be sufficient to prevent early A-type and late B-type stars with equatorial rotation velocities greater than 50 km./sec. from becoming giants as the result of inhomogeneity in the central regions. It would likewise prevent these stars from developing isothermal cores through local exhaustion of hydrogen. The corresponding figure is higher for the earlier B types.

(iv) The effects of accretion of small quantities of interstellar material would be more likely to form giants from highly rotating stars than from slowly rotating ones. Giants, once formed in this way, would remain as giants even if highly rotating, since a discontinuity in molecular weight, once formed, cannot easily be broken down by meridian-plane circulation.

(v) The observed rotation velocities of early-type stars are of the same order of magnitude as the critical values. This would produce bifurcations in the evolutionary tracks of stars of a given mass, according to rotation, if acted on by the processes mentioned in (iii) and (iv). Stars later than F5 have small rotation velocities, and are not subject to a significant mixing effect due to rotation.

University Observatory,
Glasgow :
1950 *October* 11.

References

(1) A. S. Eddington, *M.N.*, **90**, 54, 1929.
(2) M. Schönberg and S. Chandrasekhar, *Ap. J.*, **96**, 161, 1942.
(3) M. Hall Harrison, *Ap. J.*, **103**, 193, 1946; *Ap. J.*, **106**, 322, 1947.
(4) F. Hoyle and R. A. Lyttleton, *M.N.*, **102**, 218, 1942; *M.N.*, **109**, 614, 1949.
(5) Li Hen and M. Schwarzschild, *M.N.*, **109**, 631, 1949.
(6) J. Wasiutynski, *Astrophysica Norvegica*, **4**, 1946.
(7) M. Schwarzschild, *Ap. J.*, **106**, 427, 1947.
(8) See A. S. Eddington, *Internal Constitution of the Stars*, Cambridge, 1926.
(9) S. Chandrasekhar, *M.N.*, **93**, 390, 1933.
(10) T. G. Cowling, *M.N.*, **96**, 42, 1936.
(11) G. P. Kuiper, *Ap. J.*, **88**, 429, 1938.
(12) O. Struve, *Pop. Astron.*, **53**, 201, 1945.
(13) V. C. A. Ferraro, *M.N.*, **97**, 458, 1937.
(14) P. A. Sweet, *M.N.*, **110**, 69, 1950.

TRANSPORT OF HEAT AND MATTER BY CONVECTION IN STARS

E. J. Öpik

(Received 1950 December 1)*

Summary

A quantitative analysis of the transport of heat in thermal convection is developed. An essential improvement consists in allowing for the lateral exchange of heat between the turbulent elements. The analysis is applied to the case of a medium with an originally stable stratification by molecular weight†, and to Coriolis stratification of convection itself produced by rotation.

The start of small-scale convection may be prevented by the radiative exchange of heat. Quantitative conditions of the start of convection are investigated. As compared with radiation, viscosity is an insignificant factor in impeding thermal convection.

The mixing efficiency, or the transport of matter by thermal convection in a stratified medium is investigated.† The mixing efficiency is strongly influenced by rotation. At a certain limiting angular speed of rotation thermal convection may be stopped altogether.

The propagation of convection in a metastable " super-adiabatic " layer (in which the temperature gradient exceeds the adiabatic value, but which possesses a stable stratification by molecular weight) is investigated. The process of mixing in such a layer involves time intervals of the order of 10^5–10^6 years, for a solar mass. The bearing of these results upon a theory of the ice ages is considered.

---

1. *General survey and introduction.*—Formulae for the *convective transport of heat* in free thermal circulation are improved by allowing for the lateral exchange of heat; the corrected formulae represent experimental data within ± 20 per cent, whereas the earlier formulae overestimate the transport by a factor of about 30. The formulae are extended to the cases of *stratification by molecular weight* and *Coriolis deflection in a rotating medium*; in the latter case, when the angular velocity of rotation exceeds about one-tenth of the solar value, a fixed average thermal gradient establishes itself as given by formula (31), independent of the absolute value of the convective transport. For solar rotation the relative *excess of the temperature gradient* is about 5×10^{-5}, which is small but much larger than former estimates indicated; in the convective regions of fast-rotating stars the gradient may reach two or three times the adiabatic value.

A *necessary condition for convection to persist* in a stratified rotating medium is given by formula (44). Radiative transfer of heat impedes small-scale convection by equalizing the differences of temperature before regular motion can start; on this account an initial "push" is required to set convection going. At the solar rate of rotation the "push" amounts to a differential velocity about 0·5 cm./sec. in the deep interior, and about 200 cm./sec. in subphotospheric regions; differences in the angular velocity of rotation accumulating within 10^8–10^9 years can provide for the "push" required to overcome the damping of

* Received in original form 1950 September 28.

† The stratification persists, although in a smaller degree, while convection is active.

convection by radiation. As a result, convection is expected to set in suddenly over a zone of finite width.

Viscosity (gas and radiative) is capable of preventing small-scale circulation from starting, but its effect is subordinate to the much more powerful damping of convection by radiative exchange of heat and need not be considered.

Formulae for the *convective transport of matter* and mixing in a stratified rotating medium are derived, based upon the same principles as the formulae for the transport of heat. In the particular case of stratified hydrogen and for an established steady flow of heat formula (77) gives the material flow as a function of the logarithmic gradient of the molecular weight, μ'; the flow does not steadily increase with the gradient but, attaining a maximum at μ'_m (depending upon rotation), drops down to zero at μ'_0 which corresponds to the limiting case of formula (44); the material flow cannot exceed the absolute maximum set by formula (80) save in the case of a violent upset of hydrostatic equilibrium.

In a *convective core* convection is impeded by rotation; at the centre and at the boundary of the core convection is stopped and replaced by radiative equilibrium; these zones of calmness increase in extent with increasing speed of rotation, until they join and convection ceases in the core altogether, at about $\omega = 9 \times 10^{-4}$ for a solar model. For solar rotation, $\omega = 3 \times 10^{-6}$, the effect is negligible. From a consideration of the balance between the transmutation of hydrogen by nuclear reactions and the supply from outside by convection, another closer lower limit to ω stopping convection in the core may be set; for a solar model the limit is only about 7 per cent below the above-mentioned absolute limit.

In a *super-adiabatic* layer, in which the temperature gradient exceeds absolutely the adiabatic value but which still remains in radiative equilibrium on account of stratification by molecular weight, convection once locally started spreads gradually over the whole layer. The mixing of material and the simultaneous changes of structure may cause changes in the luminosity; such changes in luminosity may possibly be responsible for the terrestrial climate anomalies during "ice ages". The time of spread of the disturbance is calculated (Table VIII) for a particular model with pronounced internal stratification of hydrogen; for solar dimensions one-half of the zone (of a total width of 60,000 km.) is covered in 200,000 years, but the rate of propagation is gradually decreasing and the most important "deep" stage of mixing is covered between two and six million years; these figures are well within the order of magnitude of the Quaternary—Pre-Quaternary duration of the climatic changes on the Earth's surface.

With nuclear energy generation and an adiabatic equation of state governing mixing, a small contrast in the hydrogen abundance leads to a decrease, a large contrast to an increase in the energy output as the result of mixing. The latter case, i.e. an increase of the energy output, is required to explain the decrease in external radiation, which should thus correspond to an advanced "deep" stage of mixing (**14**).

The main theses of the present paper were worked out by the writer in 1939–1943, at Tartu Observatory. The paper is one of a series of publications, all considering the problems of stratification and convection in stars from the standpoint of evolution and long-term variability of the luminosity; special

attention is paid to the Sun, as geological records provide observational evidence of its variability, indisputable for the Quaternary and more vague for the earlier periods of the Earth's life. Continued research on these lines may throw more light on the general trend of stellar evolution and perhaps also on such particular problems as the cluster-type variables and the difference between stellar populations I and II, to be explained as difference in age.

The author's thanks are due to Dr Eric M. Lindsay, Director of Armagh Observatory, for providing facilities for these researches; to Dr L. Biermann for valuable discussions on related subjects; and especially to Professor T. G. Cowling for critical comments and help in preparing the manuscript for press.

2. *Convective transport of heat.*—For the theory of stellar structure the knowledge of the turbulent transport of heat is in certain cases of primary importance. However, the theory of turbulence developed by Taylor (**1**), Prandtl (**2**), Schmidt (**3**), and others, is far from satisfactory in this respect. Biermann (**4**) has used formulae which are in agreement with Prandtl's conception of the mixing length and with the theory of Schmidt; a review of the question is given by Wasiutynski (**5**). From mere dimensional considerations Öpik (**6**) deduced independently a formula for the convective vertical transport of heat (formula (22) in (**6**)) which, upon check, is found to coincide exactly with Biermann's corresponding formula. Unfortunately, the formula must be acknowledged to be incorrect, yielding vertical heat transport values which are too large by a factor of the order of 30; the agreement between Öpik and Biermann can be traced to their common postulate "that the turbulent elements undergo adiabatic processes along their mixing paths . . . but that at the terminating points of their paths, they discontinuously exchange heat with the medium under constant pressure" ((**5**), p. 20). Now, if "the simple formulae of Schmidt and Prandtl prove to account approximately for the mechanical and thermal effects of turbulence by horizontal linear mean flow and horizontal stratification" ((**5**), p. 24)*, in the absence of the forced horizontal flow, in free thermal convection in which temperature differences are the immediate cause of motion, the result is quite different. The turbulent element *does* interchange heat with the medium all along its path, its motion being far from adiabatic; at the "terminating points", on the contrary, there is no reason to assume a discontinuous complete exchange of heat, the exchange rate being there about the same as it is along the path. If the continuous exchange of heat is allowed for, a radical change in the coefficient of the formula for convective transport results.

By the condition of continuity each rising element of mass has its counterpart in an equal descending mass; the two elements will interchange heat by lateral contact (direct or indirect) and part of the heat which should have gone up is intercepted by the descending element and transported back. This process we try to evaluate by approximate or dimensional formulae, assuming as a guiding framework the model of cellular turbulence (**7**) without implying necessarily the existence of the cellular type in any particular case; formulae derived for the cellular model will apply, within an order of magnitude, to the general case of turbulent interchange of heat. The turbulent stresses $\Delta p/p$ being small, the ordinary equations of hydrostatic equilibrium remain practically valid.

* Such as in the case of wind sweeping over a horizontal surface, the flow being independent of existing local temperature differences and turbulence being produced by mechanical effects—the common case of Micro-Meteorology.

Consider a gaseous turbulent layer of depth H, assumed flat and horizontal, "heated from below", i.e. transporting heat outwards; let the average diameter of the *major* convective cells (elements) be D (the polygonal cross-sections of the cells we represent by circles, to simplify the order-of-magnitude formulae). Further let K be the vertical (radial) convective transport of heat (erg/sec./cm.^{2} of horizontal cross-section); v, the effective *mean* vertical velocity of ascent or descent; ΔT_l, the mean "lateral" difference of temperature on the same level between the ascending and descending currents; ΔT_r, the mean excess vertical difference of temperature (positive when decreasing outward, as is in practice the case) at the bottom, or at the top of the cell, i.e. the temperature "jump" (in excess of the normal gradient) between the layers outside and inside the bottom or inside and outside the top surface (polygon); s, the effective coefficient of "contact" heat transfer (erg/cm.^{2}/sec./deg.), consisting of a turbulent, a radiative and a conductive component; ρ, the density; c_p, the specific heat; $\xi = dT/dr (<0)$, the vertical temperature gradient; ξ_i, the effective vertical gradient inside the cell; $\bar{\xi}$, the average radial gradient (including the temperature "jump", and the average gradient of hydrostatic equilibrium); ξ_a, the adiabatic gradient. The warm ascending current occupies the core of the cell (**7**), of a diameter $D/\sqrt{2}$ and a conventional cross-section $\pi D^2/8$; the cold descending current covers an equal cross-section in the polygonal ring (between $D/\sqrt{2}$ and D) enclosing the core; the area of lateral surface of separation between the ascending and descending branches is set equal to $\pi DH/\sqrt{2}$.

The coefficient of contact heat transfer s is defined as such that $s\Delta T$ is the flux of heat per unit area across an interface at which there is a temperature jump ΔT. Thus the contact flux of heat (in excess of the average radiative flux) directed upward across the bottom or the top surface of the cell is $s\Delta T_r . \pi D^2/4$. On the other hand, the flux is equal to the difference in the heat content of the ascending and descending current, or to

$$\rho v c_p . \Delta T_l . \frac{\pi D^2}{8} = s . \Delta T_r . \frac{\pi D^2}{4} = K . \frac{\pi D^2}{4}. \tag{1}$$

Hence
$$\Delta T_r = \Delta T_l / 2f, \tag{2}$$

where
$$f = \frac{s}{\rho v c_p} \tag{3}$$

is a non-dimensional parameter of the heat transfer.

Inside the cell, the lateral flux of heat from the ascending toward the descending current is equal to the loss of the potential heat content along the ascending current, or

$$s . \Delta T_l . \frac{\pi DH}{\sqrt{2}} = \rho v c_p (\xi_a - \xi_i) H . \frac{\pi D^2}{8}. \tag{4}$$

Further, the average radial gradient is

$$-\bar{\xi} = -\xi_i + \frac{\Delta T_r}{H}. \tag{5}$$

From (4), (5), (3) and (2) it is easy to obtain

$$\Delta T_r = \frac{H(\xi_a - \bar{\xi})}{B}, \tag{6}$$

$$\Delta T_l = \frac{2fH(\xi_a - \bar{\xi})}{B}, \tag{7}$$

where B is a second non-dimensional parameter of the turbulent system

$$B=1+8\sqrt{2}f^2.H/D. \tag{8}$$

From (1) we obtain

$$K=\rho v c_p H(\xi_a-\bar{\xi}).f/B; \tag{9}$$

this differs from the former expression (**4, 6**) mentioned above by the factor f/B (of the order of 0·1).

Assuming the average stream velocity equal to one-half of the "top" velocity acquired in falling a distance H under the excess gravity $g\Delta T_l/T$, $\Delta T_l/T$ being small,

$$v\cong\tfrac{1}{2}\sqrt{2gH.\Delta T_l/T}, \tag{10}$$

g denoting the effective acceleration of gravity. With the aid of (7) we obtain

$$v=H\sqrt{\frac{g(\xi_a-\bar{\xi})}{T}.\frac{f}{B}}, \tag{11}$$

and from (9) and (11) the formula for the turbulent flow of heat

$$K=\rho c_p.H^2\left(\frac{g}{T}\right)^{1/2}(\xi_a-\bar{\xi})^{3/2}.\left(\frac{f}{B}\right)^{3/2}. \tag{12}$$

Here the correction factor $(f/B)^{3/2}\sim 1/30$ represents the difference as compared with the former formula (**4, 6**).

From (11) and (12) we obtain also

$$v=\left(\frac{HgK}{\rho c_p T}\right)^{1/3}, \tag{13}$$

in which now the correction factor has disappeared; this remarkable formula used by Biermann (**4**) thus remains unchanged.

All the above dimensional formulae assume the relative vertical variation of ρ over H to be small. In such a case we may apply the principle of the approximate constancy of the stream cross-section along the circuit (in the case of non-forced circulation); equating the lateral upper or lower half cross-section $\pi DH/2\sqrt{2}$ to the horizontal cross-section of the ascending or descending branch, $\pi D^2/8$, we get as an order-of-magnitude approximation

$$\frac{D}{H}=2\sqrt{2}, \tag{14}$$

whence (8) becomes

$$B=1+4f^2. \tag{15}$$

For a purely turbulent transport of heat f is usefully interpreted as

$$f=\tfrac{1}{2}\overline{|\sin\alpha|}, \tag{16}$$

where α is the angle of meridional deviation of the motion at a given point from the mean direction, so that $w\sin\alpha$ is the "mixing component" or the turbulent component of velocity normal to the gliding surface, w denoting the absolute average of the velocity vector. Thus f is a measure of "micro-turbulence" of the first order of smallness relative to the "macro-turbulence" of the regular cellular circuit which we have used as a model; it determines the dissipation rate of the major circulation. Terrestrial wind near the Earth's surface represents an observable case of such dissipation (although here the "gliding surface" is

not determined as the ever-changing surface of contact of two gaseous stream elements, but is fixed by the solid but rough surface of the soil). From unpublished micro-meteorological observations with a special hand-anemometer, Öpik has observed the fluctuations of α as the inclination of wind motion to the horizon. Values of $\overline{|\sin\alpha|}$ from 0·1 to 0·3 were obtained, according to locality and weather, with an average of 0·2, whence a provisional value of $f=0{\cdot}1$ may be assumed; this figure corresponds to a feeble persistence of a given cellule of circulation, amounting to from one to three cycles of the circulation, which is about the persistence of photospheric granules. For a completely random distribution of velocities $\overline{|\sin\alpha|}=0{\cdot}50$; hence an upper limit for f in the case of pure turbulence can be assigned,

$$f<0{\cdot}25.$$

Perfectly regular (laminar) motion corresponds to $f=0$; in this case by (12) the convective transport vanishes, and all the transport that remains is by conductivity and radiation.

Generally $f=f_t+f_r$, f_t referring to turbulent transport (when necessary, together with conductivity), f_r to radiative. f_r decreases with opacity and with the increasing size of the turbulent elements. In stellar interiors f_r is estimated at about 10^{-8} to 10^{-10} or less and is negligible, so that for the major portion of the star $f=f_t=0{\cdot}1$ can be assumed, neglecting altogether the component f_r. For a subphotospheric layer, however, $T=12{,}700$ deg., $\rho=5\times10^{-8}$ g./cm.^{3}, opacity $\kappa=70$, $v=10^5$ cm./sec., we find $f_r\cong1$, thus large.

Table I gives the value of the "convective transport factor", f/B and $(f/B)^{3/2}$, with B given by (15).

TABLE I

Convective Transport Factor (for $B=1+4f^2$)

f	0	0·05	0·10	0·15	0·20	0·25	0·5	1	2	5	∞
f/B	0	0·050	0·096	0·14	0·17	0·20	0·25	0·20	0·12	0·050	0
$(f/B)^{3/2}$	0	0·011	0·032	0·05	0·07	0·09	0·125	0·09	0·04	0·011	0

The factor is zero both for $f=0$ (no exchange) and $f=\infty$ (perfect exchange of heat and equalization of the temperature of the ascending and descending elements); its slow variation with f is worthy of comment, its value remaining within the same order of magnitude for f between 0·05 and 5. This circumstance is rather advantageous, a change of f especially toward the higher values being of little consequence. In the following we may assume with confidence the provisional value $f=0{\cdot}1$, $(f/B)^{3/2}=0{\cdot}032$; the data for aerodynamical friction confirm this value (*cf.* Section 8).

An observational check of the theory can be provided by laboratory experiments on free thermal convection in air between two horizontal surfaces (warm lower surface). Because of the small scale ξ_a may be neglected; $-\bar{\xi}$ is $(T_1-T_2)/b$, where b is the distance between the surfaces and T_1, T_2 are their temperatures ($T_1>T_2$). Thus (12) yields

$$K=\rho c_p\,.\,\frac{H^2(T_1-T_2)^{3/2}}{b^{3/2}}\left(\frac{f}{B}\right)^{3/2}\left(\frac{g}{T}\right)^{1/2}. \qquad (17)$$

For horizontal surfaces $H=b$. Unfortunately the experiments available refer to vertical surfaces (**8**). A modification of the theory is thus required, to adapt it

to vertical surfaces. Without going into details, we may say that an additional factor k in (17) is required; with a model of polygonal cells of 45° inclination,

$$k=\sqrt[4]{2}\left(\frac{1+4f^2}{1+4\sqrt{2}f^2}\right)^{3/2}=1{\cdot}17;$$

with solenoidal circulation at 45° inclination,

$$k=\sqrt{1+\sqrt{2}}\left(\frac{1+4f^2}{1+16f^2}\right)^{3/2}=1{\cdot}32.$$

The average may be taken as $k=1{\cdot}24$. On the other hand, there is a general upward flow along the warm surface, a downward flow along the cold surface; by the shearing action of these opposite currents the space in between must be divided into two convectional systems of circulation, with $H=b/2$ in each. The convective flow for the vertical surfaces should thus be

$$K'=0{\cdot}31\rho c_p b^{1/2}(T_1-T_2)^{3/2}\left(\frac{f}{B}\right)^{3/2}\left(\frac{g}{\bar{T}}\right)^{1/2}, \tag{18}$$

or 0·31 of the flow for the horizontal surfaces, which agrees, qualitatively at least, with the statement that for a horizontal space the convectional loss "is greater than for a similar vertical space" (**8**). The comparison of formula (18) with the laboratory data is as follows, the experimental data being corrected, first for radiation and then for conductivity of air, to obtain pure turbulent transport (for $b\leqslant 1{\cdot}5$ cm. the flow is apparently laminar and the share of turbulent transport is almost nil):

TABLE II

Turbulent Transport of Heat, cal./cm.² hour

$b=2$ cm. $T_1-T_2=10°$		$b=2$ cm. $T_1-T_2=25°$		$b=3$ cm. $T_1-T_2=10°$		$b=3$ cm. $T_1-T_2=25°$	
obs.	calc.	obs.	calc.	obs.	calc.	obs.	calc.
0·89	0·72	3·62	2·85	1·24	1·14	4·28	4·50

As to the order of magnitude, the agreement is excellent. The omission of the factor $(f/B)^{3/2}$ would yield values 30 times larger.

3. ***Convection in a medium stratified according to molecular weight.***—Set $d\mu/dr=-\eta$ ($\eta>0$ normally), μ being taken at equal conditions of ionization, i. e. η is not the true gradient of molecular weight, but the difference between the true gradient and the gradient which would obtain in a medium of uniform chemical composition.

Instead of (10),

$$v\cong\tfrac{1}{2}\sqrt{2gH\left(\frac{\Delta T_l}{T}-\frac{\Delta\mu_l}{\mu}\right)}, \tag{19}$$

where $\Delta\mu_l$ is the difference in molecular weight between the ascending and descending branches at the same level. By analogy with formula (7), $\Delta\mu_l$ depends upon $d\mu/dr$ exactly in the same manner as ΔT_l depends upon $\bar{\xi}=dT/dr$; thus, with $\eta_a=0$ ("adiabatic gradient of molecular weight"),

$$\Delta\mu_l=\frac{2f}{B}H\eta, \tag{20}$$

with $f/B=(f/B)_t$ (corresponding to turbulence only).

Setting

$$\theta=(\eta/\mu)/[(\xi_a-\bar{\xi})/T], \tag{21}$$

and neglecting f_r as before, the formulae of Section 2 are transformed with the aid of (19), (20) and (21) into

$$K=\rho c_p \cdot H^2\left(\frac{g}{T}\right)^{1/2}(\xi_a-\bar{\xi})^{3/2}\left(\frac{f}{B}\right)^{3/2}\cdot(1-\theta)^{1/2}; \tag{22}$$

$$v=\left[\frac{HgK(1-\theta)}{\rho c_p T}\right]^{1/3}; \tag{23}$$

$$v=H\sqrt{\frac{g(\xi_a-\bar{\xi})}{T}\cdot\frac{f\cdot(1-\theta)}{B}}. \tag{24}$$

In the case when f_r is not negligible, putting $f=f_t+f_r$, and

$$m=\left(\frac{f}{B}\right)\Big/\left(\frac{f_t}{B_t}\right)>0, \tag{25}$$

the new forms of formulae (22), (23), (24) are found by substituting $m-\theta$ for $1-\theta$, $m\rho$ for ρ, and $(f/B)_t$ for (f/B).

4. *Rotation and thermal convection.*—In a medium where horizontal shearing motions are absent, the effective value of $H=r_2-r_1$ may be assumed equal to the whole depth of the unstable layer provided that this does not exceed the maximum value corresponding to the condition

$$\frac{\rho_2 r_2^2}{\rho_1 r_1^2}\cong e^{-1} \tag{26}$$

(*cf.* (**6**), p. 12), where ρ_1, r_1 are density and radius at the bottom, ρ_2, r_2 those at the top of the layer H; if the depth of the unstable layer exceeds the limit, two or more superposed convective layers should be postulated. Shearing motion with a velocity of the order of v or larger will produce additional stratification. The Coriolis deflection in a rotating body is a cause of such stratification. As long as $\omega(r_2-r_1)=\omega H$ is small as compared with v(ω = angular velocity of rotation), the limitation to H is set by equation (26); such is apparently the case near the surface of the Sun. In the interior, however, v is small (because ρ is large) and rotational deflection of the vertical current produces stratification into layers of a thickness $H=H_r$, smaller than the limit set by (26). For the order of magnitude we set in this case

$$H_r\cong\frac{v}{\omega\cos\phi}, \tag{27}$$

where ϕ is the latitude (*cf.* below).

Substituting (27) for H in (23) we obtain a different expression for velocity:

$$v=\left[\frac{gK(1-\theta)}{\rho c_p T\cdot\omega\cos\phi}\right]^{1/2}. \tag{28}$$

Substituting this into (27):

$$H_r=\left[\frac{gK(1-\theta)}{\rho c_p T}\right]^{1/2}(\omega\cos\phi)^{-3/2}, \tag{29}$$

valid only when H_r falls below the limit (26).

Substituting (29) into (22), K cancels and the remarkable formula is obtained (also obtainable from (24) and (27)):

$$\xi_a-\bar{\xi}=\frac{T(\omega\cos\phi)^2}{g(1-\theta)\cdot(f/B)}. \tag{30}$$

When convective equilibrium is established, the temperature gradient $\bar{\xi}$ is determined by $\omega\cos\phi$ (if not too small) independently of the flux K, or of the velocity v.

Substituting (21) into (30), it is easy to obtain

$$\frac{\xi_a-\bar{\xi}}{T}=\frac{(\omega\cos\phi)^2}{g\cdot(f/B)}+\frac{\eta}{\mu}. \tag{31}$$

If f_r is not negligible, in equations (28)–(31) $1-\theta$, ρ, f/B and in (31) $(\xi_a-\bar{\xi})/T$ are replaced by $m-\theta$, $m\rho$, $(f/B)_t$ and $m(\xi_a-\bar{\xi})/T$. Equation (31) imposes a condition upon the temperature gradient which is not *a priori* in agreement with the equations of hydrostatic equilibrium of the rotating star. This means zonal instability in a sense analogous to the instability required by von Zeipel's theorem (**9**); purely radial turbulence is impossible, meridional circulation inevitably arising in the convective region of a rotating star.

Let us inquire closer into the reasons for the assumption expressed by equation (27). Consider the Coriolis deflection of a small turbulent element moving without friction and assuming everywhere the density of the medium; for simplicity take $\omega=$const., and suppose the element to move in the equatorial plane, with coordinates x, y, $(r^2=x^2+y^2)$. Such an element is subject to the same gravitational force and pressure gradient as the medium itself; thus it is given the same (centripetal) acceleration as the medium, and its equations of motion are

$$\frac{d^2x}{dt^2}=-\omega^2x, \quad \frac{d^2y}{dt^2}=-\omega^2y.$$

Starting with the following initial conditions at $t=0$: $x=r_0$, $y=0$, $dx/dt=u\omega r_0$ (initial vertical velocity), $dy/dt=\omega r_0(1+w)$ ($w\omega r_0$ is the initial tangential velocity), the equations of motion lead to the solution

$$x=r_0\sqrt{1+u^2}\cos(\omega t+c),$$
$$y=r_0(1+w)\sin(\omega t),$$

with

$$\cos c=\frac{1}{\sqrt{1+u^2}}, \quad \sin c=-\frac{u}{\sqrt{1+u^2}}.$$

With respect to the radius it is a periodic solution with a period π/ω, or half the period of revolution. Take the simplest case of a vertical initial velocity, $w=0$:

$$r^2=x^2+y^2=r_0^2[(1+u^2)\cos^2(\omega t+c)+\sin^2(\omega t)].$$

From that the extreme values of r are found:

$$\binom{\text{max.}}{\text{min.}}\left(\frac{r}{r_0}\right)=\sqrt{(1+\tfrac{1}{2}u^2)\left(1\pm\frac{u}{\sqrt{1+u^2}}\right)}.$$

Between these extreme distances a closed trajectory is described with respect to the rotating medium, the direction of the vortex being opposite to rotation.

When u is small,

$$\left(\frac{r}{r_0}\right)_{\text{max.}}=1+\tfrac{1}{2}u, \quad \left(\frac{r}{r_0}\right)_{\text{min.}}=1-\tfrac{1}{2}u,$$

and the total amplitude in r becomes $r_{\text{max.}}-r_{\text{min.}}=H=ur_0$, or, with $v=u\omega r_0$, $H=v/\omega$ which is identical with formula (27). Even when the whole medium is

stirred by convection, the medium as a whole, consisting of a great number of turbulent elements with random characteristics, may be assumed at rest except for the general rotation, wherefore the Coriolis deflection as considered above applies to thermal convection, and the dimensions of the vortices created, or the vertical free paths of the turbulent elements, are of the order given by equation (27).

5. *Thermal convection in dwarf stars.*—Within a turbulent region we may assume constancy of molecular weight, thus $\eta = 0$ as a first approximation. The temperature gradient is given by the formula (*cf.* (42) below)

$$\frac{dT}{dr} = \xi = -\frac{g\mu}{\mathfrak{R}(n+1)}, \tag{32}$$

where g is the effective acceleration of gravity (depending itself upon ω and ϕ), $n = d\log P/d\log T - 1$ the polytropic index.

Hence

$$\xi_a - \bar{\xi} = \frac{(n_a - n)}{(\bar{n}+1)(n_a+1)} \frac{g\mu}{\mathfrak{R}} = \frac{T(\cos\phi)^2}{g\,.\,(f/B)}$$

according to (31) ($\eta = 0$), and with ξ_a determined by (32) with $n = n_a$,

$$\frac{\xi_a - \bar{\xi}}{-\xi_a} = \frac{(n_a - \bar{n})}{\bar{n}+1} = \frac{(n_a+1)\,\mathfrak{R}}{\mu(f/B)} \frac{T(\omega\cos\phi)^2}{g^2}. \tag{33}$$

For average conditions in the interior

$$\bar{T} = \tfrac{2}{3}T_c = -\tfrac{2}{3}\bar{\xi}R = \frac{2}{3}\frac{\bar{g}\mu R}{\mathfrak{R}(\bar{n}+1)}, \quad \bar{g} \cong 2g_0,$$

(g_0 = surface gravity, R = surface radius), whence (33) yields for an assumed completely convective structure,

$$n_a - \bar{n} \cong \frac{(n_a+1)}{3(f/B)} \frac{R(\omega\cos\phi)^2}{g_0}. \tag{34}$$

For a convective Sun, with $\omega = 3\times10^{-6}$, $\overline{\cos^2\phi} = 2/3$, $f/B = 0{\cdot}096$, $n_a = 1{\cdot}5$, $R \cong 7\times10^{10}$, $g_0 \cong 3\times10^4$, we find $n_a - \bar{n} \cong 1{\cdot}3\times10^{-4}$, $(\xi_a - \bar{\xi})/(-\xi_a) \cong 5\times10^{-5}$. This deviation from adiabatic equilibrium is still quite small and justifies the use of $n = n_a$ in calculations of stellar structure over thermal convective regions; the deviation is, however, much larger than former estimates gave (**4, 6**) when f/B and rotation were not allowed for.

Our formulae hold as long as H_r does not exceed its limit given by (26). For average conditions in the interior as assumed above,

$$\bar{\rho} = 0{\cdot}55\rho_c = 3{\cdot}3\rho_m (n = 1{\cdot}5,\ \rho_c/\rho_m = 6), \quad \overline{K} \sim L/12R^2,$$

formula (29) yields

$$\bar{H}_r \cong \left(\frac{L}{8{\cdot}8\rho_m \pi R^3}\right)^{1/2} (\omega\cos\phi)^{-3/2} = \left(\frac{L}{6{\cdot}6M}\right)^{1/2} .\, (\omega\cos\phi)^{-3/2}. \tag{35}$$

On the other hand, condition (26) for the average interior (not near the surface) requires $H \leqslant 0{\cdot}4R$, whence from (35)

$$\omega\cos\phi \geqslant \left(\frac{L}{1{\cdot}06MR^2}\right)^{1/3} \text{ in c.g.s. units} \tag{36}$$

is the condition of the validity of equations (27)–(35).

For the solar luminosity, mass and radius the limit is at

$$(\omega\cos\phi)_\odot \geqslant 7\times10^{-8}\,(\text{sec.}^{-1}). \tag{37}$$

For the solar rotation, $\omega = 3 \times 10^{-6}$; this gives $\cos\phi \geqslant 0{\cdot}023$, $\phi < 88°{\cdot}7$ and, as with $H \sim 0{\cdot}4R$ the diameter of the turbulent cell is much larger than the $90° - 88°{\cdot}7 = 1°{\cdot}3$ of latitude, there is no "loophole" in polar direction; for the main bulk of the star with about solar rotation (or faster), the equations are valid in all latitudes. Near the surface, however, (29) ceases to be valid, with ρT and the limit given by (26) both decreasing.

For larger masses of the main sequence $R \sim M^{0{\cdot}72}$ (**10**), and roughly $L \sim M^{3{\cdot}5}$, whence the limit of validity (36) reduces to

$$\omega \cos\phi \geqslant 7 \times 10^{-8} \left(\frac{M}{M_\odot}\right)^{0{\cdot}35} \text{(sec.}^{-1}\text{)}. \tag{38}$$

If satisfied at $\phi = 60°$, the condition may be assumed fulfilled effectively for the whole star; with $M/M_\odot < 10$, an overall certain limit of validity is $\omega > 3 \times 10^{-7}$ or one-tenth of the solar value.

As it is highly probable that the rate of solar rotation is unusually slow, we feel entitled to conclude that the equations of Sections 4 and 5 are applicable to internal convective regions of most stars, including the Sun; the peripheral convective regions are, however, excepted.

In (34), $R\omega^2/g_0 = \alpha_0$ is of the order of the oblateness of the spheroid of rotation at photospheric level; with $n_a = 1{\cdot}5$, $f/B = 0{\cdot}096$, $\cos^2\phi = 2/3$, we obtain

$$\bar{n} = 1{\cdot}5 - 5{\cdot}8\alpha_0. \tag{39}$$

For $\alpha_0 = 0{\cdot}1$, $\bar{n} = 0{\cdot}9$; $\alpha_0 = 0{\cdot}26$, $\bar{n} = 0{\cdot}0$; $\alpha_0 > 0{\cdot}26$, $\bar{n} < 0$. The average polytropic index in the convective regions of fast rotating stars may be considerably lower than the standard value $n_a(1{\cdot}5)$ and may even become negative, requiring negative density gradients. It seems that, if the major portion of the star is in convective equilibrium, in this way low values of $\bar{n}$ and of the density concentration ρ_c/ρ_m suggested by Kopal (**11**) for some binaries can be produced, especially as all these cases are connected with fast rotation. The actual conditions in fast-rotating stars are, of course, of a very complex nature.

6. *Persistence of convection in a stratified medium.* In slowly rotating stars, $\omega \ll 10^{-7}$ sec.$^{-1}$, or a period of rotation over two years (main sequence), the most general equations are those of Section 3; the equations refer to settled thermal convective equilibrium, as well as to convection starting in a stratified medium. A real solution is possible only when $1 - \theta \geqslant 0$; at the start, $v = 0$, which requires by (24) $1 - \theta = 0$, or

$$\frac{\xi_a - \bar{\xi}}{T} = \frac{\eta}{\mu}. \tag{40}$$

In the case of not negligible rotation the necessary general condition (31) must be fulfilled (at $\omega = 0$, this equation becomes identical with (40)); the excess of the temperature gradient, $\xi_a - \bar{\xi}$, has to increase until the value of (31) is reached, when convection may start.

The gas equation for total pressure $P = \mathfrak{R}\rho T/\mu\beta$, the equation of hydrostatic equilibrium $dP/dr = -G\rho M_r/r^2$, and the special definition of the polytropic index

$$n + 1 = \frac{d\log P}{d\log T} = \frac{T}{P}\frac{dP}{dT} \tag{41}$$

yield quite generally, for variable μ as well as β,

$$\xi = \frac{dT}{dr} = -\frac{G\mu\beta}{\mathfrak{R}(n+1)}\frac{M_r}{r^2} \tag{42}$$

(to be compared with (32) which is even more general as g may include also the effect of centrifugal force).

Substituting (42) into (31) and setting (with $\eta = -d\mu/dr$ and $(f/B) = (f/B)_t = 0{\cdot}096$)

$$A = \frac{\mathfrak{R}T}{G\beta\mu} \cdot \frac{r^2}{M_r}\left[-\frac{1}{\mu}\frac{d\mu}{dr} + \frac{(\omega\cos\phi)_2}{g.(f/B)}\right], \tag{43}$$

we have the condition for convection to continue after starting

$$n+1 \leqslant n_c+1 = \frac{n_a+1}{1+(n_a+1)A}\,; \tag{44}$$

as normally $A>0$, $n_c<n_a$; n_c is the limiting value of the polytropic index for convection to persist.

With $n_a = 1{\cdot}5$ as the adiabatic value and for $\omega = 0$, (44) becomes identical with the condition set up by Ledoux (**12**), in which $A = d\log\mu/d\log P$.

The preceding refers to pure turbulent exchange of heat. When the radiative exchange, f_r, is not zero, according to Section 3 and (25) the condition becomes $m-\theta = 0$, which leads finally to

$$n_c+1 = \frac{n_a+1}{1+(n_a+1)A/m}\,. \tag{45}$$

As $f = f_t + f_r$, with $f_t = 0{\cdot}10$ and with increasing f_r, according to Table I $m = (f/B)/(f/B)_t$ increases until $f = 0{\cdot}5$ is reached and then decreases toward an ultimate value zero. Thus, according to (45) moderately strong radiative exchange makes the persistence of initial convection easier (by increasing n_c); a very strong one, however, impedes convection. (44) and (45) are necessary but not sufficient conditions for the start of convection as shown next below.

7. *Radiative transfer and start of convection.*—In an established large-scale turbulent system, radiative transfer is insignificant in the interior of a star. When turbulence is starting, however, the situation may be different; at the start radiation may equalize the differences in temperature before these have time to produce appreciable motion. To estimate the radiation damping of turbulence at its start, we keep to the model of the cellular turbulent element depicted in Section 2; for this it is estimated that the average distance between the middle streamlines of the two adjacent currents of opposite direction (with $D/H = 2\sqrt{2}$) is $0{\cdot}54H$ along the lateral section and about $0{\cdot}5H$ at the bottom or top. We assume an average thickness of the "layer of interchange" $\Delta x = \frac{1}{2}H$; over this thickness a temperature difference ΔT gives rise to an average gradient $\Delta T/\Delta x$ along the direction x, normal to the surface of separation. The flux of radiation may be expressed through the well-known formula

$$q_x = -\frac{4ac}{3\kappa\rho}T^3\frac{dT}{dx}\,;$$

the coefficient of radiative "contact" transfer is $s_r = |q_x|/\Delta T$, and by (3) $f_r = |q_x|/\rho v c_p \Delta T$, whence, with $dT/dx = 2\Delta T/H$, we have

$$f_r = \frac{8acT^3}{3\kappa\rho^2 v c_p H} = \frac{N}{vH}, \tag{46}$$

with

$$N = \frac{8acT^3}{3\kappa\rho^2 c_p}, \tag{47}$$

a number of the order of 10^5 for stellar interiors.

When v is small, f_r may become very large; as $f=f_t+f_r=0{\cdot}1+f_r$, $f=f_r$ very nearly if $f_r>2$, whereas, according to Table I, if $f_r<2$, f/B does not vary much and may be assumed roughly constant.

Imagine convection starting spontaneously from an initial stage of $v_1\to 0$; at this stage by (46) $f_r\to\infty$, $f\to\infty$, $f/B=f/(1+4f^2)\to 0$, $m\to 0$, and formula (24) (with $m-\theta$ for $1-\theta$) yields v imaginary: convection cannot be maintained. An initial finite impulse $v_1\neq 0$ is required to set convection going when $\theta\neq 0$, i. e. when there is a finite gradient of μ.

In non-rotating stars ($\omega=0$) at constant molecular weight an infinitesimal impulse is sufficient, the question being only one of time. Without going into the rather complicated details, it may be mentioned that the following case was worked out numerically. With a certain stellar model "B_0'" in mind (**13**), $\mu=$ const., a potential convective core in which convection had not yet started was considered:

$M=M_\odot$; $L\sim L_\odot$; $\bar{r}=4\times 10^9$ cm.; $H=2{\cdot}4\times 10^9$ cm.; $\bar{\rho}=234$ g./cm.^{3};
$\bar{T}=2{\cdot}15\times 10^7$ deg.; $\kappa=1{\cdot}42$ cm.^{2}/g. (opacity); $c_p=2{\cdot}5\ \mathfrak{R}/\mu=3\times 10^8$ erg/g. deg.;
$N=2{\cdot}62\times 10^5$ cm.^{2}/sec.; $g=1{\cdot}8\times 10^5$ cm./sec.^{2}; $\xi_a=6\times 10^{-4}$ deg./cm.;
$\bar{\xi}=9\times 10^{-4}$ deg./cm.,

i. e. an "oversteep" gradient, 1·5 times in excess of the adiabatic value, sufficient to transport by radiation all the energy generated inside. If the gradient were ξ_a, a normal convective core would result with an excess heat $K=3\times 10^{12}$ erg/cm.^{2} sec. to be transported by convection at $r=\bar{r}$, with $v=950$ cm./sec. according to formula (13) ($\mu=$ const., $\theta=0$). For $f_r<5$, or $v>2\times 10^{-5}$ (equation (46)), the formulae with $f/B=(f/B)_t=0{\cdot}096$ were assumed and for $v<2\times 10^{-5}$, $f/B=(f/B)_r$. The following order-of-magnitude figures were found*:

TABLE III

v_1, cm./sec. (starting velocity)	10^{-8}	3×10^{-8}	9×10^{-8}	7×10^{-7}	5×10^{-6}	2×10^{-5}
Time to reach $v=950$ cm./sec.	500 years	150 years	50 years	12 years	4 months	10 hours

The final velocity attained is 10 km./sec., far in excess of v as given above—on account of the excessive thermal gradient, which leads to a sort of violent readjustment to new conditions of equilibrium. However, for time intervals of the order of the Helmholtz–Kelvin time scale, $\sim 10^7$ years, no such violent upset would take place; a non-rotating sun gradually contracting from a more diffuse state will develop smoothly a convective core in accordance with the gradual growth of the nuclear energy sources, with $\xi_a-\bar{\xi}$ very small (Section 5), and with v agreeing with the equilibrium formula (13). 10^{-8} cm./sec. is about the differential effect over $H=2{\cdot}4\times 10^9$ cm. from the tidal action of Jupiter. Once a turbulent element has come into being, it will start by contact a complete zone of potential turbulence. Once turbulence has started, its vibrational energy propagating over the whole mass of the star furnishes another source of initial impulses. Meteorite impact may be invoked, especially for the outer layers (although there the obstacle set up by the radiative transfer is more efficient).

* The velocity is given by $\sqrt{v}=7{\cdot}7\times 10^{-7}\,h^{3/2}+\sqrt{v_1}$ (equations (46), (15) and (11) with $h\equiv H$ and f_r large), where h is the path travelled by the turbulent element since the start, and the time is given by $t=\int dh/v$.

Thus it seems that there is no difficulty about the star (with $\mu = \text{const.}$, $\omega = 0$) getting over the dead point.

The case of appreciable rotation, in which H is a function of the velocity itself, is different. Assume a stratified medium which has become ripe for turbulence, i. e. in which the temperature gradient has attained the critical value given by (31). We assume

$$f = f_r + 0{\cdot}1\,; \quad \frac{f}{B} = \frac{f}{1+4f^2} = \frac{1}{4f(1+1/4f^2)}\,;$$

for $f_r > 2$ we may safely assume $f/B = 1/4f_r$ with an inaccuracy of 5 per cent at the worst. Thus $m = (f/B)/(f/B)_t = (1/4f_r)/0{\cdot}096 = 2{\cdot}6/f_r$, and, according to (46), $m = 2{\cdot}6Hv/N$.

The equation of velocity (24) becomes

$$v = H\sqrt{\frac{g(\xi_a - \bar{\xi})}{T} \cdot \left(\frac{f}{B}\right)_t \cdot \left(\frac{2{\cdot}6Hu}{N} - \theta\right)}. \tag{48}$$

Here the actual velocity upon which f_r depends (equation (46)) is denoted by u, whereas v denotes the turbulent velocity expected to establish itself under the given circumstances.

It is obvious that, when starting with $u = v_1$, turbulence will develop when $v > u$ and will fade out when $v < u$; further, a certain set of finite H and u in (48) yields $v = 0 < v_1$, thus no convection; the starting velocity cannot therefore be arbitrarily small and must be finite. Evidently the critical value v_0 of the starting velocity is that which yields $v = u = v_0$ according to (48); when $v_1 > v_0$, turbulence develops, when $v_1 < v_0$, it fades out. Hence, setting in (48) $v = u = v_0$, and according to (27), $H = v_0/\omega\cos\phi$ (which is legitimate because in this special case the velocity remains constant during the whole circuit, as in steady state), we obtain

$$1 = \frac{1}{\omega\cos\phi}\sqrt{\frac{g(\xi_a - \bar{\xi})(f/B)_t}{T}\left(\frac{2{\cdot}6v_0^2}{N\omega\cos\phi} - \theta\right)}\,;$$

with $\theta = 0$ and $\bar{\xi}$ from (30) corresponding to pure turbulent transport this is reduced to

$$v_0^2 = \frac{N\omega\cos\phi}{2{\cdot}6}. \tag{49}$$

Formula (46) reduces to $f_r = N\omega\cos\phi/v_0^2$, or, by (49), $f_r = 2{\cdot}6$ at $v = v_0$, a general result depending solely upon the assumed value of $f_t = 0{\cdot}10$. At this value for $f_r > 2$ our formulae are valid and the critical velocity as given by (49) may be accepted. When the temperature gradient exceeds the normal value of (30) or (31), a smaller starting velocity may be sufficient, $v_0 \sim (\xi_a - \bar{\xi})^{-1/2}$.

For solar mass and data as quoted above, $N = 2{\cdot}6 \times 10^5$, $\omega\cos\phi = 3 \times 10^{-6}$, $v_0 = 0{\cdot}55$ cm./sec. To obtain turbulence around the core of the rotating Sun, in which the condition (31) is already fulfilled, a "push" of $v_1 > 0{\cdot}55$ cm./sec. must be given for the start; the figure is small but quite considerable, and none of the impulses mentioned above would be sufficient (except already existing turbulence in the central region).

Nevertheless, a major source of impulse is the non-uniformity of rotation itself. Even assuming constancy of ω throughout the whole mass at the beginning, non-homologous contraction will produce sufficient differences in the course of

time. Thus, assume as an example two models of solar mass calculated by the writer (**13**), "B_0'" as the initial stage, "B_c'" with an almost exhausted central hydrogen content as a supposed advanced stage of evolution after the lapse of about 3×10^9 years. In the first model, $(\rho_c/\rho_m)_1=72{\cdot}6$; in the second, $(\rho_c/\rho_m)_2=428$; in the absence of friction $\omega r^2=$const., and the ratio of angular velocity of centre and surface would become

$$\frac{\omega_c}{\omega_p}=\left[\left(\frac{\rho_c}{\rho_m}\right)_2\Big/\left(\frac{\rho_c}{\rho_m}\right)_1\right]^{2/3} \text{ or } \frac{\omega_c}{\omega_p}=3{\cdot}3$$

for the advanced stage. In agreement with this we may assume that in t years a difference in angular velocity between two strata r_1 and r_2 establishes itself of the order of

$$2{\cdot}3\,\omega_p\left(\frac{t}{3\times10^9}\right)\frac{(r_2-r_1)}{R}=\Delta\omega,$$

which corresponds to a difference in linear velocity $\Delta\omega(r_2-r_1)=v_1$, and may be assumed to be the required "push". With $v_1=v_0$ according to (49) this yields for the time required to establish a differential velocity v_1 inside the layer (with $r_2-r_1=\Delta r$ as the width of the prospective convective zone, and $M=M_\odot$, $R=R_\odot$):

$$t\text{ (years)}=\frac{3\times10^{22}\sqrt{N}}{(\Delta r)^2}. \qquad (50)$$

For the circumcentral region ($T=2{\cdot}15\times10^7$, etc.) as quoted above, $N=2{\cdot}6\times10^5$, $v_1=0{\cdot}55$ cm./sec. we have:

Δr, cm.	1×10^8 (minimum start)	5×10^8 (normal "ripe" start)	$2{\cdot}4\times10^9$ (maximum width admissible)
t, years	$1{\cdot}5\times10^9$	6×10^7	$2{\cdot}5\times10^6$

Thus, a narrow region will not easily start convection (too long a waiting time for the push); it is likely that convection starts at once in a strip of finite width, producing thus suddenly (within a few hours for a solar model) a discontinuous change in the structure of the model (a "pure change of structure" (**14**) along the line of constant potential energy), and a sudden mixing of its material.

For the subphotospheric region of the same model, at $T=2\times10^5$, $N=3\times10^{10}$, $v_1\sim v_0=184$ cm./sec., and $\Delta r=1\times10^9$ cm. as a normal thickness, t is 5×10^9 years, so that in practice a metastable state could persist for a life-time somewhat less than the above figure; $\Delta r=3\times10^9$ cm. as a possible maximum yields $t=6\times10^8$ years. The metastability in the peripheral convective region is very large indeed, implying the possibility of sudden changes in structure and luminosity of the star from this cause. The upset of equilibrium in the metastable layer may be evoked by certain changes in the deep interior which the writer has considered as a possible cause of the "ice ages" (**14**); this might lead to secondary fluctuations of luminosity superimposed on the general depression of the "major ice age", fluctuations that might correspond to the repeated advance and retreat of glaciation during the Quaternary. A similar metastability in subphotospheric layers may be produced by the stratification of hydrogen as illustrated by certain models calculated by the writer (**13**).

The impact of external bodies and the tremors from already existing turbulent layers may, however, ease very much the start of convection in the peripheral zone.

8. *Viscosity, parameter f_t, and persistence of turbulent circulation.*—Two radically different kinds of viscosity are to be distinguished: (*a*) viscosity proper, or gas-viscosity, and radiative viscosity produced by the kinetic diffusion of individual molecules or photons; the coefficient of viscosity depends upon the kinetic properties of these particles, and the tangential force per unit surface is proportional to the velocity gradient normal to the surface; (*b*) turbulent or eddy-viscosity, produced by the interpenetration of the turbulent elements; the effective coefficient of viscosity is proportional to vH, $dv/dH \sim v/H$, and the average drag resulting is proportional to $vHv/H = v^2$; here v is the velocity, H the linear dimension of the turbulent circulation.

By the very nature of things turbulent viscosity cannot prevent a turbulent circulation from coming into being; its damping effect enters as an inherent property of turbulence itself, being balanced by the corresponding exciting forces. It would therefore be superfluous to consider the persistence of turbulent circulation under the influence of turbulent viscosity.

On this occasion we notice that our non-dimensional parameter of turbulent heat transfer, f_t (Section 2), is at the same time the parameter of the transfer of kinetic momentum by eddy-viscosity. The turbulent transfer of momentum across a cellular interface is effected by the same agency as the turbulent transfer of energy; thus it can be found from the expression for the energy transfer, simply replacing the difference in the heat content $c_p . \Delta T$ per gram, by the difference in momentum content, $2v$ per gram. Now the rate of transfer of heat per cm.^{2} is $f_t \rho v c_p \Delta T$; hence the rate of transfer of momentum per cm.^{2}, which equals the tangential friction per cm.^{2}, is given by $F_t = 2 f_t \rho v^2$. If v_e is the extreme amplitude in the velocity of flow on the two sides of the interface, the picture of Section 2 requires $v_e = 4v$ *; thus $F_t = \frac{1}{8} f_t \rho v_e^2$. Experiments with flat wings moving parallel to their plane with a velocity u yield for the aerodynamical friction $F_t = 0{\cdot}012\, u^2$ dyne/cm.^{2} (**16**); on the one side of the wing the total amplitude of velocity is evidently $v_e = u$ (the "interface" to be placed at a certain distance from the plane, the wing moving with a velocity $+\frac{1}{2}u$, the free atmosphere with $-\frac{1}{2}u$ relative to this fictitious average interface), whence the experimental aerodynamical value is $\frac{1}{8} f_t = 0{\cdot}012$, or $f_t = 0{\cdot}096$, in fair agreement with our value $f_t = 0{\cdot}10$ adopted on the basis of other data.

The viscosity proper may set a lower limit to the size of the turbulent elements. From dimensional considerations it is roughly estimated that the life-time of a vortex (dimensions according to equation (14)), measured by U, the number of circuits completed until the angular velocity is reduced to a fraction $1/e$ of its initial value, is

$$U = \frac{Hv}{45(\nu/\rho)}, \tag{51}$$

where ν is the ordinary coefficient of viscosity, ν/ρ the kinematic viscosity. $U > 1$ may be taken as a condition for the persistence of a circulation. The numerical factor $45 = 2\pi k e/(e-1)$, with $k = 4{\cdot}5$ depending upon assumption (14), is but a guess. According to Jeans, the radiative viscosity ν' is more important than gas viscosity ν'' in the interior of most stars, including the Sun (*cf.* (**15**), p. 281); $\nu' = aT^4/3\kappa\rho c$ (a = radiation constant, κ = opacity, c = velocity of light;

* v is the average velocity in a layer across which the velocity changes from zero to about the double value, $2v$; in the adjacent cellular section the flow is in the opposite direction, attaining an extreme velocity $-2v$. The extreme difference in velocity is thus $4v$.

the numerical factor may be slightly different). With Kramers' opacity $\kappa \sim \rho T^{-3.5}$, and a rough average equation of state $\rho \sim T^{2.5}$ for composite stellar models, the kinematic viscosity ν'/ρ remains practically constant throughout the star. For homologous stellar models the luminosity is $L \sim RT_c^4/\kappa_c \rho_c$, whence $\nu'/\rho \sim LR^2/M$ can be inferred from the observed luminosity, radius and mass of a star independently of assumptions with respect to molecular weight. The kinematic viscosity increases rapidly with the mass; if $L \sim M^{3.5}$, $R \sim M^{0.75}$, then $\nu'/\rho \sim M^4$ (valid only for the main sequence). For the Sun $\nu'/\rho = 0.2$ may be assumed (*cf.* (**15**), p. 281). Gas viscosity, chiefly produced by the diffusion of electrons (**17**), is $\nu'' \sim \mu T^{2.5}$, whence the kinematic viscosity ν''/ρ is again practically constant throughout the star (when $\mu \sim$ const.), and for stars of the main sequence if homologously built it is $\nu''/\rho \sim \mu^{3.5} M^{1.5} R^{0.5}$. According to Eddington (**15**), $\nu''/\nu' = \frac{1}{3}$ in the Sun and may be much smaller when μ is low. In any case, for the Sun $\nu = \nu' + \nu'' = 0.3\rho$ may be safely assumed.

In the absence of rotation, or for a forced circulation like the rotational currents where Coriolis deflection does not influence the system of circulation, the minimum average velocity of circulation to persist unobstructed follows from (51) with $U = 1$ as

$$v \geqslant \frac{45(\nu/\rho)}{H}. \tag{52}$$

For a system of Eddington–von Zeipel rotational circulation (**18**), $H = 4 \times 10^{10}$ cm., $\nu/\rho = 0.3$ whence, as $v \cong \frac{1}{4} v_0$, $v_0 \geqslant 1.4 \times 10^{-9}$ cm./sec. is the condition of undisturbed persistence. The condition is well fulfilled for the above-mentioned data (Table I, (**18**)), at $\omega = 10^{-4}$. However, for solar rotation, $\omega = 3 \times 10^{-6}$, the average value of v_0 is much below the limit, which means that, although the forced circulation cannot be stopped, it will go on, as it were, under great friction, which means that changes of ω corresponding to conservation of angular momentum will not take place (except in the outer layers where v_0 is large, *cf.* **18**). In other words, the time of circulation ($\sim 10^{13}$ years) being longer than the time of relaxation with respect to viscosity (10^{12} years), serious differences in angular velocity are impossible. For thermal convection in a rotating star, with (27) and (51) we obtain

$$U = \frac{v^2}{45(\nu/\rho)\omega \cos\phi},$$

or for the limit of persistence $U \geqslant 1$,

$$v \geqslant \sqrt{45(\nu/\rho)\,\omega \cos\phi}. \tag{53}$$

If v falls below the limit, the circulation cannot continue—it will stop completely. For the Sun $\nu/\rho = 0.3$, $\omega \cos\phi = 2 \times 10^{-6}$, whence $v \geqslant 0.005$ cm./sec. is required as a minimum push to overcome viscosity. This is 100 times smaller than the minimum required in Section 7, wherefore we conclude that viscosity does not play a role in preventing the start of thermal convection (the ratio of the two limiting values of the velocity push is $v_0^2/v^2 = c^2/14.6 c_p T$ and remains large for all imaginable values of T in main sequence stars).

9. *Transport of matter by convection.*—The question is of importance only in a stratified medium where

$$\mu' = -\frac{1}{\mu}\frac{d\mu}{dr} = \frac{\eta}{\mu}$$

is different from zero. Let X be the concentration (by weight) of a particular element (e. g. hydrogen). The material flow of this element caused by convection may be assumed to be governed by the ordinary diffusion formula

$$\delta M = -D\rho\left[\frac{dX}{dr} - \left(\frac{dX}{dr}\right)_0\right],$$

where $(dX/dr)_0$ is the equilibrium gradient of abundance, equal to zero in the case of convection, as the ultimate state after mixing is uniform composition, and the effective coefficient of "convectional diffusion", $D = D_c$, is independent of the properties of the element under question. Hence

$$\delta M = -D_c\rho\frac{dX}{dr}\,(\text{g./cm.}^2\,\text{sec.}). \tag{54}$$

We may consider heat as an "element" of concentration c_pT, with the adiabatic gradient $d(c_pT)/dr = c_p\xi_a$ as the equilibrium state; the convectional transport of heat is therefore given by the diffusion formula

$$K = -D_c\rho c_p(\bar{\xi} - \xi_a), \tag{55}$$

where D_c is exactly the same as in (54) when the transport of heat is exclusively by convection ($f_r = 0$).

Substituting into this $\bar{\xi} - \xi_a$ from (31), we find

$$D_c = \frac{K}{\rho c_p T}\left[\frac{(\omega\cos\phi)^2}{g(f/B)} + \mu'\right]^{-1}. \tag{56}$$

Substituting $(\bar{\xi} - \xi_a)$ from (30) into (55), and the resulting K into (28) and (29), we get

$$v = \left[\frac{D_c\omega\cos\phi}{(f/B)}\right]^{1/2} \quad \text{and} \quad H_r = \left[\frac{D_c}{(f/B)\,.\,\omega\cos\phi}\right]^{1/2},$$

whence

$$D_c = \frac{f}{B}H_r v. \tag{57}$$

This corresponds to the definition of the coefficient of diffusion as the product of free path (H_r), velocity (v), and a constant factor f/B. In the kinetic theory of gases the constant factor is $\frac{1}{3}$; here it is $f/B = 0{\cdot}096$, or considerably smaller, allowing for the lateral interchange of matter by the turbulent element.

In the notation of Sections 6 and 7, the convective transport of heat, being the difference between the total energy generated inside r and the amount transported by radiation, is

$$4\pi r^2 K = L - Q, \tag{58}$$

where

$$Q = \frac{16\pi acr^2T^3}{3\kappa\rho}(-\xi). \tag{59}$$

At given fixed conditions of state the radiative flux is proportional to the absolute value of the temperature gradient, ξ; let ξ_0 be the gradient corresponding to the possible radiative flow $Q_0 = L$ (or $K = 0$), i. e. to the case of radiative equilibrium:

$$L = \frac{16\pi acr^2T^3}{3\kappa\rho}(-\xi_0). \tag{60}$$

From (59) and (60) we get

$$Q = L \cdot \frac{\xi}{\xi_0}. \tag{61}$$

From (42) we introduce the more convenient notion of the local polytropic index*, $\xi/\xi_0 = (n_0+1)/(n+1)$, where n_0 is the radiative equilibrium value of n (n being defined by (41)); substituting this into (61) and (58), we get

$$4\pi r^2 K = \frac{L(n-n_0)}{n+1}. \tag{62}$$

Let the total material flow of the element (X) be defined as

$$F_x = 4\pi r^2 \cdot \delta M \text{ (g./sec.)}. \tag{63}$$

With δM from (54), D_c from (56) and K from (62), the general formula for the material flow of the particular element becomes

$$F_x = -\frac{(n-n_0)LX'}{(n+1)c_p T(\omega'+\mu')}; \tag{64}$$

here $X' = dX/dr$ and

$$\omega' = \frac{(\omega \cos\phi)^2}{g \cdot (f/B)_t}. \tag{65}$$

Formula (64) applies to a steady state of the energy transport when (58) or (62) is valid and when hydrostatic equilibrium remains practically undisturbed. In the case of a rapid re-adjustment to another state of hydrostatic equilibrium K is not bound to these conditions but may attain very large values, as may F_x also.

We notice that in (64) n is the actual average polytropic index in the turbulent medium, whereas $n_0 < n$ is a limiting potential value defined (*cf.* (42) and (60)) by

$$n_0 + 1 = \frac{16\pi ac\mu\beta G}{3\mathfrak{R}} \cdot \frac{T^3}{\kappa\rho} \cdot \frac{M_r}{L}. \tag{66}$$

Now, in a steadily persisting turbulence the temperature gradient and thus also n is prescribed by (31) independently of the amount of the actual convective transport:

$$\frac{\xi_a - \xi}{T} = \omega' + \mu'; \tag{67}$$

further, $\xi = \xi_a(n_a+1)/(n+1)$ and by (42) or (32)

$$\xi_a = -\frac{g\mu}{\mathfrak{R}(n_a+1)} = -\frac{g}{c_p}, \tag{68}$$

as $c_p = \gamma c_v$, $\mathfrak{R}/\mu = (\gamma-1)c_v$, $n_a = 1/(\gamma-1)$.

Hence from (67)

$$(n+1)c_p T(\omega'+\mu') = g(n_a - n), \tag{69}$$

and formula (64) is very much simplified:

$$F_x = -\frac{(n-n_0)}{(n_a-n)} \frac{LX'}{g}. \tag{70}$$

Whereas n_0 and n_a may be considered as given, n remains to be determined from condition (69):

$$n = \frac{gn_a - c_p T(\omega'+\mu')}{g + c_p T(\omega'+\mu')}. \tag{71}$$

* Convenient as a dimensionless quantity.

Substituting this into (70), setting

$$\mathfrak{a} = \frac{(n_0+1)c_p T}{g(n_a-n_0)} = \frac{(n_0+1)(n_a+1)\mathfrak{R}T}{g\mu(n_a-n_0)}, \tag{72}$$

the following general formula for the material flow by convection is obtained (using for c_p its former expression):

$$F_x = -\frac{(n_a-n_0)L}{(n_a+1)^2\mathfrak{R}T}\cdot\mu X'\left(\frac{1}{\omega'+\mu'}-\mathfrak{a}\right); \tag{73}$$

also

$$F_x = -\frac{(n_0+1)}{(n_a+1)}\frac{LX'}{g}\left[\frac{1}{\mathfrak{a}(\omega'+\mu')}-1\right]; \tag{74}$$

$\mathfrak{a}$ is a parameter having the dimension of a radius; $\mathfrak{a}$ and ω' are independent of the gradient X', whereas μ' does depend on it.

10. *Transport of stratified hydrogen by convection.*—The molecular weight in a mixture containing the fraction X of hydrogen, Y of helium, the rest being "metals", is conveniently schematized by the formula

$$\mu = \frac{1}{\frac{1}{2}+\frac{3}{2}X+\frac{1}{4}Y};$$

when Y itself is a linear function of X, the formula may be reduced to

$$\mu = \frac{k}{X+b}. \tag{75}$$

For $Y=0$, $k=\frac{2}{3}$, $b=\frac{1}{3}$; for $X+Y=C=1-Z$ (Z = constant metal content), $k=0{\cdot}8$, $b=0{\cdot}4+0{\cdot}2C$. Thus, formula (75) may be looked at as typical, with b between $\frac{1}{3}$ and $0{\cdot}6$. From (75)

$$\mu' = -\frac{d\mu/dr}{\mu} = \frac{X'}{X+b} = \frac{\mu X'}{k}. \tag{76}$$

Hence $\mu X' = k\mu'$. Further, take the simplest case of a monatomic gas, $\gamma=\frac{5}{3}$, $n_a=1{\cdot}5$; formula (73) is then transformed into

$$F_x = -\frac{4k(1{\cdot}5-n_0)L}{25\mathfrak{R}T}\cdot\mu'\left(\frac{1}{\omega'+\mu'}-\mathfrak{a}\right), \tag{77}$$

in grams of hydrogen per second. For $dX/dr>0$ as a normal case of a stable stratification, $\mu'>0$ and $F_x<0$: the flux is directed inward. The flux becomes zero for $\mu'=0$, $X'=0$, and for

$$\mu_0' = \frac{1}{\mathfrak{a}} - \omega', \quad X' = X_0 = (X+b)\mu_0', \tag{78}$$

which latter case corresponds exactly to condition (44) of persisting convection, with

$$A = \frac{c_p T}{(n_a+1)g}(\omega'+\mu_0')$$

yielding $n_c = n_0$ as the limiting value.

A maximum value of the flux depending upon μ' is attained at

$$\mu_m' = \sqrt{\frac{\omega'}{\mathfrak{a}}} - \omega'. \tag{79}$$

The maximum possible material flow at $\mu' = \mu'_m$ is then, from (77),

$$F_{\max.} = -\frac{4k(1{\cdot}5 - n_0)L}{25\mathfrak{R}T}(1 - \sqrt{\mathfrak{a}\omega'})^2. \tag{80}$$

On both sides of μ'_m the flow decreases, although the decrease may be very flat toward $\mu' > \mu'_m$ (when ω' is small).

Confining ourselves to the normal case of a mechanically stable stratification where the molecular weight decreases outwards, $dX/dr \geqslant 0$ or $\mu' \geqslant 0$, and where the flow necessarily must be directed inwards, $F_r \leqslant 0$, together with $n_0 \leqslant 1{\cdot}5$ as a necessary condition of thermal convection, from (74) we get the following limiting condition of validity: $(\omega' + \mu')^{-1} - \mathfrak{a} \geqslant 0$, or

$$\mathfrak{a}\omega' \leqslant 1 - \mathfrak{a}\mu', \tag{81}$$

which in any case means also

$$0 \leqslant \mathfrak{a}\omega' \leqslant 1, \tag{82}$$

as $\mathfrak{a}$, ω' and μ' are all positive.

On the other hand, except when $n_0 = -1$, which however is impossible, $\mathfrak{a}$ is finite or large (when $1{\cdot}5 - n_0$ is small, equation (72)), and the product $\mathfrak{a}\omega'$ at a given point inside a star may be made equal to or to exceed 1 by suitably increasing the angular velocity, ω. There exists therefore an upper limit ω_0 to the angular velocity at which thermal convection is rendered impossible even when there is no stratification, $\mu' = 0$; from the condition $\mathfrak{a}\omega' = 1$ (81) the limiting value of the angular velocity is given by (72) and (65), assuming $(\cos\phi)^2 = \frac{2}{3}$ and $(f/B)_t = 0{\cdot}096$, with $n_a = 1{\cdot}5$ as

$$\omega_0 = 2{\cdot}64 \times 10^{-5} g \sqrt{\left\{\frac{\mu(1{\cdot}5 - n_0)}{(n_0 + 1)T}\right\}}. \tag{83}$$

When the angular velocity of rotation attains or exceeds ω_0, thermal convection excited by the normal energy exchange becomes impossible, even in the absence of stratification by μ, and is replaced by radiative equilibrium with a super-adiabatic gradient corresponding to n_0. On account of the factor $\cos\phi$ in ω', the limit is not sharp, convection tending to persist in the polar direction; however, because of the finite size of the turbulent elements, turbulence in the polar direction will also come to a stop at somewhat larger values of ω. On the other hand, for a finite value of the gradient μ' the stop, according to (81), may take place at $\omega < \omega_0$.

The limiting value ω_0 is not too high, corresponding to a moderate oblateness, except near the surface of the star:

$$\alpha_0 = \frac{\omega_0^2 r}{g} = 6{\cdot}98 \times 10^{-10} \cdot \frac{\mu(1{\cdot}5 - n_0)gr}{(n_0 + 1)T}. \tag{84}$$

For an interior point inside the core of a solar model, $n_0 \sim 0{\cdot}5$ (or $\frac{2}{3}$ of energy transported by convection), $g \sim 2 \times 10^5$, $r \sim 6 \times 10^9$, $\mu = 0{\cdot}8$, $T = 2 \times 10^7$, the oblateness of the level surface corresponds to $\alpha_0 = 0{\cdot}022$, and the surface is still satisfactorily spherical; $\omega_0 = 8{\cdot}6 \times 10^{-4}$ (period of revolution about two hours) is nevertheless rather high and hardly comes into question for the interior of the Sun. For fast rotating stars, in which the interior rotates still faster, a cessation of convection in the core may be quite possible.

In the outskirts of the star, with decreasing temperature the convective limit given by (83) or (84) increases; at about $T < 10^6$ convection (at $\mu' = 0$) cannot be stopped by rotation before the star starts breaking up from centrifugal force.

11. *Persistence of convection in the core.*—From (83) it appears that ω_0 is zero at the centre ($r=0$, $g=0$), and at the theoretical boundary of the core ($n_0=1{\cdot}5$); thus, the centre and the boundary are theoretically not stirred by convection however slow the rotation is. Obviously, with the increasing speed of rotation, the convective zone in the core becomes narrower, at the expense of the increasing size of the central and peripheral regions of rest (in radiative equilibrium with a super-adiabatic temperature gradient); when ω approaches ω_0 all over the core, convection stops altogether. The process of decay of convection in the core is thus a gradual one, starting at the lowest values of ω. It is worth while to consider this process in connection with the stratification produced by the nuclear reactions inside the core.

When the maximum possible material flow (80) is unable to balance the differentiation produced by the nuclear reactions, the gradient μ' will increase at an accelerated rate (because after the optimum gradient (79) is exceeded, a further increase in μ' makes F_x (77) smaller) until $\mu'=\mu'_0$ (78) is reached and convection ceases; this happens somewhat earlier than would be the case according to the overall limit (83).

The rate of change of the average hydrogen concentration in the core produced by nuclear reactions is $d\bar{X}_1/dt=-L_1/c_0M_1$, where $L_1=$total energy production, $M_1=$mass of the core, and $c_0=6{\cdot}4\times10^{18}$ erg/g. is the energy released by the transmutation of one gram of hydrogen into helium. For an interior zone in the core, at radius r, mass M_r and energy production L_r, the rate of change is

$$\frac{d\bar{X}}{dt}=-\frac{L_r}{c_0M_r}-\frac{F_x}{M_r}\,.$$

(loss of hydrogen from transmutation $=L_r/c_0$, gain from turbulent flow $=-F_x$, F_x being negative). To prevent increasing stratification, $d\bar{X}_1/dt=d\bar{X}/dt$ must be fulfilled, whence the condition of persistence becomes

$$F_x=-\frac{L_1}{c_0}\left(\frac{L_r}{L_1}-\frac{M_r}{M_1}\right)=F_0. \tag{85}$$

F_0 is thus the material flow required to counterbalance stratification from nuclear reactions. The requirement can be met only when $|F_0|\leqslant|F_{\max.}|$, or $F_{\max.}/F_0\geqslant1$.

To estimate this ratio, we assume conventionally the structure of the core to be a polytrope of $n=n_a=1{\cdot}5$; actually this is not correct, as, according to (71), $n\neq n_a$ and is variable. However, no radical difference is produced by this simplification, the representation by $n=1{\cdot}5$ being very close (the central portions of Emden's polytropes vary little with n). If Q_a is the radiative flux at $n=n_a$, evidently, by our definition (66) (same T, ρ, M_r, κ),

$$n_0+1=(n_a+1)\frac{Q_a}{L_r}, \tag{86}$$

or, as $Q_1=L_1$ at the boundary, we may write

$$n_0+1=2{\cdot}5\frac{Q_a/Q_1}{L_r/L_1}. \tag{87}$$

This gives

$$1{\cdot}5-n_0=2{\cdot}5\frac{L_1}{L_r}\left(\frac{L_r}{L_1}-\frac{Q_a}{Q_1}\right),$$

to be substituted into (80). Using this and (85), the critical ratio is obtained as

$$\frac{F_{\max.}}{F_0} = \frac{4kc_0(1-\sqrt{\mathfrak{a}\omega'})^2}{25\mathfrak{R}T_c} \cdot \chi \geqslant 1, \tag{88}$$

where

$$\chi = \frac{L_r/L_1 - Q_a/Q_1}{(T_r/T_c)(L_r/L_1 - M_r/M_1)}. \tag{89}$$

Using Emden's relative variables, z = the relative radius, $u = T_r/T_c$, $m = -z^2u'$, $u' = du/dz$, with Kramers' opacity and $n = 1{\cdot}5$, the relative radiative flux is $q_a = q = mu^{3{\cdot}5}$, and with ρT^{15} as the law of energy generation, the relative energy production is $l = \int_0^m u^{16{\cdot}5}\,dm$; the following table is calculated for $z_1 = 1{\cdot}1$, nearly corresponding to the size of the core of a dwarf composite model (**13**). The last column gives another function,

$$\lambda = \frac{u(n_0+1)}{(u')^2(1{\cdot}5-n_0)}, \tag{90}$$

to be referred to below.

TABLE IV

Polytrope $n = 1{\cdot}5$; $z_1 = 1{\cdot}1$; $\epsilon \sim \rho T^{15}$; *Kramers' opacity*

z	n_0	χ	λ
0·0	0·09	0·72	∞
0·1	0·10	0·72	680
0·2	0·13	0·71	180
0·3	0·19	0·70	92
0·4	0·28	0·69	61
0·5	0·40	0·67	48
0·6	0·54	0·65	42
0·7	0·70	0·62	42
0·8	0·89	0·58	48
0·9	1·09	0·55	62
1·0	1·30	0·51	120
1·1	1·50	0·48	∞

Now, the critical product $\mathfrak{a}\omega'$ follows from (72) and (65), with $\overline{\cos^2\phi} = \frac{2}{3}$ and $(f/B)_t = 0{\cdot}096$, as

$$\mathfrak{a}\omega' = 1{\cdot}43 \times 10^9 \lambda \cdot \frac{(u_1')^2 T_c}{g_1^2 \mu} \cdot \omega^2, \tag{91}$$

λ being given by (90).

The core of a model "B_0'" (*cf.* (**13**)), with $z_1 = 1{\cdot}082$, closely corresponds to the case of Table IV. In this case $\mu = 0{\cdot}8/(X + 0{\cdot}594)$ or $k = 0{\cdot}8$, $\log T_c = 7{\cdot}368$ (reduced to $M = M_\odot$), and $4kc_0/25\mathfrak{R}T_c = 425$. Using this value, (88) yields as an upper limit $\mathfrak{a}\omega' \leqslant 0{\cdot}865$ at the boundary of the core ($\chi = 0{\cdot}48$) and $\mathfrak{a}\omega' \leqslant 0{\cdot}889$ at the centre ($\chi = 0{\cdot}72$); the difference is unimportant and the figures are close to the absolute limit (82). Assuming $\mathfrak{a}\omega' \leqslant 1$ in (91), the limiting values ω_0 given below will exceed the narrower limit by not more than 5–7 per cent:

TABLE V

Core of Model " B_0' *",* $M = M_\odot$

(*taking* $z_1 = 1{\cdot}1$ *instead of* 1·082)

Absolute limit for rotation to stop convection in the core

z	0·0	0·1	0·2	0·3	0·4	0·5	0·6	0·7	0·8	0·9	1·0	1·1
$\omega_0 \times 10^4$	0	2·2	4·1	5·9	7·2	8·2	8·7	8·7	8·2	7·1	5·2	0·0

Between $z=0{\cdot}0-0{\cdot}1$, $\omega_0 \sim z$; between $z=1{\cdot}0-1{\cdot}1$, $\omega_0 \sim \sqrt{1{\cdot}1-z}$. Thus, for $\omega=3\times10^{-6}$ (solar rotation), $\omega=\omega_0$ at $z=0{\cdot}0014$ and $z=1{\cdot}099997$, and between these two limits convection persists; the minute zones of rest are, however, only about 10^7 cm. and 2×10^4 cm. in thickness and are certainly overcome by gas diffusion (which is not considered here). At $\omega=5\times10^{-4}$, the convective region stretches from $z=0{\cdot}25$ to $z=1{\cdot}0$, the regions of rest being of considerable extent; the oblateness at the boundary of the core ($r_1=6\times10^9$ cm.) is still only 0·004, thus quite small. At $\omega=8{\cdot}7\times10^{-4}$, oblateness 0·012, all convection in the core should cease. On account of the circumstances here considered, the structure and course of evolution of fast rotating stars (or stars with fast rotating cores) should differ considerably from those of slow rotating stars even before the oblateness becomes appreciable. Of course, the rotational currents will be more intense in this case but will never be able to produce complete mixing.

12. *Spread of turbulence in a super-adiabatic layer.*—Below we keep to the picture of hydrogen stratification in slowly rotating stars, $\omega<\omega_0$, which probably is also the case of our Sun. In a stratified medium the polytropic index may fall below the adiabatic value, the stratification remaining convectionally stable as long as the inequality

$$n_c<n<n_a \qquad (92)$$

holds, n_c being defined by (44). A layer answering condition (92) we call a super-adiabatic layer; also $n=n_0$ is the "radiative equilibrium value of n" of Section 9. If a portion of such a layer becomes suddenly mixed, so that the stratification of molecular weight is almost blotted out, n_c in this portion jumps up to a higher value near n_a, $n_c>n_0$, the instability persists and convection in the once disturbed portion may continue indefinitely. The undisturbed portion will at the same time continue to remain in radiative equilibrium. In the disturbed portion $n>n_0$ and by (62) the convective transport of heat will assume a certain finite equilibrium value. The same holds at the interface between the disturbed and undisturbed portions of the layer; on the disturbed side of the interface convection is active, on the undisturbed side convection is absent. This discontinuity in n, or in the temperature gradient, leads to a certain "surf effect" at the interface; as the result of mixing toward the disturbed region, a discontinuity in X, the hydrogen content, will establish itself at the interface, and by contact (gas diffusion at the discontinuity and the beat of the convective "surf") an interchange of hydrogen takes place through the interface; the next adjacent part of the undisturbed layer gets its hydrogen content equalized with the convective portion, which allows convection to stretch out over this adjacent part and so forth. From a disturbed shell, however narrow, convection spreads in two directions, inwards and outwards, until mixing becomes complete over the entire super-adiabatic layer. As the result of mixing, the distribution of hydrogen, and so of the energy sources in the star, is changed, which affects the luminosity of the star directly, as well as indirectly through changes of structure. Mixing in super-adiabatic layers has been suggested by the writer as a possible cause of the dimming of solar luminosity, which may be responsible for the ice ages on the Earth (**13, 14**).

The first disturbance may start as the consequence of gradual evolution, when in a certain narrow zone the decreasing polytropic index n_0 reaches the stability limit n_c; from this zone the "infection" spreads out as described above. The

rate of the spread depends upon the efficiency of the surf effect which we are going to evaluate below. The theoretical basis is given in Sections 9 and 10 and consists in the application of smooth functions of flow to the irregular phenomena of turbulence; it may be believed, nevertheless, that the schematization used is a fair approximation to the average effect (statistical average) of these complex phenomena.

For a spherical shell between r and $r+dr$, containing a mass of hydrogen $4\pi r^2\rho X\,dr$, $\partial X/\partial t$ is the change of concentration per unit of time; evidently, with a flow of hydrogen F_x at r and F_x+dF at $r+dr$ (F positive when directed outwards), $4\pi\rho r^2(\partial X/\partial t)\,dr=-dF$, or

$$\frac{\partial X}{\partial t}=-\frac{1}{4\pi r^2\rho}\frac{\partial F_x}{\partial r}. \tag{93}$$

Consider first, for the sake of simplicity, a very narrow shell, such that over it $r^2\rho$, L, T, ω', $\mathfrak{a}$ and n_0 may be considered as constant; also, let $X+b$ change relatively little over our narrow region, so that according to (76) X' and μ' are proportional to each other, and $dX'/dr\sim d\mu'/dr$. In such a case, from (77) and (93)

$$\frac{\partial X}{\partial t}=C\frac{\partial X'}{\partial r}\left[\frac{\omega'}{(\omega'+\mu')^2}-\mathfrak{a}\right]; \tag{94}$$

here C is a certain positive factor, assumed to be constant in the present case of a narrow strip. However, μ' cannot be taken as constant near the interface even for the narrow region here considered, as the gradient may change there steeply up to practical discontinuity. Assume schematically a continuous variation of X' (μ') at the interface, X' increasing to large values when the margin is approached as represented schematically in Fig. 1. Let the broken line PQ symbolize the undisturbed distribution of X (increasing with r), and let the disturbance spread symmetrically around CC′, from position I between AA′–BB′ toward position II between DD′–EE′; let the distribution of X be represented by the full curve A′aC′bB′ for I, and D′dC′eE′ for II, equality of the areas being maintained: AA′aC′bB′B = AA′mC′mB′B, and DD′dC′eE′E = DD′A′mC′mB′E′E. Evidently at C′, by reason of symmetry $(\partial X/\partial t)_C=0$ which by (94) requires either $(\partial X'/\partial r)_C=0$, or

$$\mu'_C=\sqrt{\frac{\omega'}{\mathfrak{a}}}-\omega'=\mu'_m \quad (cf.\ (79)).$$

At b the transition is from C′bB′ toward C′eE′, thus X is decreasing, or $(\partial X/\partial t)_b<0$; as on this branch $(\partial X'/\partial r)_b>0$ (the gradient becoming steeper is the only possibility of a continuous transition), (94) gives

$$\frac{\omega'}{(\omega'-\mu_b)^2}-\mathfrak{a}<0, \quad \text{or} \quad \mu'_b>\sqrt{\frac{\omega'}{\mathfrak{a}}}-\omega'=\mu'_m.$$

Similarly, on the branch A′aC′, $\mu'_a>\mu'_m$, with $(\partial X'/\partial r)_a<0$. On account of the postulated continuity of curvature from $(\partial X'/\partial r)_a<0$ toward $(\partial X'/\partial r)_b>0$, $(\partial X'/\partial r)_C=(\partial^2X/\partial r^2)_C=0$ necessarily takes place at C′, the middle of the disturbance: C′ is a point of inflexion. By the same requirement of continuity the gradient exceeding μ'_m on both sides of C′ cannot be less than μ'_m at this point, thus $\mu'_C\geqslant\mu'_m$ is a second necessary condition. The gradient μ'_C determines the total flow of material from the excess half (C′bB′) toward the deficit half (C′aA′) of the zone of disturbance.

In the "surf" region (a, b, d, e in Fig. 1) the gradient μ' establishes itself automatically, to respond to arbitrary values of $\mu'_C \geqslant \mu'_m$. The inferior limit determines the *maximum* efficiency of the surf effect; it cannot yield more, but it will automatically fulfil all requirements which do not exceed the maximum efficiency. Therefore, *a priori* all values of μ'_C above the limit are possible, each value leading to *indifferent* equilibrium, without a tendency of increasing or decreasing.

These considerations refer to the transport of matter purely by convection, in which case the material flow decreases with the increasing gradient. Should, in some place of the surf region, the transport by convection fail, on account of too steep a gradient, a discontinuity may arise, with $\mu' \to \infty$. In this case, however, gas diffusion will come into play, with an efficiency limited only by the velocity of the gas molecules, and will provide the supply required to keep the transport going. It is therefore safe to conclude that any material flow with $\mu'_C \geqslant \mu'_m$ tapped at the inside edge of the surf region (to the left of b, Fig. 1) will be met somehow inside the surf region, if necessary through gas diffusion and a discontinuity in the gradient. (*Cf.* also *Addendum.*)

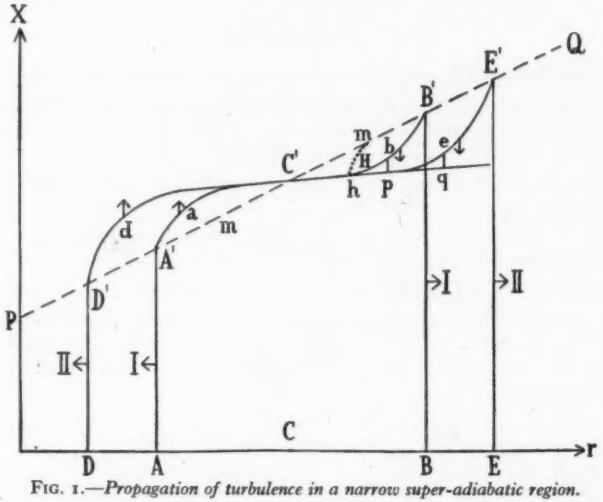

FIG. 1.—*Propagation of turbulence in a narrow super-adiabatic region.*

The above uncertainty in the gradient μ'_C is removed by the following considerations. As shown in Section 7, convection is likely to start suddenly over a strip Δr of finite width, of the order of 10^8 to 5×10^8 cm. where the critical temperature gradient is already surpassed. The disturbance when once started is one of readjustment of hydrostatic equilibrium and as such is not governed by the restrictive formulae (74) or (80); the mixing all over the strip (where $n < n_c$ has been reached) will be practically complete at the first moment, $\mu'_C \cong 0$, and after the violent motion has calmed down, the further development requiring $\mu'_C \geqslant \mu'_m$ will force μ'_C to increase until μ'_m is attained, and never beyond that—simply because of the indifferent equilibrium reached. Therefore it appears that the second condition, $\mu'_C = \mu'_m$ is practically, although not necessarily fulfilled at C'; the optimum gradient and the maximum possible material flow establish

themselves automatically in a narrow starting region of turbulence. Actually the central portion at C′ will stretch out into an almost straight line at the optimum inclination, whereas the curved ends b, e, a, d, representing the "surf" range, will remain of a more or less fixed effective width.

In the case of a finite or large width of the convective zone, when the different variables can no longer be considered as constant, the circumstances are more complicated. However, the above reasoning may be applied to narrow regions of the "surf" near the two interfaces. It follows that at each interface the gradient (μ' or X') assumes a value equal to the corresponding optimum value (μ'_m), when the solution of the differential equation (93) is such that everywhere except at the interfaces $|F_x|<|F_{\max.}|$ and $\mu'<\mu'_m$; this is the case of the numerical example given below. When the above condition cannot be fulfilled, another type of solution follows with $\mu'=\mu'_m$ and $F_x=F_{\max.}$ at a certain median point, and $\mu'>\mu'_m$, $|F_x|<|F_{\max.}|$ everywhere else including the interfaces.

Below are given results of the computation of the time of mixing for a particular model. To apply the results in other cases, homologous transformations with the following proportionalities can be used: $X=f(Mr/M)$, thus μ kept same, as well as $n_0=f_1(Mr/M)$; $r\sim R$; $\mathfrak{a}\sim R$; $X'\sim\mu'\sim\omega'\sim R^{-1}$; $\omega^2\sim\bar{\beta}MR^{-3}$; $g\sim\bar{\beta}MR^{-2}$; $F_x\sim F_{\max.}\sim LT^{-1}\sim LR(\bar{\beta}M)^{-1}$; hence the time of mixing becomes

$$t\sim M/F_x\sim\frac{\bar{\beta}M^2}{LR}. \tag{95}$$

Table VI contains abbreviated data for Model "C_3" (**13**), in which a considerable region outside the core is in a super-adiabatic state. For more detail about the model we refer to the original publication (**13**).

TABLE VI

Model "C_3"

$\mu=\frac{8}{5}/(X+\frac{1}{3})$; $\epsilon=1\cdot766\times10^{-109}\,X\rho T^{15}$; $M=3\cdot27\times10^{33}$ g.;
$T_c=2\cdot5\times10^7$ deg.; $\rho_c=100$ g./cm.^{3}; $L=1\cdot92\times10^{34}$ erg/sec.;
$R=1\cdot05\times10^{11}$ cm.

(Super-adiabatic region ($n_0=1\cdot5$) extends from $r=5\cdot87$ to $r=14\cdot85\times10^9$ cm.)

r, 10^9 cm.	6·0	6·2	6·8	8·4	10·4	12·8	13·6	14·4
T, 10^7 deg.	21·3	21·1	20·8	19·8	18·7	17·5	17·1	16·7
$4\pi r^2\rho$, 10^{22} g./cm.	1·92	1·96	2·12	2·78	3·86	5·29	5·77	6·24
M_r, 10^{31} g.	6·54	6·93	8·15	12·0	18·7	29·6	34·0	38·8
L_r, 10^{33} erg/sec.	6·33	7·01	8·90	12·8	15·9	17·9	18·2	18·5
X_0	0·294	0·320	0·377	0·449	0·480	0·494	0·496	0·497
n_0	1·45	1·40	1·23	1·10	1·12	1·30	1·38	1·46
n_c	Small.....				0·64	1·19	1·29	1·36
$F_{\max.}$, 10^{16} g./sec.	−1·4	−5·0	−15·0	−33·6	−41·7	−27·4	−19·1	−7·5

In the table X_0 is the original distribution of hydrogen abundance before mixing; as $n_0>n_c$ throughout, the region is in the stable state of radiative equilibrium with $n=n_0$. The closest approach of n_0 to n_c takes place at $r=13\cdot6$ and we assume that at this spot the disturbance is somehow started.

The characteristic parameters for the turbulent flow, on the assumption of unchanged state after turbulence has started, are given below for the two extreme and the middle points of the region, for $\omega=2\times10^{-6}$ (homologously corresponding to $\omega=3\times10^{-6}$ at solar mass), $\cos^2\phi=\frac{2}{3}$:

TABLE VII

r	ω'	a		μ'_m	X'_m	X'_0	
10^9 cm.	10^{-18} cm.$^{-1}$	10^{11} cm.	$\sqrt{a\omega'}$	10^{-14} cm.$^{-1}$	10^{-14} cm.$^{-1}$	10^{-12} cm.$^{-1}$	X'_m/X'_0
6·0	2·30	16·7	0·020	1·19	0·75	135	$5{\cdot}6\times10^{-5}$
10·4	2·42	3·41	0·009	2·68	2·17	9·6	0·0023
14·4	2·23	20·1	0·021	1·07	0·89	1·49	0·0060

Here $\sqrt{a\omega'}$ is so small that it exerts little influence in formula (80). $X'_m=(X+\frac{1}{3})\mu'_m$ (equation (79)) is the optimum gradient of hydrogen concentration, the true gradient $X'\leqslant X'_m$ according to the preceding theory. $X'_0=\partial X_0/\partial r$ is the original undisturbed gradient. The ratio X'_m/X'_0 is so small throughout that, for the purpose of calculating the time intervals, we may neglect the gradient, assuming $X'=0$ all over the disturbed region, which greatly simplifies our solution; in the disturbed region $X=$const. is a pure function of time alone, $\partial X/\partial t$ is independent of r, whence from (93)

$$\frac{\partial F_x}{\partial r}=-4\pi\rho r^2C_1,$$

or

$$F_x=C_1\int_{r_1}^{r}4\pi r^2\rho dr+C_2. \tag{96}$$

The constants C_1 and C_2 are determined from the condition that at $r=r_1$ and $r=r_2$ (limits or interfaces of the disturbed region), $(F_x)=F_{\max.}$; at $r=r_1$, $F_x=(F_{\max.})_1=C_2$; at $r=r_2$,

$$C_1=-\frac{(F_{\max.})_2-(F_{\max.})_1}{\int_{r_1}^{r_2}4\pi\rho r^2dr}. \tag{97}$$

Equation (93) is then represented simply as $\partial\overline{X}/\partial t=C_1$, where

$$\overline{X}=\frac{\int_{r_1}^{r_2}X_0dM_r}{M_2-M_1}. \tag{98}$$

The time interval is approximately given by $t=\Delta\overline{X}/C_1$. The limiting radii r_1, r_2 should not be taken arbitrarily, but in agreement with the relative speed of the propagation of the turbulence in the two directions:

$$\left(\frac{dr_1}{dt}\right):\left(\frac{dr_2}{dt}\right)=\frac{(F_{\max.})_1}{(F_{\max.})_2}\cdot\frac{[\rho r^2(X_0-\overline{X})]_2}{[\rho r^2(X_0-\overline{X})]_1}. \tag{99}$$

The method is applicable only when $\overline{X}$ changes definitely with time. Actually another method was used which may be applied also in the case of $\overline{X}$ remaining constant. Let $\bar{r}$ be the median radius of the disturbance where $\overline{X}=X_0$ and let us consider two consecutive stages of the disturbance: r_1, r_2, $\overline{X}$ (preceding stage); r'_1, r'_2, $\overline{X}_f$ (following stage). Let

$$\Delta M_x=\int_{r_1'}^{\bar{r}}(X_0-\overline{X}_f).4\pi\rho r^2dr-\int_{r_1}^{\bar{r}}(X_0-\overline{X}).4\pi\rho r^2dr, \tag{100}$$

a negative quantity which represents the mass of hydrogen flowing over the median $\bar{r}$ from the outer half of the region toward the inner half between the two stages. Further, let

$$\overline{F}_x=\tfrac{1}{2}[(F_x)_{\bar{r}}+(F_x)_{\bar{r}}'\,]\,; \tag{101}$$

the time interval between the two stages is then

$$\Delta t = \frac{\Delta M_x}{\bar{F}_x} \text{(seconds)}. \tag{102}$$

It may be added that in the solution, F_x as determined from (96) always did conform with the conditions $|F_x| \leqslant |F_{\max.}|$ which is a check upon the choice of the method applied, i. e. upon the assumption that the first case of the solution of (93) with $F_x = F_{\max.}$ at $r = r_1$ and $r = r_2$ is to be taken.

By solving graphically equations (96)–(101), with the numerical data as illustrated by Table VI, the results of Table VIII were obtained (the calculations are rather approximate, of course). The last three columns contain the data reduced to solar dimensions according to the homology relations (95); these time intervals by (95) are 2·8 times larger than those for the original model; t is the duration from the start to the given stage. The figures are well within the order of magnitude of the time intervals involved in the last (Quaternary and pre-Quaternary) ice age (**14**).

TABLE VIII

Time of Propagation of a Turbulent Disturbance in the super-adiabatic Zone of Model "C_3" (**13**)

Stage	X	$M = 3{\cdot}27 \times 10^{33}$, $R = 1{\cdot}05 \times 10^{11}$				$M = M_\odot$, $R = R_\odot$, $L = L_\odot$		
		r_1 10^9 cm.	r_2 10^9 cm.	$\bar{r}$ 10^9 cm.	Δt sec.	r_1 10^9 cm.	r_2 10^9 cm.	t years
I	0·4956	13·6	13·6	13·6		9·07	9·07	0
II	0·4942	12·0	14·4	13·18	$7{\cdot}0 \times 10^{11}$	8·00	9·60	$6{\cdot}2 \times 10^4$
III	0·4933	11·2	14·6	12·74	$5{\cdot}7 \times 10^{11}$	7·47	9·73	$1{\cdot}1 \times 10^5$
IV	0·4900	9·6	14·70	11·95	$2{\cdot}0 \times 10^{12}$	6·40	9·80	$2{\cdot}9 \times 10^5$
V	0·4850	8·0	14·78	11·00	$4{\cdot}8 \times 10^{12}$	5·33	9·85	$7{\cdot}1 \times 10^5$
VI	0·4791	6·8	14·84	10·32	$9{\cdot}9 \times 10^{12}$	4·53	9·89	$1{\cdot}6 \times 10^6$
VII	0·4748	6·2	14·85	9·95	$1{\cdot}9 \times 10^{13}$	4·13	9·90	$3{\cdot}3 \times 10^6$
VIII	0·4728	6·0	14·85	9·73	$3{\cdot}2 \times 10^{13}$	4·00	9·90	$6{\cdot}1 \times 10^6$
IX	0·4721	5·87	14·85	...	∞	3·91	9·90	∞

It must be pointed out that the effect of the mixing upon the energy production is rather complicated. Although more hydrogen is transported towards the hotter regions, the temperature of these regions will be lowered as the result of mixing because the adiabatic gradient, according to which the temperature of the transported hydrogen rises, is lower than the former super-adiabatic gradient ($\mu < \bar{\mu}$, $n_0 < n_a$).

Take a unit of mass at r_1, T_1, ρ_1, P_1, X_1, $\mu_1 = k/(X_1 + b)$, another at r_2, T_2, P_2, etc., and a law of energy generation $\epsilon \sim X\rho T^s$; interchange these two units, the second being transferred to pressure P_1, the first to P_2, assuming adiabatic changes of state. The ratio of the energy output after the interchange to the original output of these two units of mass is then

$$\frac{\bar{\epsilon}'}{\bar{\epsilon}} = \frac{A/B + B}{A + 1}, \tag{103}$$

where

$$A = \frac{X_2}{X_1}\frac{\rho_2}{\rho_1}\left(\frac{T_2}{T_1}\right)^s,$$

and

$$B = \left(\frac{P_2}{P_1}\right)^{\frac{s+n_a}{n_a+1}}, \text{ with } \frac{P_2}{P_1} = \frac{\rho_2 T_2 \mu_1}{\rho_1 T_1 \mu_2}.$$

The normal case is of X increasing outwards, thus of $X_2 > X_1$ when $P_2 < P_1$, $T_2 < T_1$. A gain in the energy production is expected after the interchange, when $A/B + B > A + 1$ by (103), which yields $A > B$; when $A < B$, the mixing will lead to a decrease in the energy production. Evidently, for a given change of state, and for a given value of B, A is proportional to X_2/X_1; the result depends thus upon the contrast in the hydrogen content: small values of X_2/X_1 yield a negative effect, large values a positive effect of mixing upon energy generation. Thus, for Model "C_3" (Table VI), with $s = 15$ and $n_a = 1{\cdot}5$, an interchange between $r_1 = 6{\cdot}8 \times 10^9$ and $r_2 = 10{\cdot}4 \times 10^9$ cm. yields $A = 0{\cdot}2140$, $B = 0{\cdot}2389$, $\bar{\epsilon}'/\bar{\epsilon} = 0{\cdot}93 < 1$ at $X_2/X_1 = 1{\cdot}27$; an interchange between $r_1 = 6{\cdot}0$, $r_2 = 8{\cdot}4 \times 10^9$ yields $A = 0{\cdot}4011$, $B = 0{\cdot}3668$, $\bar{\epsilon}'/\bar{\epsilon} = 1{\cdot}04 > 1$ at $X_2/X_1 = 1{\cdot}53$. In any case, for a moderate contrast in X, the effect upon the energy production is rather small as compared with X_2/X_1.

Complications from general changes of the structure of the model will add to that. To produce a dimming of solar luminosity by 10–20 per cent, required to explain the Quaternary ice age, an equal relative increase in the internal energy production is needed (**14**); for that, an even more contrasty distribution of X is required, as compared with the distribution in Table VI.

In the mixing, the chief effect will appear at the end (stages VII–VIII of Table VIII), when the greatest contrast in X is obtained. Tables VI–VIII represent, of course, one of the many possibilities, to be considered only as an example of what may happen.

Armagh Observatory,
Northern Ireland:
1948 *November* 2.

References

(1) G. I. Taylor, *Phil. Trans.* A, **215**, 1, 1915; *Proc. Roy. Soc.* A, **135**, 685, 1932.
(2) L. Prandtl, *Zts. f. Angew. Math. u. Mech.*, **5**, 136, 1925 a.o.
(3) W. Schmidt, *Wiener Sitzber.*, **IIa**, 126, 1927 a.o.
(4) L. Biermann, *Zeit. f. Astrophys.*, **5**, 117, 1932; *A.N.*, **264**, 361, 1938.
(5) J. Wasiutynski, *Astroph. Norvegica*, **4**, 1946.
(6) E. Öpik, *Tartu Obs. Pub.*, **30**, No. 4, 1938.
(7) H. Bénard, *Revue gen. d. Sc.*, **11**, 1261 and 1309, 1900; *Ann. d. Phys. et de Chim.*, 7e série, **23**, 62, 1901.
(8) H. C. Dickinson and M. S. van Dusen, *A. S. Refrig. Eng. Journ.*, **3**, No. 2, 1916; cited from *Smithsonian Phys. Tables*, 8th ed. 1933, p. 327.
(9) H. von Zeipel, *Festschrift f. H. v. Seeliger*, 144, 1924.
(10) E. Öpik, *Tartu Obs. Pub.*, **30**, No. 3, 1938.
(11) Z. Kopal, *M.N.*, **96**, 854, 1936.
(12) P. Ledoux, *Ap. J.*, **105**, 305, 1947.
(13) E. Öpik, *Proc. Roy. Irish. Acad.*, A, **54**, 49, 1951; *Contrib. Armagh Obs.*, No. 3.
(14) E. Öpik, *M.N.*, **110**, 49, 1950.
(15) A. S. Eddington, *Internal Constitution of the Stars*, Cambridge, 1926.
(16) F. W. Lanchester, *Aerodynamik* (German translation), p. 187, Leipzig-Berlin, 1909.
(17) S. Chapman, *M.N.*, **82**, 292, 1922.
(18) E. Öpik, *Rotational Currents*, unpublished.

ADDENDUM

In connection with the problem of the spread of turbulence (Section 12), consider two similar points, b and e, in the two consecutive "surf" regions (bB′→eE′, Fig. 1), such that their elevations over the X'_C level (straight line C′pq) are equal, bp = eq. Let the displacement pq = Δr be infinitesimal and correspond

to a time interval Δt (in Fig. 1, the displacement is too large ; imagine e to fall closely below bB′). If $X' = (\partial X/\partial r)_b$, evidently

$$(X' - X'_C)\Delta r = -\frac{\partial X}{\partial t}\Delta t,$$

whence the rate of propagation of the surf is given by

$$\frac{\Delta r}{\Delta t} = -\frac{\partial X}{\partial t}/(X' - X'_C).$$

Substituting $\partial X/\partial t$ from this into (94), and considering that for the narrow layer of turbulence $X' = \mu' \times \text{const.}$, we obtain

$$\frac{\Delta r}{\Delta t}(\mu' - \mu'_C) = -C\frac{\partial \mu'}{\partial r}\left[\frac{\omega'}{(\omega' + \mu')^3} - a\right]. \tag{A}$$

As $\Delta r/\Delta t$ is always finite, a singular solution of (A) is the straight line $\mu' = \mu'_C$, $\partial\mu'/\partial r = 0$.

$\Delta r/\Delta t$ may be variable inside the surf region, especially at the beginning, during the transition from the first violent upset of hydrostatic equilibrium toward regular convection; depending upon this variable, the general solution for μ' is defined by equation A. However, over a long run, the surf region should displace itself along similar configurations, which means that the speed of propagation of the disturbance will become nearly the same for the whole surf region *at a given moment*, or

$$\Delta r/\Delta t \to \text{const.} \tag{B}$$

With this condition (A) can be integrated and yields

$$x = \frac{(1+y_c)^2}{(1+y_c)^2 - a}\ln(y - y_c) + \frac{\sqrt{a}}{2(1+y_c+\sqrt{a})}\ln(1+y+\sqrt{a}) - \frac{\sqrt{a}}{2(1+y_c-\sqrt{a})}\ln(1+y-\sqrt{a}) + \text{const.}, \tag{C}$$

where $x = [(\Delta r/\Delta t)a/C]r$, $y = \mu'/\omega'$, $a = 1/a\omega' > 1$. The optimum gradient μ'_m corresponds to $y_m = \sqrt{a} - 1$.

With $y > y_c$, (C) is finite. However, at $y \to y_c > y_m$, the first term in (C) tends to $-\infty$; the transition from the curved portion toward the straight line (Fig. 1) is asymptotical, or the distance C′b (Fig. 1) is infinite. At $y > y_c = y_m$, the first and third terms in (C) are infinite, their sum tending to $-\sqrt{a}/2(y - y_c)$, thus to $-\infty$ again as $y \to y_c = y_m$. A finite interval of r between the straight and curved portions of the surf can be obtained only with $\Delta r/\Delta t$ infinite, or an infinite speed of propagation at $y \to y_c$. The straight-line portion of the surf region expands quickly and replaces the curved portion, reducing the latter to infinitesimal dimensions.

Thus the region of transition, $\mu' > \mu'_C$, in the surf region disappears as (B) is fulfilled. In the limiting case the surf effect may be represented by a straight line (C′h, Fig. 1) with the optimum inclination corresponding to μ'_m, almost suddenly changing into a "cliff" (dotted line hH in Fig. 1) of a gradient steep enough to effect all the transport of matter by gas diffusion. The analogy with a real surf is much closer than was anticipated at first.

With condition (B), gas diffusion requires an exponential run of μ' asymptotically merging into the original undisturbed distribution. The fitting of this exponential "cliff" (hH, Fig. 1) to the convective linear region (C′h) is always possible.

TWO-COLOUR INDICES AND GENERAL RELATIVITY

G. C. McVittie

(Received 1950 August 22)

Summary

When the system of the extra-galactic nebulae is represented by a homogeneous model of general relativity, it is shown that the formula for the two-colour index measured by Stebbins and Whitford can be established theoretically. Comparison of this theory with the observations leads to the conclusion that the interpretation of the reddening of remote nebulae as a time-effect cannot be regarded as proven because of the paucity of data, but that there is a strong presumption in its favour.

The " two-colour " indices of certain elliptical extra-galactic nebulae measured by Stebbins and Whitford* suggest that there is a change of colour-index with distance and that there is possibly a consequential change of spectral energy-distribution. Since the light by which we observe a distant nebula left it at an earlier date than the light by which we see a nearer one, these measurements may well prove to be the first observational data for an evolutionary process in the elliptical nebulae. At the suggestion of Dr Martin Schwarzschild, I have attempted to present in this paper a theory of the two-colour index in general relativity and to interpret the observations in terms of this theory. I am also indebted to Dr Schwarzschild for his help in making clear to me the technical details of the photometry involved in S. & W.

Theory of the two-colour index.—In general relativity, when abstraction is made of the observed irregularities in the spatial distribution of the extra-galactic nebulae and they are replaced by a uniform system, the set of idealized nebulae is " mapped " in one of the Riemannian space-times with metric of the form†

$$ds^2 = dt^2 - \frac{R^2(t)}{c^2}\left(\frac{dr^2 + r^2 d\theta^2 + r^2 \sin^2\theta d\phi^2}{(1 + kr^2/4)^2}\right).$$

Each nebula has fixed coordinates (r, θ, ϕ) and the observer, O, may be taken to be at the origin (0, 0, 0) whilst the mechanical properties (pressure and density) of the whole system of nebulae depend only on t and the constant k. We shall make the further assumption that, at each instant t, the energy-distribution function of every nebula is the same but that this function varies with t. Consider a nebula N and a comparison nebula S which is so "near" to O that the spectral energy-distribution of S which O would observe with a perfect measuring instrument is the same as the distribution emitted by S. On the other hand, let N be so distant that the moment of emission, t_1, of the radiation by N is very different from the moment of its receipt, t_0, by O. Since it can be shown that $(t_0 - t_1)$ may be expanded as a power-series in the red-shift δ ($= \Delta\lambda/\lambda$) we are, in effect, defining S as

* J. Stebbins and A. E. Whitford, *Ap. J.*, **108**, 413, 1948. Hereinafter this paper is referred to as "S. & W.".

† See, e. g., G. C. McVittie, *Cosmological Theory*, Methuen & Co. (London), and John Wiley & Sons (New York), Chap. IV, 1949.

a nebula whose red-shift is sensibly zero, whereas N shows an appreciable red-shift.

The energy-distribution will depend on the wave-length, λ, of the radiation and on certain parameters $A, B, C, \ldots$ defining the condition of the emitter. It is these parameters which we are assuming to be functions of t. Let N emit, at time t_1, in the range of wave-length λ_1 to $\lambda_1 + d\lambda_1$ an amount of energy $E_1(\lambda_1)\,d\lambda_1$, where, in the energy-distribution function E, the suffix 1 denotes that the parameters $A, B, C, \ldots$ have been evaluated at the instant t_1. When this light reaches O it is observed by him to lie in the range of wave-length λ to $\lambda + d\lambda$, where*

$$\lambda = (1+\delta_1)\lambda_1, \quad d\lambda = (1+\delta_1)\,d\lambda_1,$$

and its amount is

$$\frac{G}{1+\delta_1} E_1\left(\frac{\lambda}{1+\delta_1}\right) d\lambda, \tag{1}$$

where G is a function depending on the r-coordinate of N and on t_0 and t_1. Similarly, in the range λ_1' to $\lambda_1' + d\lambda_1'$ emitted by N, O observes

$$\frac{G}{1+\delta_1} E_1\left(\frac{\lambda'}{1+\delta_1}\right) d\lambda', \tag{2}$$

where G has the same value as in (1). We assume that the observer allows for galactic absorption, atmospheric extinction, the sensitivity of his apparatus and all other local effects. We must also allow for the fact that measurements such as those of Stebbins and Whitford are expressed in certain conventional units and we can do this by introducing an unknown function α of the *observed* wave-length, λ, and saying that the measured energies are, respectively,

$$F_1(\lambda)d\lambda = \frac{\alpha(\lambda)}{1+\delta_1} GE_1\left(\frac{\lambda}{1+\delta_1}\right) d\lambda \tag{3}$$

and

$$F_1(\lambda')d\lambda' = \frac{\alpha(\lambda')}{1+\delta_1} GE_1\left(\frac{\lambda'}{1+\delta_1}\right) d\lambda'. \tag{4}$$

The observer can now introduce a " two-colour " index

$$(I_{\lambda\lambda'})_N = 2{\cdot}5 \log_{10} \frac{F_1(\lambda)d\lambda}{F_1(\lambda')d\lambda'} = 2{\cdot}5 \log_{10} \frac{E_1\left(\frac{\lambda}{1+\delta_1}\right)\alpha(\lambda)d\lambda}{E_1\left(\frac{\lambda'}{1+\delta_1}\right)\alpha(\lambda')\,d\lambda'} \tag{5}$$

as a measure of the ratio of the intensity of radiation at wave-length λ to that at wave-length λ'. We assume that δ_1 is small, so that its square and higher powers can be neglected, and we write

$$\epsilon = 2{\cdot}5/\log_e 10 = 1{\cdot}086.$$

Then by (5)

$$\begin{aligned}(I_{\lambda\lambda'})_N &= \epsilon\left\{\log_e \frac{\alpha(\lambda)d\lambda}{\alpha(\lambda')d\lambda'} + \log_e \frac{E_1(\lambda) - \lambda\delta_1 E_1'(\lambda)}{E_1(\lambda') - \lambda'\delta_1 E_1'(\lambda')}\right\} \\ &= \epsilon\left[\log_e \frac{\alpha(\lambda)d\lambda}{\alpha(\lambda')d\lambda'} + \log_e \frac{E_1(\lambda)}{E_1(\lambda')} - \delta_1\left\{\lambda\frac{E_1'(\lambda)}{E_1(\lambda)} - \lambda'\frac{E_1'(\lambda')}{E_1(\lambda')}\right\}\right],\end{aligned} \tag{6}$$

where $E_1'(\lambda) = \dfrac{d}{d\lambda} E_1(\lambda)$, etc. But now by hypothesis S is so near to O that we can take the moment of emission as being effectively t_0 so that the energy-distribution

* See, e. g., W. H. McCrea, *Zeit. f. Astrophys.*, **9**, 290, 1935.

function is $E_0(\lambda)$. Hence for S

$$(I_{\lambda\lambda'})_S = \epsilon\left[\log_e \frac{\alpha(\lambda)d\lambda}{\alpha(\lambda')d\lambda'} + \log_e \frac{E_0(\lambda)}{E_0(\lambda')}\right]. \tag{7}$$

If therefore the observer subtracts (7) from (6), he gets rid of the unknown function α and finds that

$$(I_{\lambda\lambda'})_N - (I_{\lambda\lambda'})_S = \epsilon\left[\log_e\left\{\frac{E_1(\lambda)}{E_0(\lambda)}\Big/\frac{E_1(\lambda')}{E_0(\lambda')}\right\} - \delta_1\left\{\frac{\lambda E_1'(\lambda)}{E_1(\lambda)} - \frac{\lambda' E_1'(\lambda')}{E_1(\lambda')}\right\}\right]. \tag{8}$$

Suppose now that we have a number of nebulae $N_a, N_b, \ldots N_q, \ldots$ whose light, emitted at times $t_a, t_b, \ldots t_q, \ldots$, respectively, is received simultaneously at time t_0 by O. Denote by the suffixes $a, b, \ldots q, \ldots$ quantities associated with the times of emission, respectively, and let the two-colour index of the nebula N_q be $(I_{\lambda\lambda'})_q$. Using the formula (8) for N_q and N_a, respectively, and subtracting, we find our fundamental formula for the difference of the two-colour indices, viz.—

$$\begin{aligned}(I_{\lambda\lambda'})_q - (I_{\lambda\lambda'})_a = \epsilon\Bigg[&\log_e\left\{\frac{E_q(\lambda)}{E_a(\lambda)}\Big/\frac{E_q(\lambda')}{E_a(\lambda')}\right\} \\ &+ \delta_a\left\{\frac{\lambda E_a'(\lambda)}{E_a(\lambda)} - \frac{\lambda' E_a'(\lambda')}{E_a(\lambda')}\right\} - \delta_q\left\{\frac{\lambda E_q'(\lambda)}{E_q(\lambda)} - \frac{\lambda' E_q'(\lambda')}{E_q(\lambda')}\right\}\Bigg].\end{aligned} \tag{9}$$

A particular case of the foregoing theory is that in which the parameters $A, B, C, \ldots$ which occur in the function E are all constants, so that there is no secular change in the energy-distribution function of a nebula. If in (9) we write

$$E_q = E_a = E \text{ (say)},$$

we obtain

$$(I_{\lambda\lambda'})_q - (I_{\lambda\lambda'})_a = \kappa(\delta_q - \delta_a), \tag{10}$$

where κ is a constant for a given pair of wave-lengths, and

$$\kappa = \epsilon\left\{\frac{\lambda' E'(\lambda')}{E(\lambda')} - \frac{\lambda E'(\lambda)}{E(\lambda)}\right\}. \tag{11}$$

Comparison with observation.—The following data are taken from S. & W. Table 6, except that the " velocities of recession ", V, have been converted back to the red-shifts (which are observed) by means of the formula $\delta = V/c$.

Cluster and Nebula	δ	C_p
18 nebulae in Virgo	·0041	0·86
Coma; NGC 4872 and Anon	·0219	0·96
Coma; NGC 4889	·0219	1·05
Cor. B.: Nos. 1, 3, 4	·0733	1·13
Cor. B.: No. 2	·0733	1·15
Bootes: No. 1	·1297	1·36

Apart from the zero-point (irrelevant in this connection), our $I_{\lambda\lambda'}$ is identical with C_p. The effective wave-lengths are (S. & W. Table 3)

$$\left.\begin{aligned}\lambda &= 5{\cdot}29 \times 10^{-5} \text{ cm. (Yellow)}, \\ \lambda' &= 4{\cdot}32 \times 10^{-5} \text{ cm. (Blue)}.\end{aligned}\right\} \tag{12}$$

Let us assume, firstly, that E is the same for all nebulae and interpret the observations in terms of (10) and (11) as is done by S. & W. (their Fig. 6). We identify N_a with the 18 nebulae in Virgo and N_q in turn with each of the nebulae

in the other clusters. The values of κ so found are listed in Table A in which we have also given the approximate times of travel* of the light by which we see the nebulae. It is interesting to observe that κ has approximately the same value for the five nebulae in the Cor. Bor. and Bootes clusters, though the time of travel of the light from the latter cluster is nearly twice the time of travel from the former. This might be regarded as evidence that the function E was independent of the time, were it not that the three nebulae in Coma give κ's that are different. If there were sufficient measurements to provide the same value of κ for a more numerous selection of nebulae at different distances from the Galaxy than the eight with which we are dealing, it would be worth while to use this κ to find a corresponding function E from formula (11). Such a procedure seems premature at the present stage. But, as a second way of interpreting the data, it is instructive to abandon the assumption that E is independent of t and to assume that each nebula radiates like a black body at a single temperature $T(t)$. Undoubtedly this is an over-simplification in view of S. & W.'s conclusion that a nebula radiates like a mixture of black bodies.

TABLE A

N_q	κ	T_q	(t_a-t_q) in 10^8 years
(N_a=18 nebulae in Virgo)	...	(T_a=6000 deg.)	7½
Coma : NGC 4872 and Anon	5·6	5600	45
Coma : NGC 4889	10·7	5200	45
Cor. B. : Nos. 1, 3, 4	3·9	5200	130
Cor. B. : No. 2	4·2	5100	130
Bootes : No. 1	4·0	4700	240

Black-body radiation.—Let us assume that the S. & W. measurements refer to black-body radiation of wave-lengths (12). We have also

$$E_1(\lambda)=\frac{c_1\lambda^{-5}}{\exp(c_2/\lambda T_1)-1},\quad E_0(\lambda)=\frac{c_1\lambda^{-5}}{\exp(c_2/\lambda T_0)-1},$$

so that there is now but one parameter A, B, C, . . . , which is the temperature T and it is, by hypothesis, a function of t. We have thus

$$\frac{E_1(\lambda)}{E_0(\lambda)}=\exp\left\{\frac{c_2}{\lambda}\left(\frac{1}{T_0}-\frac{1}{T_1}\right)\right\}\frac{1-\exp(-c_2/\lambda T_0)}{1-\exp(-c_2/\lambda T_1)}.$$

If λ is measured in centimetres we have $c_1=3{\cdot}71\times10^{-5}$, $c_2=1{\cdot}435$, and so, if λ is about 5×10^{-5} cm. and T_0, T_1 are each about 5000 deg., the value of $\exp(c_2/\lambda T)$ is about 310. Thus, as a first approximation, we may write

$$\left.\begin{aligned}\log_e\frac{E_1(\lambda)}{E_0(\lambda)}&=\frac{c_2}{\lambda}\left(\frac{1}{T_0}-\frac{1}{T_1}\right)\\ \text{and}\qquad\log_e\frac{E_1(\lambda')}{E_0(\lambda')}&=\frac{c_2}{\lambda'}\left(\frac{1}{T_0}-\frac{1}{T_1}\right).\end{aligned}\right\}\qquad(13)$$

Again,

$$\frac{\lambda E_1'(\lambda)}{E_1(\lambda)}=-5+\frac{c_2}{\lambda T_1}\{1-\exp(-c_2/\lambda T_1)\}.$$

* E. Hubble, *The Observational Approach to Cosmology*, Oxford, 1937.

Hence, with these approximations, (8) is

$$(I_{\lambda\lambda'})_N-(I_{\lambda\lambda'})_S=\frac{\epsilon c_2}{T_0}\left(\frac{1}{\lambda}-\frac{1}{\lambda'}\right)\left\{1-\frac{T_0}{T_1}(1+\delta_1)\right\}, \tag{14}$$

whilst (9) becomes

$$(I_{\lambda\lambda'})_q-(I_{\lambda\lambda'})_a=\frac{\epsilon c_2}{T_a}\left(\frac{1}{\lambda'}-\frac{1}{\lambda}\right)\left\{\frac{T_a}{T_q}(1+\delta_q)-(1+\delta_a)\right\}. \tag{15}$$

We regard this as a formula for T_q in terms of T_a and so we write it as

$$\frac{T_a}{T_q}=1+\left\{\frac{\{(I_{\lambda\lambda'})_q-(I_{\lambda\lambda'})_a\}(1-\delta_q)}{\frac{\epsilon c_2}{T_a}\left(\frac{1}{\lambda'}-\frac{1}{\lambda}\right)}-(\delta_q-\delta_a)\right\}, \tag{16}$$

neglecting powers of δ_q higher than the first. Using again the S. & W. data we find the values of T_q listed in the third column of Table A. It is hard to escape from the conclusion that there is indeed a progressive fall in black-body temperature of the radiation as we proceed to nebulae of increasing red-shift, the rate of fall being, however, difficult to estimate in view of the curious case of NGC 4889.

In researches on the system of the extra-galactic nebulae—the so-called "cosmological problem"—it is too often the practice of theoreticians, and even sometimes of observers, to draw positive and far-reaching conclusions from the slenderest of data. We have here a case in point: two-colour indices have been measured for 26 nebulae, of which 18 lie in the "nearby" Virgo cluster. These measurements do indeed suggest—but do no more than suggest—that the average spectral energy-distribution of the elliptical nebulae undergoes a secular reddening as we recede in time from the present moment. But to conclude from measurements on 26 nebulae, of which only 8 lie in distant clusters, that "there is every reason to believe that this reddening is a universal effect for E (elliptical) nebulae at all distances in every part of the sky" (S. & W. p. 426) seems premature, even when the conclusion is qualified by the remark that "we (i. e. S. & W.) are well aware of the danger of drawing far-reaching conclusions from the observations of only a few objects". The correct conclusion, in the present author's opinion, is that more measurements of red-shift and of two-colour index are urgently needed and should be made for nebulae in as many clusters as possible. When we have these data for, say, 20 nebulae in *each* of the clusters Pegasus, Perseus, Coma, etc., for which red-shifts have been measured, we should possess a surer foundation for comparison with the 18 nebulae in Virgo and be in a position to determine whether this secular effect exists or not.

Queen Mary College,
Mile End Road,
London, E.1:
1950 *June* 29.

ON THE INTERPRETATION OF THE HERTZSPRUNG-RUSSELL DIAGRAM

H. Bondi

(Received 1950 August 26)

Summary

A general discussion of laws of energy generation and opacity is given, together with a brief account of stellar evolution based on the view that stars consist almost entirely of hydrogen and helium. The Hertzsprung-Russell diagram is drawn, using mainly Kuiper's data on the nearest stars and also his estimates of surface temperatures and bolometric corrections. It is shown that this diagram strongly indicates that a switch of the law of energy generation occurs for stars of a luminosity about one-sixth that of the Sun. The brighter stars draw their energy from a highly temperature-sensitive process which is probably the Bethe cycle. The fainter stars draw their energy from a much less temperature-dependent process the proton-proton reaction (presumably).

Consideration of the Sun's central temperature shows that the astrophysical data definitely contradict the earlier estimates for the critical temperature of the Bethe cycle and tend to show that this temperature may even be slightly lower than the more recent experiments indicate.

---

1. Comparisons between the results of the theory of stellar constitution and the observations have generally been carried out by considering the mass-luminosity and the mass-radius relations. This approach has some advantages, especially in that it makes use of all the observable properties of stars and in that the physically fundamental quantity, the mass, appears as independent variable. On the other hand, the smooth outlines of the Hertzsprung-Russell diagram, when compared with the scatter of the empirical mass-luminosity relation, indicate that the observational determinations of the stellar masses are perhaps not as accurate and certainly not as numerous as measurements of luminosity and type. Accordingly it may be advantageous to compare the theoretical luminosity-surface temperature relation with the observational one. This task is simplified and greatly aided by the fact that the theoretical interpretation of the red giants and of the white dwarfs is now fairly certain. It is the purpose of the present paper to carry out such a comparison and it is claimed that, in spite of the exclusion of the observational determinations of stellar masses, valuable conclusions can be drawn. In the last section of the paper one special stellar mass is also considered, namely the mass of the Sun, which is known to a high degree of accuracy, and some further deductions are made.

2. The problem of the source of stellar energy has long been one of the most difficult questions of astrophysics. The modern development of nuclear theory has shown beyond reasonable doubt that, at least in the vast majority of all stars, thermonuclear processes are responsible for the generation of energy, and that the ultimate effect of these processes is the conversion of hydrogen into helium. Although this conversion usually takes place in several stages, one of these will

normally be far less likely to occur than the others and will therefore limit the rate of generation of energy. It may perhaps be useful to discuss the general properties of these critical stages of the various processes in some detail.

Owing to the relatively large amount of energy released in the conversion of four protons into a helium nucleus the energy requirements of a star are covered if only a minute fraction of the inter-particle collisions near the centre of the star leads to the requisite nuclear reaction. The investigation concerns therefore highly improbable processes and this naturally adds to its difficulties (only about one collision in 10^{20} is required to produce energy).

The only collisions of interest are those in which the participating nuclei are of the requisite types. One of them must be either hydrogen or must be derived from hydrogen by a process more likely to occur than the critical stage now under discussion. Hence one of the nuclei must be fairly common. The other one may have to be a comparatively rare one like, say, carbon, but the abundance of no element is likely to be so low as to contribute a very substantial factor to the improbability of the reaction.

It follows then, that the collision is still very unlikely to lead to the reaction even if the two nuclei are of the required types. In the terms of nuclear physics, a very small cross-section for the energy-generating process will be sufficient to keep up the energy supply of the star.

Collision cross-sections are in general functions of the relative velocity of the particles, increasing rapidly with the velocity. While, however, for most reactions the dependence on relative velocity is extremely steep (30th to 40th power of the velocity), for a very few it is less critical and for at least one the effective dependence, in the important range, may be as low as the 6th power.

If the cross-section depends extremely sensitively on the relative velocity, then the rate of energy generation in a star will depend very critically on the central temperature. For only the very fastest particles will make an effective contribution to the rate of energy generation, and their number depends, by the Maxwell distribution law, very critically on the temperature. Accordingly the energy-producing region will be closely confined to the innermost parts of the star. It is also well known that in this case the core of the star must be in convective equilibrium (**13**). A final consequence of this extreme sensitivity of the cross-section is that the process may be investigated in the laboratory. For it is possible to produce much faster particles than occur in stars and hence the cross-section may become large enough to be measurable.

If the cross-section does not depend so sensitively on the relative velocity, then the rate of energy generation in the star will vary only like a low power of the temperature. Accordingly the energy-producing region will occupy a substantial fraction of the star and the core need not be convective, owing to the low-power dependence on velocity it is not possible to increase the cross-section sufficiently in laboratory conditions to make it measurable. Hence such processes can only be investigated theoretically. Although only one process of this type is known, the possibility of the existence of others cannot yet be absolutely excluded.

A further sub-division of thermonuclear processes can be carried out by examining whether (*a*) they concern only hydrogen nuclei and those others which are produced in the process, or whether (*b*) other elements take part. In case (*b*), owing to the very small abundance of elements other than hydrogen, it is probably only necessary to consider processes in which the other elements act purely as

catalysts and are therefore not used up in the reaction. It is possible, though unlikely, that stars of very low luminosity use non-catalytic processes of type (*b*).

All processes of type (*a*) must start with the formation of deuterons from two protons, although various subsequent developments are possible. However, the first stage imposes the most severe limitation. This process is well known (**1**), but owing to its low-power velocity dependence can only be studied theoretically. In stellar conditions the rate of energy generation due to it is given approximately by

$$\epsilon_{pp} = \epsilon_0 X^2 \rho^2 T^{3.5}, \tag{1}$$

where ϵ_0 is a constant, X the hydrogen abundance and ρ is the density.

Highly velocity-sensitive processes are amenable to laboratory study and the only one of importance is of class (*b*) and is the famous carbon-nitrogen cycle discussed first by Bethe (**2**) and recently re-examined experimentally (**3**). It appears that in stellar conditions

$$\epsilon_{CN} = \epsilon_1 X Z_{12} \rho^2 T^n, \tag{2}$$

where ϵ_1 is a constant and Z_{12} is the abundance of carbon.

Low-power chain processes can only be studied theoretically, and although the discussions given tend to show that no such process is of importance, the existence of an important process of this type (temperature-insensitive catalytic chain) cannot yet be completely excluded.

Finally it may be mentioned that processes involving triple and higher collisions between atomic nuclei have been shown to be of no importance.

3. A knowledge of the coefficient of opacity of stellar material at all relevant temperatures and densities is required for a discussion of stellar structure. Since these are far beyond the range of laboratory conditions the coefficient of opacity must be determined theoretically. This is unfortunately not an easy matter, since extensive computations are required, and hence our knowledge of the coefficient of opacity is a little vague.

The two main contributions to the opacity are the scattering of light by free electrons and the photoelectric effect. The first leads to a coefficient which is proportional to the number of free electrons but otherwise constant. In a state of complete ionization

$$\kappa_{el} = 0{\cdot}19(1+X)\,\text{cm.}^2/\text{g}. \tag{3}$$

The photoelectric effect was first investigated by Kramers (**4**) who showed that hydrogen and helium atoms were far less effective agents of opacity than the heavier elements. At that time it was believed that these heavier elements were a considerable fraction of the stellar material and unfortunately all his and subsequent investigations and computations (**5**) were carried out on that basis, which is now known to be quite incorrect.

Kramers found that

$$\kappa_{\text{p.e.}} = \kappa_{00} \frac{Z(1+X)\rho}{gT^{3.5}}, \tag{4}$$

where Z is the abundance of elements other than *H* and *He*, κ_{00} is a constant equal to about 10^{25} in c.g.s. units, whereas g is the so-called guillotine factor which depends on the density, temperature and composition of the material, but generally only varies slowly. Extensive tabulations of g have been made by Strömgren and by Morse (**5**) but unfortunately on the erroneous assumption that

Z is not too small (say $Z>0{\cdot}05$). New tabulations of g for very small Z are sorely needed.

Various formulae of approximations to the somewhat irregular variations of g have been tried, notably $g=\text{const.}$, $g\sim\rho^{1/4}$, $g\sim\rho^{1/2}T^{-3/4}$, $g\sim T^{3/2}$, etc.

At low densities (such as are more common in more massive and luminous stars) electron scattering predominates, but in average and small stars the photoelectric effect is probably more important.

The present situation is far from satisfactory, but it seems justified to put

$$\kappa=\kappa_0(1+X)\rho^{\sigma-1}/T^{\nu-3}, \tag{5}$$

where Z has been included in the constant κ_0, and

$$\text{in big stars: } \sigma=1, \quad \nu=3,$$

$$\text{in other stars: } 1{\cdot}5\leqslant\sigma\leqslant 2, \quad 6\leqslant\nu\leqslant 8.$$

An additional complication may arise in very massive stars through the action of radiation pressure, but this is probably quite unimportant in all other stars and its effects will be neglected.

4. Even without detailed integrations of the equations of stellar structure, deductions of considerable interest can be made from homology relations.

We consider general models of stars. Universal constants will be left out in the proportionality relations. Similarly the abundance Z of elements other than *H* and *He* will be taken to be constant and will hence be omitted.

The notation used will be:—

L = luminosity of star, T_c = central temperature,

M = mass of star, ρ_c = central density,

r = radius of star, μ_c = central molecular weight,

μ_s = surface molecular weight, X_c = central hydrogen abundance,

X_s = surface hydrogen abundance, T_e = effective surface temperature,

$D=\dfrac{\mathscr{R}T_c}{\mu_c}\dfrac{r}{GM}$ = an invariant characteristic of the whole structure of the star (**6, 7**)

$F=\dfrac{\rho_c}{\rho_{\text{mean}}}=\dfrac{4\pi r^3\rho_c}{3M}$ = an invariant characteristic of the whole structure of the star (**6**),

A = numerical constant characteristic of the structure of the surface layers (**6**).

If $\epsilon\sim X^\nu\rho^\alpha T^\eta$ ($\psi=1$ for catalytic reactions, $\psi=2$ for the p–p reaction, $\alpha=2$ usually), then by the definitions of D and E

$$L\sim r^3X_c^\nu\rho_c^\alpha T_c^\eta\sim D^\eta\mu_c^\eta E^\alpha X_c^\nu M^{\alpha+\eta}/r^{3\alpha-3+\eta}.$$

Also if

$$\kappa\sim(1+X)\rho^{\sigma-1}/T^{\nu-3}, \tag{6}$$

then the mass-luminosity-radius relation is

$$L\sim A^{\nu+\sigma}\frac{\mu_s^{\nu+1}}{1+X_s}\frac{M^{\nu+1-\sigma}}{r^{\nu-3\sigma}}. \tag{7}$$

Finally,

$$L\sim r^2T_e^4. \tag{8}$$

We shall first derive the relation between L and T_e if only M and r are allowed to vary, that is we are considering a homologous sequence of stars. If M and r are eliminated between (6), (7) and (8), then

$$L \sim T_e^q, \tag{9}$$

where

$$q = 4\frac{\eta(2\sigma+1)+\alpha(2\nu+3)-3(\nu+1-\sigma)}{\eta(2\sigma-1)+\alpha(2\nu+1)-(\nu+1-\sigma)}. \tag{10}$$

In the most important case $\alpha = 2$ and then

$$q = 4\frac{\eta(2\sigma+1)+\nu+3+3\sigma}{\eta(2\sigma-1)+3\nu+1+\sigma}. \tag{11}$$

Values of q for a number of representative values of α, η, σ and ν are tabulated below.

TABLE I

α	η	σ	ν	q		α	η	σ	ν	q
2	16	1	3	8·44	Electron opacity *C–N* cycle	2	5	1	3	6·00
2	18	1	3	8·69		2	3·5	1	3	5·38
2	20	1	3	8·90		2	2·5	1	3	4·89
2	16	2	6·5	5·43		2	5	2	6·5	4·32
2	18	2	6·5	5·51		2	3·5	2	6·5	4·00
2	20	2	6·5	5·60		2	2·5	2	6·5	3·73
2	16	2	8	5·17		2	5	2	8	3·43
2	18	2	8	5·28		2	3·5	2	8	3·04
2	20	2	8	5·38	Kramers' opacity *C–N* cycle	2	2·5	2	8	2·72
2	16	1·75	6·5	5·57		2	5	1·75	6·5	4·29
2	18	1·75	6·5	5·69		2	3·5	1·75	6·5	3·93
2	20	1·75	5·6	5·80		2	2·5	1·75	6·5	3·65
2	16	1·50	5·75	5·98		2	5	1·50	5·75	4·47
2	18	1·50	5·75	6·12		2	3·5	1·50	5·75	4·08
2	20	1·50	5·75	6·24		2	2·5	1·50	5·75	3·76
1	18	1	3	10·80		1	3·5	1	3	5·60
3	18	1	3	8·00		3	3·5	1	3	5·30
1	18	2	6·5	5·73		1	3·5	2	6·5	3·58
3	18	2	6·5	5·37		3	3·5	2	6·5	4·02

This table indicates the variation of L with T_e for stars of different masses but the same constitution. This variation will be of considerable assistance in interpreting the Hertzsprung-Russell diagram, but it will also be necessary to consider what different types of composition are likely to arise and how they affect the distribution of stars in the Hertzsprung-Russell diagram. For this purpose stellar evolution has to be considered to some extent.

5. In this and subsequent sections the term "normal star" will be used to describe a homogeneous star of arbitrary mass in equilibrium, the material of the star being mainly (say 95 per cent to 99 per cent) hydrogen, the rest consisting of a little helium and other elements. This is supposed to be the state of a star which has condensed from interstellar material and in which thermonuclear energy generation fully covers the loss of energy by radiation but has not yet converted any appreciable amounts of hydrogen into helium. The sequence of normal stars will form a curve in the luminosity-type diagram. The slope of the tangent to this curve at any point will be described by the value of q discussed in Section 4. The curvature of the curve is due to the fact that

for different sizes of star different laws of energy generation and opacity predominate and hence the value of q varies along the curve. The switch from one law to another will always lead to a convex shape of the curve (i. e. q increasing with T_c). Concave regions can only be due to a suitable variation of the exponents in any one law such as an increase of η with decreasing T_c.

In the state preceding the normal one the star is contracting under gravity without nuclear energy generation. The radius of such a "pre-normal" star will clearly be greater than the radius of a normal star of the same mass. Since for any opacity law proposed $(\nu-3\sigma)$ is small (usually positive), it follows from the mass-luminosity-radius relation that the luminosity differs little from the normal luminosity (it is probably a little smaller, especially since A is probably a little less than its normal value), but T_c will be smaller owing to the bigger radius. Accordingly the representative points of the pre-normal stars will lie to the right of the "normal" curve. Owing to the brevity of the Helmholtz-Kelvin time scale very few stars may be expected to be in this state.

Of far greater importance are the developments due to the conversion of hydrogen into helium, and those due to the accretion of interstellar matter.

Considering first the conversion of hydrogen into helium, we note that it will take place mainly close to the centre of the star. In the course of time substantial amounts of helium will be formed there, but it is an open question whether they will stay there or whether they will diffuse throughout the star. The problem is still obscure in spite of the amount of work that has been done on it, and it seems quite possible that in fact the speed of diffusion depends on the rotation rate of the star and therefore differs from star to star. In view of this uncertainty both alternatives will be considered here. Since we first leave out the question of accretion, the mass M of the star will be taken to be constant during the evolution.

(i) *Diffusion much less rapid than production of helium.*—In this case the helium will be chiefly confined to the inner regions of the star. If the core is convective the helium will be distributed throughout the core, but will not penetrate far into the radiative envelope. If the core is radiative, then this implies that η is low (high η leads to instability and convection). Accordingly the energy generation is fairly widely spread and helium will be produced in a region of similar dimension to the convective cores usually considered (radius varies between $r/10$ and $r/3{\cdot}5$).

In either case it seems (7) that the invariants D, E and A differ little from their normal values. By hypothesis μ_s and X_s are unaltered and hence by equation (7) $Lr^{\nu-3\sigma}$ is virtually unchanged. But, by (6), $Lr^{3\alpha-3+\eta}$ is changed owing to the alteration of μ_c and X_c.

Whether the product $X_c^{\psi}\mu_c^{\eta}$ increases or decreases depends on the values of ψ and η, and on the amount of helium produced. For $\mu\to\frac{4}{3}$ as $X\to 0$, and so, in the final stages of evolution, the product tends always to zero. However, in the early stages, which are more important for our purposes, the product increases or decreases according as to whether $5\eta/8$ is greater or less than ψ (since $\mu\sim 1/(1-5Y/8)$, $X=1-Y$). Since η always exceeds 2 the product will increase in the early stages of evolution for any catalytic process ($\psi=1$) but will be almost unaltered at first for the p–p reaction ($\eta=3{\cdot}5$, $\psi=2$) and will soon start to decrease. Furthermore, for all likely laws of opacity and energy generation $(3\alpha-3+\eta)>\nu-3\sigma$. Therefore r will increase in the early stages of evolution (unless the p–p reaction is responsible for energy generation, in which

case r hardly changes). The increase will be larger the greater η is. For very large values of η the radius r will be proportional to μ_c. Since $(\nu-3\sigma)$ is generally a small positive number, the luminosity L will, by virtue of (7), decrease slightly. In the early stages of evolution the representative point in the type-luminosity diagram will therefore not move if the p–p reaction predominates and will otherwise move to the right and a little down, but the displacement will not be very large (say up to at most a factor of 1·4 in T_c if both η and Y_c are large).

In the later stages of evolution there may be a movement to the left (higher T_c) and slightly upwards, particularly so in the case of the p–p reaction.

(ii) *Diffusion much more rapid than production of helium.*—In this case the star will be homogeneous. Hence D, E and A will have their normal values, but $\mu_c=\mu_s$ will be increased and $X_c=X_s$ will be decreased. It follows that

$$Lr^{3\alpha-3+\eta}\sim\mu^{\eta}X^{\nu}, \qquad Lr^{\nu-3\sigma}\sim\mu^{\nu+1}/(1+X).$$

The detailed calculations are a little tedious and the result is that in every case both L and T_e increase as μ increases, that is as hydrogen is converted into helium. The luminosity L increases for Kramers' opacity approximately like the seventh power of μ and for electron opacity more like μ^4. The increase in T_e is also fairly rapid and, in the luminosity-type diagram, the representative point moves upwards but not quite as steeply as the normal curve, so that the new position of the representative point is a little to the left of the normal curve. For each magnitude (factor of $10^{0\cdot4}$) increase in L due to this development, the increase in T_e is about 5 per cent more than would correspond to motion along the normal curve (this excess is about the same for all likely laws of opacity and energy generation).

When allowance is made for the fact that mixing is not likely to lead to a perfectly uniform star but that μ_c will probably be slightly greater than μ_s, then there will be a slight reduction in T_e, so that it is probably sufficient to say that, with good mixing and without accretion, evolution leads to upward motion more or less along the normal curve.

(iii) *Effects of accretion.*—We now consider the possibility of the accretion of interstellar matter (chiefly hydrogen). It is clear that if a normal star accretes matter substantially like its own it will merely be converted into another normal star of rather greater mass. Similarly if a star considered under (i) (which has an appreciable abundance of helium near the centre but not near the surface) accretes substantial amounts of interstellar matter it is merely turned into a similar star of greater mass.

However, if a star of the type considered under (ii) accretes interstellar hydrogen then very remarkable results occur (**7, 8**). The luminosity is little altered, but the newly acquired hydrogen envelope is very tenuous and extends to large distances. Very considerable increases in r and therefore decreases in T_e may result, leading to the formation of a red giant star. The degree of extension depends critically on the molecular weight of the original star and also on the amount of hydrogen accreted. For maximum extension this should exceed 10 per cent but not 80 per cent of the mass of the original star. It is essential for the formation of such red giants that the hydrogen of the envelope should not be mixed with the helium of the interior. Presumably the difference in molecular weight would, at least for sufficiently rapid accretion, permit the formation of such a distinct envelope. A red giant will therefore be formed if the

speed of accretion exceeds the speed of mixing, and if this in turn exceeds the rate of helium production.

The representative points of stars of this type lie to the right of the normal curve, the displacement depending on the circumstances.

6. When hydrogen conversion has progressed very considerably it becomes impossible for the star to generate enough energy. Gravitational collapse sets in and presumably continues until either disruption (novae, supernovae) due to centrifugal force occurs, or until the white-dwarf stage is reached. This final stage is known to be very long lived and has been studied in considerable detail. The intermediate stages of collapse are not so well understood but probably a star passes through them with considerable speed, so that at any given time very few stars are in this intermediate state. Accordingly it is of little importance to the interpretation of the luminosity-type diagram and will not be further considered here.

7. A fairly complete picture of the evolutionary tracks of stars in the luminosity-type diagram has now been given. Before this can be applied to the diagram representing stars of our galaxy, account has to be taken of the fact that there is an upper limit to the age of such stars. The age of our galaxy and hence the age of the oldest stars has been estimated as between 5×10^9 years and 2×10^{10} years. Of course we must expect to find numerous stars much younger than that, but none can be older than this limit.

The implications of this age limit are clear. It is readily worked out that the Sun can have converted at most 4 per cent (15 per cent for the higher age limit) of its hydrogen into helium. Since the luminosity is a very steep function of the mass, it follows that, say, stars of bolometric magnitude 7 cannot have converted more than 3 per cent of their hydrogen into helium, but stars of $M_{\text{bol}}=2$ may have converted as much as 16 per cent (or 60 per cent if the upper limit of age of the galaxy is taken). For stars of $M_{\text{bol}}>7$ there can be hardly any deviation from the normal curve if mixing is thorough (as it is likely to be in such small stars). If however the 3 per cent of helium is confined to a small region near the centre, producing there an appreciable abundance of *He*, a slight extension may result.

For stars of $M_{\text{bol}}=2$ a moderate degree of red giant formation (as discussed in 5 (iii)) becomes quite possible, but considerable red giants are not to be expected until $M_{\text{bol}}<0$.

We must therefore expect that the stars of low luminosity lie close to the normal curve and possibly a little to the right of it, but that for the more luminous stars a greater spread to the right sets in. Unless the deviation discussed in 5 (ii) becomes very important (and this is certainly unlikely for $M_{\text{bol}}>2$) the normal curve will be the lower left boundary of the band representing the stars of the main sequence. This boundary therefore has to be used for comparison with the values of q computed at the end of Section 4.

8. For our purposes it is evidently desirable to compare the theory with a highly homogeneous set of observations in which the lower part of the main sequence is well represented. For this reason the data given in Kuiper's article on the nearest stars (**9**) were taken as the primary material. These data are particularly valuable because the stars are selected by distance rather than by apparent brightness, and also because particular care was taken to determine spectral classes by consistent criteria. Even in this homogeneous collection it

was considered desirable to omit all those stars where Kuiper considers some of the data to be dubious (italicized in his list). In order to have some more material, especially for the upper ranges of the main sequence, visual and spectroscopic binaries from Kuiper's article on the empirical mass-luminosity relation (**10**) were also included. Again all data involving binaries of uncertain mass ratio were neglected.

These stars from Kuiper's article form the principal material worked on, but in order to illustrate the position of the sub-dwarfs better a few selected sub-dwarfs from Joy's list (**11**) were also included. Joy's colour classes are not in perfect agreement with Kuiper's. Therefore his general data were not included and the few sub-dwarfs selected are there solely for the purpose of illustrating the position of a class of which Kuiper gives few examples.

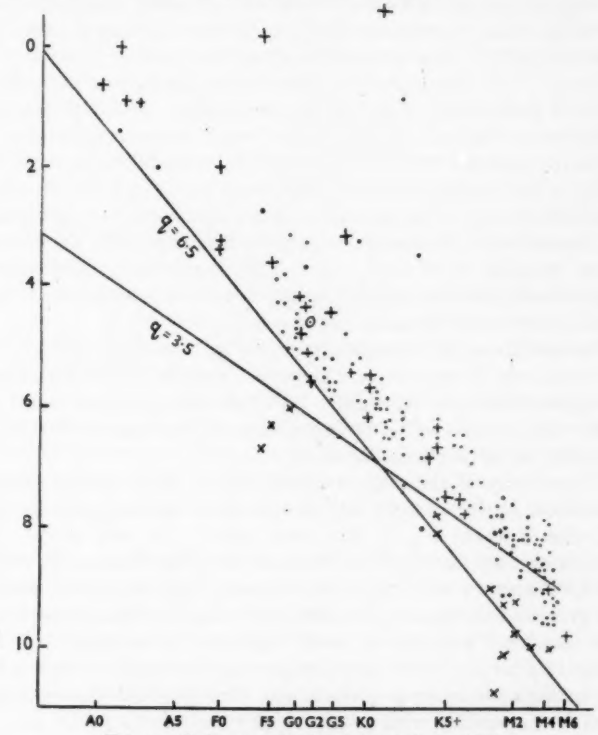

FIG. 1.—*Ordinates: Absolute bolometric magnitude.*
Abscissae: Log T_e (spectral type).
• *Stars from ref.* (9) (*nearest stars*).
\+ *Stars from ref.* (10) (*binaries*).
× *Stars from ref.* (11) (*sub-dwarfs*).

Finally the Sun was included in the collection, the data used being those given by Kuiper (**12**). The bolometric corrections and the relations between spectral type and surface temperatures were also taken from this paper. All these stars are represented in Fig. 1 in which $\log_{10} T_e$ is the abscissa and M_{bol} the ordinate.

Although in this way a very homogeneous and satisfactory set of data was obtained, it was found that data on stars of spectral type later than M2 were not usable. As Kuiper points out, the bolometric correction depends so sensitively on the spectral class and is so large that it is a very uncertain guide to the bolometric magnitudes. There are also no direct determinations of the surface temperatures of these very red dwarfs. Kuiper's doubts are strengthened by the appearance of the luminosity-surface temperature diagram in this region, which shows a sharp downward turn. As was pointed out before, such a concave shape is very unlikely on theoretical grounds and is presumably due to an over-estimate of the effective temperatures and a consequent under-estimate of the bolometric correction.

Information about these stars would be of the greatest value, since they must all be in a very early stage of evolution and should hence form a one-parameter series. Possibly the best method would be to measure red magnitudes of the stars between K6 and M8. The bolometric correction would then be small and slowly varying. The problem of determining and defining the surface temperatures of these stars would still be formidable. A complete luminosity-surface temperature diagram for this region would however give clear answers concerning the homogeneity and similarity of stellar material in our neighbourhood.

Returning to the sample taken and represented in Fig. 1, there still remains the question whether it is a fair sample. It can clearly only be representative of our galaxy, but whether dwarfs in our neighbourhood are like dwarfs elsewhere in the galaxy remains to be seen. The most important variable condition is probably the density of interstellar material, but there is little reason to believe that ours is an exceptional region in this respect.

9. The main features of the appearance of Fig. 1 are fairly clear. The band of the main sequence stands out very clearly. Near the top of the diagram the red-giant sequence starts on the right. The sub-dwarfs appear below the main sequence, the white dwarfs would be in and beyond the extreme left-hand bottom corner, but have not in fact been drawn in.

The left-hand edge of the main sequence which should be the normal curve is well represented by the straight lines drawn in on the diagram. In the upper part the q value is about 6·5, in the lower region it is only about 3·5. The transition from one line to the other seems to be quite sharp. As will be seen from Table I, the upper q value requires η to have a high value (such as the carbon cycle would give) and the opacity law seems to be intermediate between Kramers' and electron opacity. This is very much what is to be expected.

The value of q for the lower ranges points very strongly towards a low value of η such as corresponds to the p–p reaction. The opacity law must clearly be of the Kramers form, possibly with a rather high value of ν ($\nu=7$?).

The $L-T_e$ diagram lends very strong support to the view that the mechanism of energy generation has a high value of η for bright stars and a low value for small stars. The transition appears to take place fairly suddenly at $M_{\text{bol}}=6{\cdot}5\pm0{\cdot}5$, i. e. for stars one-sixth as luminous as the Sun.

The width of the main sequence in the lower ranges is probably largely due to observational errors, but for brighter stars is chiefly due to evolutionary developments.

10. Whereas the features of the diagram discussed so far are in good agreement with current theories, there are two features which cannot be so readily explained.

The first one of these is the curious "hole" in the main sequence near $M_{bol}=7$. Stars of spectral type K5–8 seem to be either of $M_{bol}=6{\cdot}5$ or $M_{bol}=7{\cdot}5$. The observations are too scanty for definite impressions but such a curious formation not far from the switch-over from low to high η may be significant.

The second odd feature is the sub-dwarfs. It is clear from the discussion of stellar evolution here given that they cannot easily be fitted into the early or middle stages of any evolutionary sequence. It is not impossible that they form part of the late stages, the final collapse to the white-dwarf stage, but their grouping, their occurrence for late spectral types and their numbers make this hypothesis unattractive. It may be that an exceptional composition, by its effect on the mode of energy generation, is responsible for the curious position of the sub-dwarfs in the diagram.

11. It will be seen from Fig. 1 that the Sun ($M_{bol}=4{\cdot}62$, dG2) is well on the part of the main sequence drawing its energy from a high-η process (carbon cycle). Information about the critical temperature of this process may be obtained from a study of the structure of the Sun.

The factor of chief interest in this connection is the invariant $D=\mathscr{R}T_c r/\mu GM$. The value of this quantity for a homogeneous star with a convective core (necessary for high η) depends slightly on the opacity law. For electron opacity ($\sigma=1$, $\nu=3$) $D=0{\cdot}80$ (**6**), for ordinary Kramers' opacity ($\sigma=2$, $\nu=6{\cdot}5$) $D=0{\cdot}90$ (**6**), while for modified Kramers' opacity ($\sigma=1{\cdot}75$, $\nu=6{\cdot}5$) $D=1{\cdot}15$ (**7**). It seems therefore that for a homogeneous star of the mass of the Sun D cannot differ very much from unity.

The central temperature of a star of solar mass and radius is readily seen to be $2{\cdot}3\mu_c D\times 10^7$ deg. If the Sun were a pure hydrogen star its central temperature would probably be between 10^7 deg. and $1{\cdot}25\times 10^7$ deg. This figure is almost certainly inapplicable for three reasons:

(i) If the Sun were a normal star its representative point would be very close to the left-hand boundary of the main sequence.

(ii) Geological evidence indicates that the Sun must be at least 4×10^9 years old and hence must contain at the very least 3 per cent *He*.

(iii) According to nuclear physics the temperature given is too low for the *C–N* cycle.

How then does the Sun differ from a normal star? If it were about 2×10^{10} years old there might be as much as 15 per cent *He*. If this were well mixed it would lead to an appreciable deviation from the normal curve but in the wrong sense. If it were well mixed and then a hydrogen envelope had accreted, the extension of radius might lead to a displacement from the normal curve in the right direction, but it would probably not be very appreciable owing to the small difference in atomic weight between envelope and interior. If however the mixing were poor there might be an appreciable concentration of helium in the core even for a moderate age. During a life of say 5×10^9 years the core would have acquired a helium abundance of some 30 per cent. The effect of this on D would be small (*cf.* Section 5), but the central value of μ would have to be substituted in the formula for T_c, leading to a value between $1{\cdot}25\times 10^7$ deg. and $1{\cdot}56\times 10^7$ deg. The upper value agrees well with estimates based on the most recent experiments on the cross-sections of the *C–N* cycle (**3**). The older figure of $1{\cdot}9\times 10^7$ deg. (**2**) is clearly almost incompatible with the astrophysical data. It might be mentioned that the author had, on the basis of these considerations,

deduced that the usual estimate for the threshold temperature of thermonuclear energy generation was a good deal too high, even before the more recent experiments had come to his notice.

In fact the correct temperature is probably still a little lower than current nuclear physics estimates, and $1{\cdot}4$–$1{\cdot}5 \times 10^7$ deg. is probably not far from correct.

Using the formulae of Section 4 and Fig. 1, it may be ascertained that the central temperature of stars of $M_{bol} = 6{\cdot}5$ is about 10 per cent lower than the Sun's central temperature. These are the stars which are close to the switch in the mode of energy generation, so that one can deduce that this switch occurs for a central temperature of about $1{\cdot}3 \times 10^7$ deg.

The results here presented are at variance with the calculations of Epstein (**14**), who deduced from the nuclear physics data that the switch in the mode of energy generation occurred for stars rather brighter than the Sun. The complete absence of a change of slope of the main sequence in that region, together with the change of slope discussed here, strongly suggests that his conclusions are erroneous, and that hence the stellar model and the nuclear data used by him stand in need of revision.

Trinity College,
Cambridge:
1950 *August* 25.

References

(1) H. A. Bethe and C. L. Critchfield, *Phys. Rev.*, **54**, 248, 1938.
(2) H. A. Bethe, *Phys. Rev.*, **55**, 434, 1939.
(3) R. N. Hall and W. A. Fowler, *Phys. Rev.*, **77**, 197, 1950.
(4) H. A. Kramers, *Phil. Mag.*, **46**, 836, 1923.
(5) B. Strömgren, *Z. Astrophys.*, **4**, 118, 1932 ; and P. M. Morse, *Ap. J.*, **92**, 27, 1940.
(6) C. M. Bondi and H. Bondi, *M.N.*, **109**, 62, 1949.
(7) C. M. Bondi and H. Bondi, *M.N.*, **110**, 287, 1950.
(8) F. Hoyle and R. A. Lyttleton, *M.N.*, **102**, 218, 1942 ; and *M.N.*, **109**, 614, 1949.
(9) G. P. Kuiper, *Ap. J.*, **95**, 201, 1942.
(10) G. P. Kuiper, *Ap. J.*, **88**, 472, 1938.
(11) A. H. Joy, *Ap. J.*, **105**, 96, 1947.
(12) G. P. Kuiper, *Ap. J.*, **88**, 429, 1938.
(13) T. G. Cowling, *M.N.*, **94**, 768, 1934.
(14) I. Epstein, *Ap. J.*, **112**, 207, 1950.

ON THE GENERATION OF MAGNETISM BY FLUID MOTION

H. Bondi and T. Gold

(Received 1950 July 31)

Summary

It is shown that in a liquid of infinite conductivity hydrodynamic motion may result in an indefinite increase of the strength of the internal magnetic field ; but that the external field is severely limited in the case when the volume occupied by the liquid is simply connected. These limitations disappear when the volume is multiply connected. The case of finite conductivity is then briefly discussed.

---

1. In recent geophysical and astrophysical researches problems of the generation of magnetic fields by fluid motion have come under discussion. The scale is there frequently so large that little comparison can be made with laboratory phenomena; and although many problems belong entirely to classical electrodynamics, the general theoretical approach is frequently too cumbersome to give much guidance or even to decide which processes are possible.

The first step to show a limitation of hydrodynamic dynamo action was taken by Cowling (**1**), who proved that a certain symmetry was incompatible with such a process. More recently Batchelor (**2**) has given the conditions necessary for turbulent motion to generate magnetic fields. Bullard (**3**), following Elsasser (**4**) and more remotely Larmor (**5**), has stimulated much interest in the subject by attempting to find patterns of fluid motion which may occur in the Earth's core and be responsible for the magnetic field of the Earth.

Owing to the large scale of geophysical or astrophysical phenomena, the decay times of electric currents may be very long. The interest of the problem may then lie in the changes which occur in much shorter intervals of time; and for such purposes the idealization of a perfect conductor may be instructive. It is known that lines of force can then be considered to move entirely with the fluid, so that any set of fluid particles once connected by a line of force remains so connected. The magnetic changes consequent upon a certain motion may then be deduced simply by finding the new positions of any set of particles previously connected by a line of force, thus specifying its new position. A dynamo action in which the magnetic energy is increased will then consist of a redistribution of the lines of force implying greater field energy, such as crowding them together and increasing their length. Commencing with an arbitrarily weak field, hydrodynamic motion may increase the magnetic energy indefinitely, or, in any practical case, until a limitation is reached which derives from some other consideration.

In the motion of a perfectly conducting fluid the energy of the magnetic field may also be decreased. Clearly a decrease would result in the case where the motion is everywhere so directed as it would be if it were caused by the magnetic forces. This implies that no general theorem can be found. But all those types of motion which "stir up" the fluid (where it is overwhelmingly more probable that any two particles which were initially a small distance δr apart should be

farther apart at a later time) will, if uncorrelated with the lines of force, be much more likely to increase the magnetic field than to decrease it. The problem is completely analogous to the stirring of a liquid, where almost any type of physically realizable motion will aid and not hinder in distributing the particles of another substance which is to be dissolved; for we may consider the particles lying on a particular line of force as belonging to another substance. As a consequence of the stirring, particles originally close to each other will in general be moved farther apart, and the line of force hence lengthened.

Steady-state motions in a closed volume are of particular interest. Whatever the initial consequences of such a motion may be, it can be seen that its continuation must eventually lengthen the lines of force, and then continue to do so indefinitely. The exceptions to this are the cases where there is no plane of shear possessing a normal component of the magnetic field (i.e. rigid body motion, or flow entirely along lines of force).

Under these circumstances there are, however, limitations imposed on the growth of the field *external* to the volume occupied by the liquid, and these will be the subject of a theorem which we shall now prove.

2. *Theorem.*—No hydrodynamic motion of a body of perfectly conducting liquid of finite dimensions in an otherwise empty space, possessing originally only arbitrarily weak magnetic fields, can generate an external field of finite moment, provided that the space external to the body is simply connected (which is always the case if the body is simply connected); but if the external space is multiply connected, an external field can be caused to grow without limit.

In this context the term "hydrodynamic motion" is taken to mean that there is no tearing of the liquid, so that if a set of particles of the liquid forms a closed curve, it will always do so. It will become clear that this condition is necessary for the theorem; but some condition of this sort is in any case implied if the motion is not to affect the topological connectivity of the body.

It can be proved rigorously that in a perfectly conducting fluid the magnetic lines of force move entirely with the fluid. (For a proof, see Dungey (**6**).) Under these circumstances the concept of lines of force becomes particularly useful, for now any given line of force remains identifiable by means of the particular fluid particles which it connects. Once a notation of lines of force is adopted in a particular case, it remains applicable throughout all motions that may take place, and within this notation there will be no new lines created and no lines lost.

The implications of this for the surface of the liquid can now be deduced. Consider a line of force which possesses an external part; there are then fluid particles at the points of exit and entry which must always have been on this line. If we were now to suppose that the external part of this line between the pair of particles did not exist at some previous time, then those particles must have been adjacent to one another. But, as the condition of hydrodynamic flow does not permit the separation of adjacent particles, no such process can have occurred. There can hence be no hydrodynamic motion whereby the number of points of exit or entry of lines of force is increased.

This number of points is proportional to the integral of the modulus of the component of H normal to the surface, taken over the entire surface, a quantity which we shall call the "total pole-strength" of the body. Hence no hydrodynamic motion of a body of perfectly conducting liquid in otherwise empty space can increase its total pole-strength.

Since, outside the liquid, space is free from currents and of permeability unity*, the field there must be expressible in terms of a magnetic scalar potential Ω. Using conventional notation,

$$\boldsymbol{B}=\boldsymbol{H}=-\operatorname{grad}\Omega, \tag{1}$$

$$\nabla^2\Omega=0, \tag{2}$$

$$\Omega=O(1/r^2), \quad |\operatorname{grad}\Omega|=O(1/r^3), \quad \text{as } r\to\infty. \tag{3}$$

The last equation is due to the fact that the sources of the field lie entirely within the body of the liquid, which is confined to the finite part of space.

By a well-known theorem of potential theory $\operatorname{grad}\Omega$ is fully determined within a simply connected region, if at infinity the conditions (3) apply, and if the normal component of $\operatorname{grad}\Omega$ is given over the finite boundary.

If the body is simply connected, then the external space is also simply connected. As the normal component of $\operatorname{grad}\Omega$ at the boundary is restricted by the limitation of the total pole-strength, there are now certain restrictions of the external field. The maximum dipole moment which the body can achieve will occur when the available pole-strength is concentrated at two poles on the surface, separated by the greatest possible distance. There is hence no motion of the liquid which could produce a finite magnetic moment, if the original total pole-strength was indefinitely small, although such motions may build up internal fields.

No systematic strengthening of the external field can result from a motion of the liquid, and hence the energy of the external field is also subject to certain limitations. Again the most favourable case would arise if all the available pole-strength were concentrated at two small areas on the surface. It is true that by letting these areas become small the external energy can be increased without limit; but the energy of the field in the part of space more than a distance $\delta>0$ from the body is again limited. The high field strength due to the concentration near the poles is purely local. Starting with an indefinitely small total pole-strength, no fluid motion could result in a finite energy of the external field, except in regions indefinitely close to the surface of the body.

In the case where the external space (and hence the body itself) is multiply connected, the limitations of the magnetic moment and the external energy will no longer apply, whilst the considerations relating to the total pole-strength remain unchanged. In a multiply connected space a knowledge of the normal component of $\boldsymbol{H}$ over the entire surface of the body is no longer sufficient to determine $\boldsymbol{H}$ throughout external space, but the integrals $\oint \boldsymbol{H}.d\boldsymbol{r}$ taken around each irreducible circuit have also to be given. In the present case there is no limitation of the values which these integrals can attain in the course of the motion of the liquid. The magnetic energy in any given external volume can hence be increased without limit, and so can the magnetic moment.

It is possible to give an interpretation to the meaning of large values of the integrals $\oint \boldsymbol{H}.d\boldsymbol{r}$ around paths which link the body. Consider the case in which the body forms an anchor ring, possessing some external parts of lines of force. A motion of the material of the surface is now possible so that the path of a fluid

* The second condition is not necessary, but simplifies the analysis considerably.

particle there is caused to link the anchor ring; and a persistent motion can cause an arbitrarily great number of linkages of the path of the particle with the ring. If a line of force emerged from the body at such a particle, and entered at a place on the surface where no such motion occurred, then it would be caused to increase the number of linkages which it makes with the body; for it would be unable to penetrate material of perfect conductivity. The external field would be increased by such a process, whilst the total pole-strength would remain unchanged. In the limit, when such a field has been built up from an arbitrarily small initial pole-strength, it would approximate to one of which the lines are entirely external; it is evident that such a field can be possessed by a multiply connected body only.

Technological dynamos are invariably multiply connected. Their function can be understood in the present terms; and it can be shown that certain types could generate external fields without the use of any dissipative circuit elements.

The electric currents responsible for the field in the example would run principally around the large circuit of the anchor ring. The "winding up" of lines of force through a ring must be identified with the induction of currents around it.

3. It is of interest to discuss the conditions under which this theory will be a fair approximation to cases of finite conductivity. There the relevant equations are (in e.s.u.'s and conventional symbols):—

$$\operatorname{curl} \boldsymbol{H} = \frac{4\pi\sigma}{c}\left(\boldsymbol{E} + \frac{\boldsymbol{v}}{c} \times \boldsymbol{B}\right), \tag{4}$$

$$\operatorname{curl} \boldsymbol{E} = -\frac{1}{c}\frac{\partial \boldsymbol{B}}{\partial t}, \tag{5}$$

where the Maxwell term has been neglected, and where σ is the conductivity. If the permeability μ is uniform, then by eliminating $\boldsymbol{E}$ we have

$$\frac{c^2}{4\pi\sigma\mu} \operatorname{curl} \operatorname{curl} \boldsymbol{B} = -\frac{\partial \boldsymbol{B}}{\partial t} + \operatorname{curl} (\boldsymbol{v} \times \boldsymbol{B}). \tag{6}$$

Hitherto we have been considering the case where σ was so large that the left-hand side could be put equal to zero so that the two terms on the right-hand side had to balance.

It is possible to characterize cases of finite conductivity according to the quality of the approximation which the perfect conductivity model is likely to give. For this purpose compare the left-hand side of (6) with the second term on the right-hand side. If l is a length characteristic of the spatial rate of change of $\boldsymbol{B}$ (this will generally be larger than the corresponding dimension for $\boldsymbol{v}$), the ratio of the two terms is of the order of magnitude

$$\frac{c^2}{4\pi\sigma\mu l\,|\boldsymbol{v}|},$$

and it is this ratio which must determine whether changes of the magnetic field are dictated principally by dissipation or by the motion of the liquid. If the ratio is large throughout the system, then the motion of the liquid has a small effect compared with that of dissipation. No dynamo action is then possible at all, for all fields will decay more quickly than they can be replenished. If the ratio is very small, then the rate of change of any field, internal or external, is determined

principally by the fluid motion, as in the case of a perfect conductor. Internal fields will then in general be built up. The system is then well represented by a model of a perfect conductor. These conditions are satisfied, for example, with a material of the conductivity of copper and permeability unity, provided that

$$l|\boldsymbol{v}| \gg 720\,\text{cm.}^2/\text{sec.}$$

The question of the growth of external fields for a simply connected body of finite conductivity is evidently difficult. They can clearly not grow, if the conductivity is too low for internal fields to grow. A very high conductivity, on the other hand, would confine the field to the interior. It cannot at present be ruled out that external fields could grow in the intermediate case, though only with a speed limited by the dissipation.

Trinity College,
Cambridge:
1950 *July* 29

References

(1) T. G. Cowling, *M.N.*, **94**, 39, 1934.
(2) G. K. Batchelor, *Proc. Roy. Soc.* A, **201**, 405, 1950.
(3) E. C. Bullard, *M.N., Geophys. Suppl.*, **5**, 248, 1948; *Proc. Roy. Soc.* A, **197**, 433, 1949; *Proc. Roy. Soc.* A, **199**, 413, 1949.
(4) W. M. Elsasser, *Phys. Rev.*, **69**, 106, 1946; *Phys. Rev.*, **70**, 202, 1946; *Phys. Rev.*, **72**, 821, 1947.
(5) J. Larmor, *Rep. Brit. Assoc.*, 159, 1919.
(6) J. W. Dungey, *Proc. Camb. Phil. Soc.*, **46**, 651, 1950.

SOME LINE STRENGTHS FOR IONIZED NEON

R. H. Garstang

(Received 1950 October 27)

Summary

Transition integrals and f-values have been calculated for the arrays $3s-3p$, $3p-3d$, and $3d-4f$ of *Ne* II using both the Coulomb approximation and the method of the self-consistent field, without exchange. The mean square radii of the outer orbitals are also given.

The absolute strength of a spectral line arising from an electric dipole transition in an atom obeying Russell–Saunders coupling can be expressed in the form

$$S = S(M)\,S(L)\sigma^2,$$

where $S(M)$ is a factor depending on the particular multiplet of the array, $S(L)$ depends on the particular line of the multiplet and σ^2 is given (in atomic units $e^2a_0^2$) by

$$\sigma^2 = \frac{1}{4l^2-1}\left(\int_0^\infty rP_iP_f\,dr\right)^2,$$

l being the larger of the two azimuthal quantum numbers involved and P_i/r, P_f/r the initial and final wave functions of the series electron. $S(M)$ has been tabulated by Goldberg (**1**) and $S(L)$ by Russell (**2**) and by White and Eliason (**3**).

Bates and Damgaard (**4**) have given a method, referred to as the Coulomb approximation, for the evaluation of σ^2. The field of the core is assumed to be Coulomb in form, the corresponding wave function being chosen to fit the observed energy levels (**5**).

Another method of calculating σ^2 is from wave functions obtained from self-consistent field calculations. The field of the *Ne* III ion was obtained from the wave functions published by the author (**6**), assuming them to be undisturbed by the series electron. The equation for the radial parts of the wave functions of the series electron was solved for the $3s$, $3p$, $3d$ and $4f$ states, the energy of these being the corresponding eigenvalues of the equation.

A partial check on the numerical work is given by applying the Coulomb approximation to the energies obtained from the self-consistent field method. The field of the *Ne* III ion is very nearly Coulomb in the region which is of significance for the series electron and the transition integrals (σ^2) should agree closely with those from the self-consistent wave functions.

Table I contains the greatest, least and adopted mean observed energy levels and the energies from the self-consistent field method. The latter are, as usual, smaller than the observed values and correspond to the well-known over-diffuseness of the wave functions. This leads to values of the transition integrals which are too large. This is shown in Table II which contains the three sets of values of σ^2. Those from the self-consistent field wave functions agree closely with those from the Coulomb approximation. This shows that

no appreciable error arises from the assumption of a Coulomb field. The values derived from the observed energies are lower than those from the self-consistent energies. These conclusions agree with those of Bates and Damgaard (**7**). In any applications of these results the values of σ^2 from the Coulomb approximation and the observed energy levels should be used.

TABLE I

[unit=13·53 e.V.]

Orbital	Observed Energy Levels			Self-Consistent Energy Levels
	Greatest	Mean	Least	
$3s$	1·023	1·000	0·972	0·882
$3p$	0·776	0·739	0·702	0·647
$3d$	0·476	0·463	0·438	0·447
$4f$	0·260	0·255	0·250	0·249

TABLE II

Values of Transition Integrals (σ^2)

Array	Coulomb Approximation		Self-Consistent Wave Functions
	Observed Energies	Self-Consistent Energies	
$3s-3p$	3·30	4·20	4·28
$3p-3d$	0·99	1·30	1·32
$3d-4f$	0·68	0·73	0·73

The mean square radii of the outer orbitals are of interest in connection with collision broadening in stellar atmospheres. They are calculated (in atomic units $e^2a_0^2$) using the Coulomb formula

$$\overline{r^2} = \frac{1}{2\epsilon}\left\{\frac{5C^2}{\epsilon} + 1 - 3l(l+1)\right\},$$

or directly from the wave functions. ϵ is the energy (units 13·53 e.V.) of the orbital and C the excess charge on the core ($C=2$ for *Ne* II). Table III contains values of $\overline{r^2}$ obtained direct from the wave functions and by using for ϵ the self-consistent energy parameters, the greatest, the least and the mean observed energies of the individual levels of the configuration. The values from the mean observed energy should be used in any applications.

TABLE III

Values of Mean Square Radii of Outer Orbitals

(atomic units=$2{\cdot}79\times10^{-17}$ cm.^{2})

Orbital	Observed Energy Values			Self-Consistent S. C. Energies	Fields Direct
	Greatest	Least	Mean		
$3s$	10·0	11·1	10·5	13·4	13·7
$3p$	12·7	16·7	15·0	20·2	20·4
$3d$	26·3	32·7	28·3	31·0	30·9
$4f$	80·6	90·0	85·1	90·0	89·7

TABLE IV

Array	Mean Wave-length (A.)	f-Value
$3s-3p$	3440	0·87
$3p-3d$	3340	0·90
$3d-4f$	4350	1·00

A further quantity of interest is the *f*-value of an array. Table IV gives the *f*-values of the three neon arrays calculated from the formulae

$$\frac{1}{\bar{\lambda}}\Sigma S = \Sigma\left(\frac{S}{\bar{\lambda}}\right),$$

$$f = \frac{1}{3\bar{\lambda}R}\cdot\frac{\Sigma S}{\omega},$$

where S is the strength of a line of wave-length λ, $\bar{\lambda}$ is the mean wave-length and ω is the statistical weight of the lower level. The values of σ^2 from the Coulomb approximation have been used in the calculation of the *f*-values.

Acknowledgments.—The writer wishes to thank Professor D. R. Hartree and Dr B. Jeffreys for their advice and encouragement during the course of this work. He is also grateful to his College for the award of a Studentship and to the Department of Scientific and Industrial Research for a grant.

Gonville and Caius College,
Cambridge :
1950 *October* 26.

References

(1) L. Goldberg, *Ap. J.*, **82**, 1, 1935; **84**, 11, 1936.
(2) H. N. Russell, *Ap. J.*, **83**, 29, 1936.
(3) H. E. White and A. Y. Eliason, *Phys. Rev.*, **44**, 753, 1933.
(4) D. R. Bates and A. Damgaard, *Phil. Trans. Roy. Soc. London*, **A 242**, 101, 1949.
(5) C. E. Moore, "Atomic Energy Levels", *Nat. Bur. Standards Circ.* 467, 1949.
(6) R. H. Garstang, *Proc. Camb. Phil. Soc.*, **47**, 243, 1951.
(7) D. R. Bates and A. Damgaard, *loc. cit.*, Table 6 and Table 7, columns 2 and 4.

VISUAL AND FAR-RED GRADIENTS AND COLOUR TEMPERATURES OF γ CASSIOPEIAE

D. R. Barber

(Communicated by the Director, Norman Lockyer Observatory)

(Received 1950 August 25)

Summary

Observed gradients, and corresponding grey-body temperatures at mean wave-lengths 5100 A. and 7090 A., are listed for γ Cass, with probable errors of ϕ, $\pm 0^{\cdot}03$ and $\pm 0^{\cdot}11$ respectively. Over the period 1945 October to 1950 April, significant departures from grey-body distribution are found associated with a general decrease of temperature.

In continuation of the routine colour temperature observations of γ Cass commenced here in 1938 *, and the short series obtained at the Lick Observatory in 1940–41 †, 38 visual gradient values have been reduced from spectrograms of this star and the Greenwich standard, δ Cass, photographed with the 12-inch McClean prismatic camera from 1945 October to 1950 April.

Up to 1948 March, the same Ilford panchromatic plates were used as formerly, and the adopted wave-lengths were 4244 A. and 6353 A., giving a mean wave-length of 5070 A. compared with 5080 A. for the 1938–41 series. After this date, Kodak I–E plates were employed and, to make full use of the spectral response of the emulsion, the red wave-length was altered to 6458 A., the mean wave-length being now 5100 A. for the visual gradient.

In addition, a supplementary set of spectrograms has been photographed with the same instrument on Kodak I.R. ER. plates since 1947 April, and from these 26 far-red gradients have been reduced from measures at wave-lengths 6458 A. (the same red wave-length as for the visual series) and 7846 A. in the near infra-red, giving a gradient value at 7090 A. Owing to the complexity of the terrestrial absorption spectrum in this wave-length interval, choice of the longer wave-length is restricted to a band of stellar continuum roughly 300 A. wide. It is just outside the infra-red wing of the oxygen [A] band, and nearly 400 A. below the Paschen series limit. Since both stars are photographed at approximately equal Z.D., any variation of the [A] band absorption will affect both spectra equally, and will not therefore distort the gradient of γ relative to δ Cass.

Photometric calibration of the I.R. ER. emulsion to red and infra-red radiation was effected in the tube sensitometer by exposing through suitable combinations of neutral absorbing screens and colour filters. The latter comprise Chance OR2 (2 mm.) with infra-red absorber ON13 (10 mm.) for red, and Chance OX4 (2 mm.) for infra-red exposures. These filters were chosen to give, as far as is practicable, the equivalent of a monochromatic calibration at each of the chosen wave-lengths.

The procedure adopted for the reduction of both visual and far-red gradients from the observed monochromatic intensities differed slightly from that previously used. Log intensity values were measured at a single wave-length in

* D. L. Edwards, *M.N.*, **103**, 222, 1943; *Comm. N.L.O.*, **58**, 232, 1943.
† D. R. Barber, *P.A.S.P.*, **58**, 363, 1946.

Gradients and Colour Temperatures of γ Cassiopeiae

Date		J.D.	ϕ 5100	ϕ 7090	T (deg.) 5100	T (deg.) 7090
1945		2431				
Oct.	7	736	0·68:	...	46,500:	...
	11	740	0·83	...	26,500	...
Nov.	10	770	0·89	...	23,000	...
Dec.	8	798	1·00	...	18,000	...
1946						
Feb.	19	871	0·83	...	26,500	...
		2432				
July	27	029	0·83:	...	26,500:	...
Aug.	25	058	0·81	...	28,200	...
Sept.	28	092	...	1·03:	...	25,700:
Nov.	14	139	0·76	...	33,000	...
Dec.	1	156	0·89	...	23,000	...
	17	172	0·81	...	28,200	...
1947						
Jan.	9	195	0·86	...	24,300	...
Mar.	24	269	0·84	...	25,800	...
Apr.	19	295	...	0·93:	...	35,200:
Aug.	8	406	0·64:	...	>50,000:	...
	15	413	...	1·05	...	24,200
Sept.	20	449	0·81:	...	28,200:	...
Oct.	4	463	0·89	...	23,000	...
	6	465	...	0·97	...	30,800
	11	470	0·87	...	24,000	...
Nov.	15	505	...	0·92	...	36,400
1948						
Jan.	5	556	0·81	0·92	28,200	36,400
	8	559	0·79	0·98	30,200	30,000
Apr.	13	655	...	1·18:	...	18,000:
May	5	677	0·88	...	23,500	...
	6	678	0·93	...	20,800	...
	26	698	0·90	...	22,200	...
Aug.	15	779	...	0·92	...	35,000
	28	792	...	0·84:	...	>50,000:
Sept.	2	797	...	1·31	...	14,800
	4	799	...	1·14	...	19,400
	11	806	...	1·39	...	12,800
	29	824	0·94	1·29	20,100	14,900
Oct.	4	829	0·94	...	20,100	...
	26	851	...	1·25	...	15,600
Nov.	8	864	0·93	1·00	20,800	28,000
	25	881	...	1·42:	...	12,500:
	30	886	0·78:	...	31,000:	...
1949						
Jan.	20	937	0·89	...	23,000	...
	27	944	...	1·57:	...	10,700:
	29	946	0·90	1·26:	22,200	15,400:
Feb.	5	953	...	1·00	...	28,000
	17	965	...	1·26	...	15,400
Mar.	3	979	0·97	...	19,200	...
	17	993	1·10	...	15,800	...
		2433				
Apr.	21	028	0·97	...	19,200	...
May	5	042	0·98	...	18,800	...
July	29	127	0·91	1·21:	21,800	16,900:
Oct.	12	202	0·83	...	26,500	...
	26	216	0·98	1·30	18,800	14,800
Dec.	21	272	0·83	1·09	26,500	21,800
1950						
Jan.	24	306	1·03	...	16,500	...
Feb.	16	329	...	1·18	...	17,800
Mar.	21	362	1·09	...	16,000	...
	25	366	1·01	...	17,400	...
Apr.	12	384	...	0·96:	...	31,800:

blue and red regions respectively by drawing in the continuum on a microphotometer tracing ($\times 7$) of each region, instead of using a mean intensity obtained from a set of six direct readings of galvanometer deflections, as in the earlier Sidmouth series. Reduction of the monochromatic intensities to relative gradients followed conventional practice; and, from these quantities, corrected for differential atmospheric extinction, the absolute gradients, ϕ_{5100} and ϕ_{7090} have been computed, using values of ϕ_{5100} and ϕ_{7090} for δ Cass, on the Greenwich scale equal to 1·24 and 1·38 respectively. The latter value is computed on the assumption of grey-body distribution in the spectrum of δ Cass corresponding to a temperature of 13,200 deg. K.

The probable error of a single determination of ϕ_{5100} is $\pm 0{\cdot}03$. On account of the shorter baseline used in the evaluation of ϕ_{7090}, giving $\Delta(1/\lambda)\,0{\cdot}273$ instead of 0·808, a probable error some three times greater is to be expected. Actually, the observed probable error of ϕ_{7090} is $\pm 0{\cdot}11$, the excess being attributable to the inferior photometric properties of the I.E.ER. emulsion. That this is so is confirmed by the greater scatter of the log intensity values reduced from the infra-red plates compared with that for the measures from panchromatic plates at the same wave-length.

The observations of gradient and colour temperature are summarized in the table, values of ϕ and T marked with a colon indicating a lower weight, due to inferior atmospheric conditions, difficulty in setting the true continuum on tracing, or photographic causes.

It will be noticed that the two gradients do not vary synchronously; and, at times, there is a pronounced departure from grey-body intensity distribution. For example, during the period, 1948 September to 1949 January, the visual gradient values were falling, while those at the longer wave-length were rising, and the mean colour temperature derived from the visual gradients was nearly 7500 deg. K. higher than for the far-red. From about J.D. 2432450 onwards, both gradient values show an upward trend (decrease of T), the increase of ϕ_{5100} being less rapid than of ϕ_{7090}. Frequent superposed fluctuations occur, of which some are probably real.

Further discussion of the results is reserved for a future paper.

Norman Lockyer Observatory of the
University College of the South-West,
Salcombe Hill, Sidmouth, Devon:
1950 *August* 23.

STELLAR PARALLAXES DETERMINED AT THE UNIVERSITY OF LONDON OBSERVATORY, MILL HILL (SECOND LIST)

(Received 1950 November 27)

(Communicated by the Assistant Director)

The following is the second list of relative parallaxes determined with the Radcliffe 24-inch photographic refractor; the first list was published in *M.N.*, **109**, 478. Of the 20 stars in the list, 19 belong to the first parallax programme and the remaining one, No. 15, was added later. Nos. 18, 19, 20 were photographed for 5 epochs, the first epoch being in 1939 (the work was interrupted from 1939 September 1 to 1946 April 3). Nos. 1, 6, 14, 16 each had one plate taken in 1939 and were then photographed for a further 6 epochs, and the remainder were photographed for 7 epochs from 1946 onwards. An average of 4·5 plates per epoch was obtained.

Two exposures were made on each plate, and these were measured in R.A. in the direct and reverse positions relative to rulings on reference plates. These plates were ruled at Greenwich through the kindness of the Astronomer Royal.

The average number of comparison stars was 5·2, with photographic magnitudes lying between 11 and 12 and with an average value of about $11^{m}\cdot5$ except where the parallax star was fainter than this magnitude. When brighter, the image of the parallax star was reduced to equality with an average $11^{m}\cdot5$ image by means of a rotating sector, as described in the first parallax list. The average distance of the comparison stars and of the parallax star from the centre of mean position of the comparison stars on the plate was 16′·4 and 2′·1 respectively, and the average parallax factor was 0·78. The plates used were Ilford Special Rapid and, for the fainter stars, Ilford Iso-Zenith, Kodak I-O and Kodak OaO. The latter plates were used at the end of the series after the manufacture of Iso-Zenith plates was discontinued by Ilford. The normal exposure time was 2½ minutes for stars not fainter than $11^{m}\cdot5$, for which no guiding was required; the hour angles were less than 20 minutes.

The photography was carried out by Mr C. C. L. Gregory, Dr E. M. Burbidge, Miss A. C. Robinson, Mr G. R. Burbidge and Mr R. W. Pring, and the plates were measured by Miss A. C. Robinson, Mr S. K. Wang, Mr C. C. L. Gregory, Mr F. Steel and Mr G. de Vaucouleurs. The plates were reduced following the method adopted by Schlesinger. As in the first list of parallax determinations, each of the two exposures on each plate was treated separately and given unit weight in the reduction.

In the following list, the second column gives the designation of each star. Greenwich numbers refer to the Greenwich catalogue of parallax determinations; Radcliffe numbers give the number of the selected area followed by the Durchmusterung number and are taken from the list of stars with proper motions exceeding 0″·100 in the *Radcliffe Catalogue of Proper Motions*, p. xl*, the third column gives the approximate visual and photographic magnitudes. These are taken from various sources and should be looked upon as provisional only. Where the photographic magnitude is bracketed, its value is estimated from the plates. Two values of the annual proper motion in R.A. are given, the first being a catalogue value and absolute (as also are the proper motions in

* In the first parallax list, the second number referred to the Radcliffe serial number in the proper motion catalogue.

declination); the second value of the proper motion in R.A. is derived from the parallax plates and is relative; omitting No. 15 for which there is no catalogue value, the average difference between this and the catalogue value is $\pm 0''{\cdot}017$. The probable errors of unit exposure were divided by $\sqrt{2}$ to give the probable errors of unit plate, which are shown in the table.

In the case of the double star No. 2 (Burnham 1239), both components were measured independently using the same comparison stars and both sets of values are given. The negative parallax of $-0''{\cdot}033$ obtained for the fainter component is probably due:—

(*a*) to the fact that the star is nearly a magnitude fainter than the brighter component, and hence its image was faint and difficult to measure on most of the plates;

(*b*) to magnitude error arising from the difference between the magnitude of the fainter component and the mean magnitude of the comparison stars, which was equal to that of the brighter component.

No. 15 was added to the parallax programme in 1946. It appeared on a plate taken at the University of London Observatory in 1946 for the determination of the position of the asteroid 51 Nemausa, and was originally chosen as a comparison star for the plate reduction, but was rejected as having a large proper motion amounting to $1''{\cdot}69$ annually. The star was added partly on account of this large proper motion and partly to see whether a reliable parallax determination of a star of south declination could be made at the University of London Observatory. The series of parallax plates shows no evidence of a large proper motion either in R.A. or in declination, and it must be assumed that the coordinates of the star in the *San Fernando Astrographic Catalogue*, Vol. 5 are in error. The values given there are $X_0 = +14{\cdot}911$, $Y_0 = +34{\cdot}110$, and the values computed at the University of London Observatory are $X_0 = +13{\cdot}872$, $Y_0 = +33{\cdot}680$.

The probable errors of unit plate are somewhat large, possibly for reasons suggested in the first list. Stellar images on the photographic plates which are now being taken for the second parallax programme, begun in 1949, are being made denser than those on the series of plates for the first programme, since it has been found that errors of measurement and errors due to irregular building up of the photographic image on the plate become larger for fainter stellar images.

No.	Designation and B.D. or *A.C.* No.	Mag. Vis. Phot.	Spec. Type	R.A. Dec. 1900.0	Unit $0''{\cdot}001$ Proper Motion R.A.	Proper Motion Dec.	P.E. Unit Wt.	Relative Parallax	P.E.
				h m s					
1	Camb. IIf, 42	9·3	K2	2 4 49	+ 142	− 72	33	+ 31*	7
	53° 467	10·7		+54° 10′	+ 151				6
2	Radcl. 70·176	...	G0	2 17 48	+ 115	+182	49	− 33*	9
	14° 387	10·8		+14° 58′	+ 66				9
	Radcl. 70·178	9·0	G5	2 17 51	+ 122	+185	32	− 1*	6
	14° 389	9·8		+14° 58′	+ 83				5
	Radcl. 49·—	8·7	G5	5 26 12	+ 33	−122	43	+ 2*	8
	29° 924	9·5		+29° 20′	+ 36				8

Unit 0″·001

No.	Designation and B.D. or *A.C.* No.	Mag. Vis. Phot.	Spec. Type	R.A. Dec. 1900.0	Proper Motion R.A.	Proper Motion Dec.	P.E. Unit Wt.	Relative Parallax	P.E.
				h m s					
4	Camb. IVc, 115	9·4	K2	6 6 2	+ 64	−160	54	+ 17*	11
	22° 1219	11·3		+22° 12′	+ 51				10
5	W Gem	6·3–7·2	G5	6 29 12	− 10	0	35	+ 2	7
	Test 6·29	var.		+15° 24′	− 13				7
	15° 1246								
6	Green. 340	7·1	Go	7 36 48	− 81	−139	28	+ 22	5
	Lal. F. 1144	7·5		+70° 27′	− 108				5
	70° 474								
7	Radcl. 4·26	...	F5	8 0 22	− 69	−268	34	+ 5*	6
	A.C. 74° 3281	12·1		+74° 28′	− 67				6
8	Radcl. 12·216	9·2	G3	9 4 16	− 80	−199	29	+ 14*	6
	59° 1224	10·9		+59° 32′	− 83				6
9	McC. 136·7a	9·4	K5	10 14 12	− 484	− 50	33	+223	7
	20° 2465	[11·0]		+20° 23′	− 494				6
10	Radcl. 30·242	9·9	K2	10 33 54	− 133	−130	38	+ 4*	6
	A.C. 45° 448–38	11·4		+45° 11′	− 87				5
11	Green. 103	10·3		10 51 1	− 630	+ 58	37	+ 14	8
	70° 639	11·6		+70° 8′	− 626				7
12	Green. 111	9·0	Ma	11 14 53	−2957	+203	33	+107	7
	66° 717	10·3		+66° 23′	−2943				7
13	Radcl. 56·210	...	G2	11 57 41	− 139	−110	42	− 1*	9
	A.C. 30° 27757	11·7		+29° 41′	− 100				8
14	Radcl. 6·181	...	G4	16 17 0	− 146	+ 64	46	− 3*	12
	A.C. 74° 5752	12·0		+74° 42′	− 156				9
15	*A.C.*−6° 3939	...		18 24 56	...	...	74	− 25*	24
	−101	11·5		− 6° 34′	− 28				17
16	Green. 222	8·0	Ko	19 42 11	+ 172	+105	41	+ 19	9
	Lal. 37923	9·0		+76° 11′	+ 164				7
	76° 750								
17	Green. 231	9·3	K5	20 13 51	+ 68	+450	35	+ 41	8
	76° 785	10·5		+76° 55′	+ 60				7
18	Green. 472	...		20 29 0	+ 449	+283	34	+114	9
	A.C. 65° 6955	11·5		+65° 6′	+ 462				6
19	Radcl. 67·453	8·8	G5	23 3 3	+ 105	− 83	42	+ 6*	8
	30° 4880	9·7		+30° 23′	+ 68				6
20	Green. 265	6·5	K2	23 47 32	+ 328	+ 52	30	+107	8
	Test 23·47	7·6		+74° 59′	+ 330				4
	74° 1047								

* No previous determination of parallax.

University of London Observatory,
Mill Hill Park :
1950 *November* 22.

OBSERVATIONS OF NOVAE, 1948 and 1949

W. H. Steavenson

(Received 1950 October 13)

Summary

These observations are in continuation of similar series communicated to the Society in past years. Unless otherwise stated, they were all made with the 30-inch Hindle reflector.

Nova Aquilae (1918)

This nova is still slightly variable, as early photographs show it to have been before its outburst.

Date	Mag.
1948 Sept. 6	11·3
17	11·2
1949 July 1	11·4

Nova Aquilae No. 6 (1936)

Date	Mag.
1948 Aug. 26	15·7
1949 July 1	16·1
29	16·1

The general fading has apparently ceased and the low value in 1949 probably represents no more than a temporary fluctuation.

Nova Aquilae (1945)

Date	Mag.
1948 Aug. 22	15·8
25	15·8
26	15·8
Sept. 11	15·8
24	15·8
28	15·8
Oct. 2	15·9
5	15·9
1949 June 23	$<16\cdot3$
July 29	$<16\cdot3$
Aug. 20	16·4
30	16·4

The nova is still fading slowly and seems likely to pass out of range of the telescope.

Nova Aurigae (1892)

Observed on 1949 December 15, when the magnitude was estimated to be 14·8, as it has been for very many years past.

Nova Cygni (1876)

This nova is definitely variable, with a range of about half a magnitude. The fluctuations appear to be quite irregular, like those exhibited by Nova Persei.

Date	Mag.	Date	Mag.
1948 July 21	14·76	1949 Aug. 15	14·55
31	14·81	20	14·60
Aug. 1	14·81	21	14·66
26	14·86	30	14·60
29	14·81	Sept. 10	14·71
Sept. 21	14·71	11	14·66
24	14·81	13	14·71
28	14·81	17	14·65
Oct. 1	14·81	25	14·65
4	15·00	27	14·71
5	15·00	28	14·71
25	15·00	Oct. 11	14·76
1949 June 23	14·76	12	14·81
July 1	14·50	13	14·86
3	14·60	15	14·76
8	14·44	21	14·55
26	14·60	24	14·57
29	14·66	27	14·65
Aug. 3	14·61	28	14·71
5	14·61	Nov. 9	14·61
11	14·45	21	14·57
14	14·50	22	14·61

Nova Cygni (1920)

The observations indicate a fall of about half a magnitude since 1947, though previously the nova had shown no change for many years, having apparently settled down to a stationary minimum. The individual estimates are given in case of further fluctuations.

Date	Mag.
1948 Sept. 6	16·1
11	16·1
24	16·2
28	16·1
Oct. 5	16·2
1949 July 1	16·1
29	16·2

Nova Cygni (1942)

The nova has probably reached or is approaching its minimum.

Date	Mag.
1948 Aug. 26	16·1
Sept. 24	16·1
1949 July 1	16·1
29	16·3
Aug. 30	16·1

Nova Cygni (1948)

Date	Mag.
1949 June 23	12·5
July 26	12·6
Sept. 6	12·7

The nova is fading normally.

Nova Geminorum (1903)

This nova is near the limit of visibility with the 30-inch telescope under average observing conditions. It was seen on 1949 February 16 and 19 and its magnitude was estimated at 16·5 ± on both occasions. So far as is known, the nova has been of this brightness for at least 30 years.

Nova Geminorum (1912)

Observed on 1949 December 19 when the magnitude was estimated to be 14·9, or much the same as for many years.

Nova Herculis (1934)

The nova appears under high powers as a planetary nebula about 3″ in diameter with a stellar nucleus. The light, almost constant at about 13·3 for some years previous to 1949, has shown some fluctuations in the period covered by the observations, but the nova remains substantially brighter than before the date of its outburst in 1934.

Date	Mag.
1948 May 2	13·3
July 22	13·3
1949 Apr. 23	13·3
July 21	14·2
26	13·6
29	13·5

Nova Lacertae (1910)

Observed on 1948 August 29 and estimated at $14^{m}\cdot4$. The light of this nova has been sensibly constant for a long time now.

Nova Lacertae (1936)

This nova seems to have reached its minimum and there is now little change in its brightness from year to year.

Date	Mag.
1948 Aug. 26	15·1
1949 July 29	15·0
Aug. 30	15·1

Nova Lyrae (1919)

The observations indicate a slight increase in brightness as compared with that of recent years.

Date	Mag.
1948 May 8	15·1
1949 June 23	14·7
July 29	14·8

Nova Ophiuchi (1848)

The slight but apparently irregular variability of this nova, first pointed out by the late Professor Barnard, persists.

Date	Mag.
1948 July 22	12·6
31	12·5
Sept. 6	12·6
24	12·6
28	12·6
1949 June 23	12·6
July 26	12·3
Sept. 6	12·2

Nova Persei (1901)

The most variable of all the old novae. Owing chiefly to the exceptionally bright maxima of 1948 July and 1949 September the range is greater than that usually observed, amounting to just over two magnitudes. The small wisp of nebulosity formerly observed in contact with the nova on its south-preceding side is now no longer observable visually with the 30-inch telescope.

Date	Mag.	Date	Mag.
1948 July 21	11·57	1949 Sept. 6	12·32
22	11·78	10	12·32
25	11·00	11	12·27
27	11·83	13	12·32
28	11·83	17	12·12
29	11·80	25	11·00
31	12·33	26	11·34
Aug. 1	12·26	27	11·81
22	12·32	28	11·30
26	12·64	30	11·08
29	12·74	Oct. 2	12·22
Sept. 6	12·64	3	12·48
11	12·79	4	12·22
14	12·74	5	12·32
17	12·64	8	12·96
18	12·69	11	12·69
20	12·64	12	12·84
21	12·64	13	12·89
24	12·84	15	12·90
25	12·90	17	12·84
28	12·84	21	12·90
29	12·90	22	12·84
30	12·90	24	12·84
Oct. 1	12·84	27	12·53
2	12·90	28	12·79
4	12·84	30	13·05
5	12·69	31	12·95
9	12·43	Nov. 7	12·79
10	12·58	9	12·95
12	12·74	10	13·00
14	12·64	13	12·95
23	12·64	15	12·84
25	12·69	18	12·95
26	12·43	21	12·84
28	12·53	22	12·79
Nov. 5	12·64	28	12·69
6	12·48	Dec. 4	12·74
8	12·64	5	12·84
25	12·48	8	12·53

Dec.	1	12·74		11	12·90
	2	12·69		15	12·84
	4	12·84		17	12·95
	21	12·95		19	12·84
1949 Jan.	3	12·85		20	12·90
	5	12·90		21	12·74
	8	12·90		27	12·84
Aug.	30	12·48		29	12·90
Sept.	4	12·47			
	5	12·27			

Nova Sagittae (1913)

The nova has returned to a nearly constant minimum following its secondary outburst in 1946.

Date	Mag.
1948 Aug. 29	14·4
June 23	14·4

Nova Scuti (1949)

Found near its maximum in 1949 August. This nova faded normally until the end of September, when the brightness began to fall much more rapidly and the star was lost in the twilight before the end of October. The observations up to that of August 17 inclusive were made with the 2-inch finder.

Date	Mag.	Date	Mag.
1949 Aug. 3	7·8	1949 Sept. 5	10·2
4	7·8	6	10·1
5	7·6	7	10·2
6	8·0	9	10·5
8	8·1	10	10·5
9	8·2	11	10·4
11	8·3	13	10·3
12	8·5	17	10·8
13	8·4	25	11·4
14	8·9	26	11·2
15	8·9	27	11·3
16	9·0	28	11·5
17	9·3	Oct. 3	13·0
19	9·4	4	12·9
20	9·6	5	13·3
21	9·7	11	14·6
22	9·6	12	14·7
25	9·8	13	14·7
30	10·1	15	15·1
Sept. 4	10·3	21	15·5

Nova Serpentis (1948)

Date	Mag.
1949 June 5	12·26
23	13·00
July 3	12·90

Cambridge :
1950 *October* 10.

IONOSPHERIC EFFECTS OF SOLAR FLARES*

M. A. Ellison

(Communicated by the Astronomer Royal for Scotland)

(Received 1950 October 11)

Summary

Intense flares generate sudden ionospheric disturbances (S.I.D.s for short). These are recorded simultaneously with the flare outbursts as seen by $H\alpha$ light in the spectrohelioscope.

Five types of S.I.D.s have been studied in relation to the flare development curves (line-width/time relationship) obtained at Edinburgh during 1949. This survey was greatly aided by two factors, a year of brilliant sunshine and a level of solar activity unexpectedly high for two years after the maximum.

The S.I.D.s, collected from continuous radio and magnetic records, were : (1) S.P.A.s : sudden phase anomalies in the reception of the Rugby 16 Kc./s. transmitter, as recorded at the Cavendish Laboratory. These give the phase difference between the ground wave and the ionospheric reflected wave and enable the level of the D-layer ceiling to be deduced. (2) G.B.R. (Ed.) : records of resultant signal strength (ground wave plus ionospheric wave) made at Edinburgh University on 16 Kc./s. (3) S.E.A.s : sudden enhancements of atmospherics on 27 Kc./s. recorded at Royal Observatory, Edinburgh. (4) S.W.F.s : D-layer absorption, giving rise to short-wave fadeouts in the 5–20 Mc./s. band. (5) C.C. : crochets recorded in the three elements, H, D and V, of the Earth's magnetic field.

The development curves produce striking evidence of the flash of radiation which occurs at the commencement of an intense flare. The D-layer ionization is found to commence simultaneously with this flash in $H\alpha$. There is evidence that the short-wave fadeout occurs at a height of about 70 km. and that the crochet currents flow at a still lower level, 60–70 km. The operative radiation must be ultra-violet light, not particles, for the D-layer effects are confined to the illuminated hemisphere and are independent of the location of the flare on the Sun's disk. Possible wave-lengths concerned are : $L\alpha$ (1215 A.), $L\beta$ (1026 A.), $He\lambda$ 584, Lyman continuum ($\leqslant$912 A.), and X-rays, formed possibly by recombination of *Fe* XIV in the corona. Cosmic-ray particles (10^{10} e.V.) accelerated by the flare may contribute to the ionization towards the end of the S.I.D. In a number of cases a lag, of the order of one hour, in the recovery of the D-layer after the visible flare is over suggests that the radiation may not arise from *H* atoms.

* The full text of this paper appears in *Publications of the Royal Observatory, Edinburgh*, **1**, No. 4, 1950.

THE ECLIPSING BINARY SV CENTAURI*

D. O'Connell, S.J.

(Received 1950 November 29)

Summary

About 1500 estimates on Riverview plates, together with 500 estimates made by Schmidt at Leiden and earlier observations by Miss Leavitt, Dawson, Dugan and Wright, were used to investigate the period of SV Centauri. Seventy epochs of primary, and twenty-seven of secondary, minimum were obtained between 1893 and 1949. It was found that the observed times of minimum could be represented by a periodic fluctuation superimposed on a parabola, which itself represents a secular decrease of period.

The secondary fluctuation has a period of 33·6 years and a semi-amplitude of 0·21 days. It can be explained as due to the motion of the binary about a third star, the variation of period being caused by the varying light-time across this orbit. The elements of the orbit were computed by Woltjer's method. The following results were obtained:—$e=0{\cdot}32$, $\omega=159°$, $a \sin i=38$ astronomical units, Periastron 1922.5, Mass-function=49.

The secular change of period is very large, from $1^d{\cdot}66151$ in 1893 to $1^d{\cdot}65929$ in 1949. If this change is periodic, the period is very long. If it were due to the motion of the triple star about a fourth star the mass-function would have to be at least 10,000. The decrease of period may be due to the interchange of matter between the components of the binary system (which are almost in contact), as suggested by Kuiper for β Lyrae. The secondary fluctuation may possibly be due to a similar cause.

The orbital elements of the binary were determined from the mean light curve derived from the Riverview plates. The orbit was found to be slightly eccentric. The stars are almost in contact. The spectrum of the companion has not yet been observed. It is estimated that at primary minimum most of the light comes from the companion and it ought to be possible to determine its spectrum at that time.

THE ECLIPSING BINARY V 525 SAGITTARII*

D. O'Connell, S.J.

(Received 1950 November 29)

Summary

875 estimates on plates taken at Lembang and Riverview were used to determine the mean light curve and orbital elements of V 525 Sagittarii, which was discovered at Riverview in 1934. Uniform and darkened solutions are given.

THE PERIOD OF THE ECLIPSING BINARY RS SAGITTARII*

D. O'Connell, S.J.

(Received 1950 November 29)

Summary

Dugan and Wright suspected a variation in the period of this binary. Epochs of minimum were determined from estimates made on 624 Riverview plates. These were combined with all other published observations to investigate the period. It is found that the times of minimum can be represented by a parabolic formula and that the period has decreased by about $0^d{\cdot}9 \times 10^{-5}$ in the 8000 epochs between 1889 and 1949.

* The full texts of these papers appear in *Riverview College Observatory Publications*, No. 9 (Vol. 2, No. 5), 1949.

S

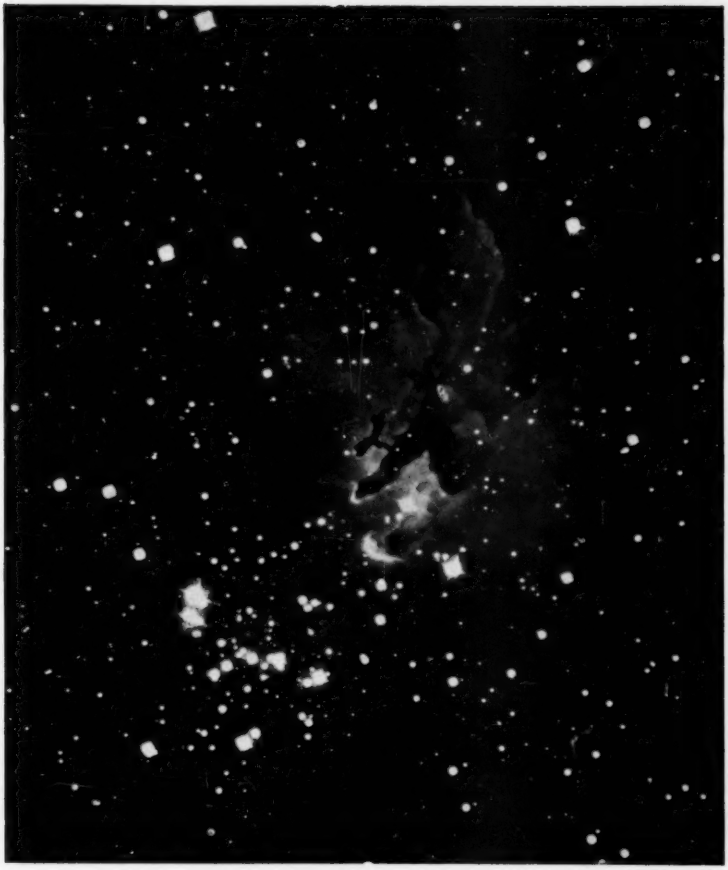

E

(*a*) *M*16. *Scale* 6″·9 = 1 *mm*.

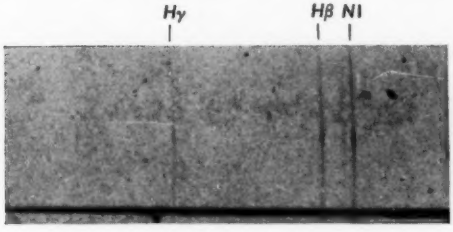

(*b*) *Rim A and reference star. Scale along lines same as for* (*a*), *east at top.*

S

E

(*a*) *M*20. *Scale* 2″·7 = 1 *mm.*

(*b*) *Spectrum of rim with slit orientated p.a.* 72° *as indicated in Fig.* 4.
Scale along lines : 6″·35 = 1 *mm., east at top.*

CONTENTS

Printed in London by Taylor & Francis, Ltd., 1951 *August.*